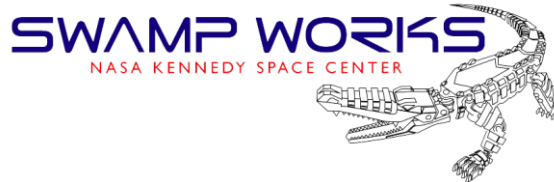


Final Phase I Report: NASA Innovative Advanced Concepts (NIAC)



Mars Molniya Orbit Atmospheric Resource Mining

FY 16 NIAC Phase I Project

Robert P. Mueller, Principal Investigator

NASA
Swamp Works Laboratory
Mail Code: UB-R1
Kennedy Space Center, Florida 32899
E-mail: rob.mueller@nasa.gov

Brandon Sforzo, PhD, Co-Investigator

Space Systems Design Laboratory
Georgia Institute of Technology
270 Ferst Drive, Atlanta, GA 30331
E-mail: brandon.sforzo@aerospace.gatech.edu

Robert D. Braun, PhD, Co-Investigator

Space Systems Design Laboratory
Georgia Institute of Technology
270 Ferst Drive, Atlanta, GA 30331
E-mail: robert.braun@aerospace.gatech.edu

Laurent Sibille, PhD, PMP, Co-Investigator

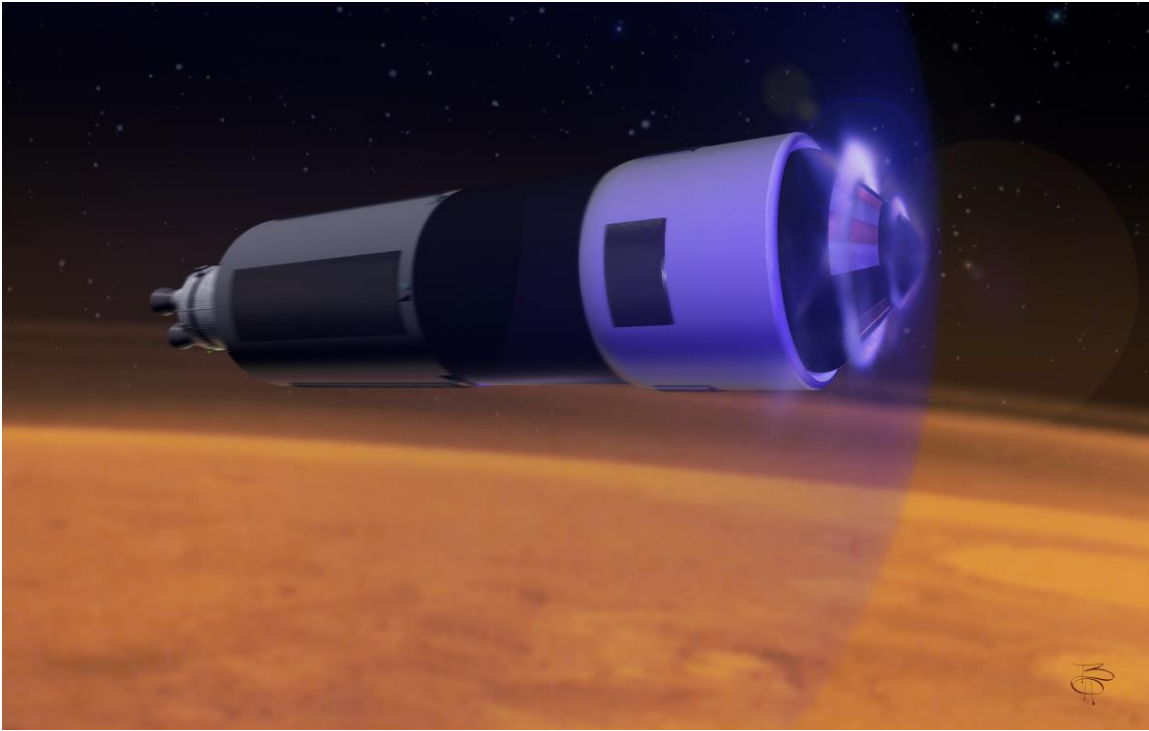
Swamp Works Laboratory
Kennedy Space Center, FL 32899
E-mail: Laurent.Sibille-1@nasa.gov

FEBRUARY 2017

Public Release Is Authorized

EXECUTIVE SUMMARY

This NASA Innovative Advanced Concepts (NIAC) Phase I study examined the revolutionary concept of performing resource collection and utilization during Mars orbital operations in order to enable the landing of large payloads. An exploration architecture was developed, out of which several mission alternatives were developed. Concepts of operations were then developed for each mission alternative, followed by concepts for spacecraft systems, which were traded to assess their feasibility.



NIAC Mars Atmospheric Gas Resources Collector Vehicle (RCV) stack during an aerobraking CO₂ collection pass in the upper atmosphere. The vehicle produces O₂ to fuel a Mars Descent and Ascent Vehicle (MDAV), for descent to the surface and subsequent launch to high Mars orbit.

A novel architecture using Mars Molniya Orbit Atmospheric Resource Mining is feasible to enable an Earth-independent and pioneering, permanent human presence on Mars by providing a reusable, single-stage-to-orbit transportation system. This will allow cargo and crew to be routinely delivered to and from Mars without transporting propellants from Earth.

In Phase I, our study explored how electrical energy could be harnessed from the kinetic energy of the incoming spacecraft and then be used to produce the oxygen necessary for landing. This concept of operations is revolutionary in that its focus is on using *in situ* resources in complementary and varied forms: the upper atmosphere of Mars is used for aerocapture, which is followed by aerobraking, the kinetic energy of the spacecraft is transformed into usable electrical energy during aerobraking, and the atmospheric composition is the source of oxidizer for a landing under supersonic retropropulsion.

This NASA Innovative Advanced Concepts (NIAC) Phase I study explores a novel mission architecture to establish routine, Earth-independent transfer of large mass payloads between Earth and the Mars surface and back to Mars orbit. The first stage of routine mission operations involves an atmospheric resource mining aerobraking campaign following aerocapture into a highly elliptical Mars orbit. During each pass through the atmosphere, the vehicle ingests the atmospheric oxidizer and stores it onboard, using solid oxide electrolysis to convert the primarily CO₂ atmosphere into usable O₂ for propellant. Power is made available through the use of magnetohydrodynamic energy generation, which converts the motion of the plasma in the shock later into usable electrical energy. Upon termination of the aerobraking sequence, the descent vehicle detaches from the orbit stack, deorbits, and executes the entry, descent, and landing sequence. Hypersonic deceleration is achieved via a deployable heat shield to lower the vehicle ballistic coefficient, and supersonic and subsonic deceleration are achieved via retropropulsion. Mars surface operations involve resource mining of the Martian regolith to produce CH₄ and O₂ propellant to be used for the subsequent MDAV ascent back to high Mars orbit (HMO) providing an apoapsis raise maneuver to initialize the aerobraking sequence, in addition to providing fuel from the Mars surface for EDL propulsive descent. The Resource Collector Vehicle (RCV), which is used for the orbital mining operations, is raised back to HMO via onboard deployable augmented solar electric propulsion. Concepts of operations were developed for each mission alternative, to evaluate between them and assess feasibility.

In Phase I, we showed that for a human-class mission, with 81 orbital scooping passes at 79 km altitude, with each atmospheric scoop varying in duration from 5.3 minutes to 7.1 minutes, at speeds ranging from 3.57 km/s to 4.5 km/s, approximately 431 kg of CO₂ can be ingested per scooping pass at periapsis and compressed by a Resource Collector Vehicle (RCV) with a hypersonic ram-compression system. The total amount of CO₂ captured and stored is approximately 34,939 kg. Because of the SOE chemical conversion process and other efficiency losses, this O₂ product amounts to an estimated 20% of the captured CO₂ mass—resulting in 6,986 kg of O₂ for EDL propulsion to provide thrust for deorbit, reorientation for entry, supersonic retropropulsion (SRP), and propulsive precision landing. A concept was developed, and the scooping analysis indicates that it would be feasible, but more detailed analysis is required in Phase II to optimize this concept and work out details of the aerodynamics and compression thermodynamics

This NASA Swamp Works/Georgia Tech team has established a first-order feasibility confirmation of the revolutionary concept of performing resource collection and utilization during orbital operations and enabling the landing of large payloads.

CONTENTS

1.	INTRODUCTION AND BACKGROUND	11
2.	DESCRIPTION AND BENEFITS OF THE CONCEPT.....	14
2.1	Description of Orbital Resource Mining and Resource Utilization	14
2.2	Architectural Advantages of Orbital Resource Mining and Resource Utilization	14
3.	STUDY APPROACH.....	17
3.1	Phase I Study Work Plan	17
3.2	Study Objectives	18
3.2.1	Objective 1: Examine Architecture Concepts.....	18
3.2.2	Objective 2: Establish Feasibility of Mars Molniya Atmospheric Resource Mining	18
3.2.3	Objective 3: Develop Systems Models and Apply Iterative Design	19
3.2.4	Objective 4: Develop a Technology Roadmap.....	20
4.	MISSION ARCHITECTURE AND CONCEPTS OF OPERATION.....	20
4.1	Ground Rules and Assumptions.....	20
4.1.1	Mission Design/ConOps.....	21
4.1.2	ConOps.....	23
4.1.2.1	Mission Architecture Elements	23
4.1.2.2	Sample Return Mission	25
4.1.2.3	Human-Crewed Mission to Mars	27
5.	ANALYSIS METHODS AND MODELING.....	30
5.1	Astrodynamics Model.....	30
5.2	Mars Atmospheric Resource Mining Model	35
5.2.1	Aerobraking and Atmospheric Resource Mining Simulation Algorithm	35
5.2.2	Mars Sample Return Mission RCV Modeling Parameters	37
5.2.3	Human Mars Mission RCV Modeling Parameters.....	37
5.2.4	Assumptions	38
5.2.5	Algorithm Characteristics	38
5.2.6	Discussion.....	38
5.2.7	Mars Atmospheric Orbital ISRU Model.....	41
5.2.7.1	Solid-Oxide Electrolysis (SOE).....	42
5.2.7.1.1	MSR Reference Case – On-Orbit O ₂ Production	44
5.2.7.1.2	Human Mission Reference Case – On-Orbit O ₂ Production.....	46
5.3	Magneto-Hydrodynamic (MHD) Model	46
5.3.1	General MHD Energy Generation, Faraday Type Flow Through	47
5.3.2	Determining the Power Available for MHD Energy Generation During Aerobraking.....	47
5.4	Electrical Energy Storage Systems	52
5.5	Entry, Descent & Landing (EDL) Model.....	57
5.5.1	EDL Simulation	57
5.6	Mars Surface ISRU Model.....	60
5.7	Spacecraft Concepts and CAD Models	62

6.	CONCEPT TECHNOLOGY DESCRIPTIONS AND TECHNICAL DETAILS TO SUPPORT FEASIBILITY	63
6.1	In-Space Transportation.....	64
6.2	Resource Collector Vehicle (RCV)	69
6.2.1	Spacecraft Systems and Operations	69
6.2.2	Hypersonic Aeroshell Coupled with CO ₂ Collection	69
6.2.3	RCV Geometry Justification	70
6.2.4	RCV Flow Capture Inlet.....	72
6.2.5	Heat Transfer and Storage.....	73
6.2.6	Magnetohydrodynamic (MHD) Energy Generation	73
6.3	Mars Descent & Ascent Vehicle/Single-Stage Reusable Lander	75
6.3.1	Spacecraft Systems and Operations	75
7.	TECHNOLOGY ROADMAPS.....	80
7.1	Reusable Hypersonic CO ₂ Collector and MHD Energy Generator.....	80
7.2	Fast-Charging Electrical Energy Storage (EES) and Augmented Solar Electric Propulsion (SEP)	81
7.3	Large-Scale Solid Oxide Electrolysis (SOE)	81
7.4	Mars Descent Ascent Vehicle.....	81
8.	SUMMARY OF THE MARS MOLNIYA ORBIT ATMOSPHERIC RESOURCE MINING CONCEPT.....	83
9.	TECHNICAL CHALLENGES THAT REMAIN TO BE ADDRESSED AND FORWARD WORK.....	85
9.1	Launch and Near-Earth Assembly.....	85
9.2	Arrival in Mars system	85
9.3	Mars Molniya Operations (orbital maneuvering, aerobraking, CO ₂ collection and processing).....	85
9.4	EDL, SRP at Mars.....	86
9.5	Mars Liftoff	86
9.6	RCV Stack LMO to HMO maneuver	87
9.7	Architecture.....	87
10.	CONCLUSIONS.....	88
11.	FORWARD WORK	90
12.	ACADEMIC INVOLVEMENT AND ACKNOWLEDGEMENTS	92
13.	REFERENCES AND CITATIONS	94
APPENDIX A.	MANAGEMENT STRUCTURE AND TEAM MEMBERS.....	97
APPENDIX B.	SPACE MISSION CAMPAIGN: ARCHITECTURE GROUND RULES & ASSUMPTIONS.....	100

FIGURES

Figure 1. A representative decaying highly elliptic Molniya orbit around Mars. 12

Figure 2. Atmospheric collector design for Earth orbit in the PHARO concept (Jones et al., 2010). 13

Figure 3. Mars sample mission architecture elements. 23

Figure 4. Human Mars mission architecture elements. 24

Figure 5. Mars Sample Return mission – Earth departure, chemical propulsion. 25

Figure 6. Mars Sample Return – MMOM and surface ISRU. 26

Figure 7. Mars Crewed Mission reference case concept of operations – Earth departure phase. 27

Figure 8. Mars Crewed Mission – Mars ops, surface ISRU, MMOM, RCV+MDAV always docked. 28

Figure 9. Example round trip ΔV as a function of total mission duration. (Source: NASA DRA 5.0) 31

Figure 10. Representative mission profiles for the major classes for human Mars missions. (Source: NASA Mars DRA 5.0) 32

Figure 11. Lunar gravity assists and maneuvers near apogee shape HEO for efficient departures (source: NASA DRA 5.0). 32

Figure 12. The aerocapture maneuver is accomplished in a single atmospheric pass to eliminate propellant. (Image: NASA) 33

Figure 13. 2035 Mars departure opportunity. (Source: NASA DRA 5.0) 34

Figure 14. Decaying elliptical orbits during aerobraking maneuver. (Target is a final altitude of 250 km.) 40

Figure 15. Mars orbital resource mining capability. 40

Figure 16. SOEC cell design for MIP experiment (2001). 43

Figure 17. SOE-ESR Dual Stack (I); 10 cm² electrodes on 8YSZ electrolyte designed for proposed use on Mars 2020 mission (Sanders, 2014). 43

Figure 18. First principles analysis of MHD energy generation. 47

Figure 19. 0% K seed postshock ionization fraction as a function of altitude and freestream velocity. 49

Figure 20. Sample power vs. time and velocity vs. time from previous work (Moses et al., 2005). 50

Figure 21. Reconstructed altitude velocity history for vehicle studied in previous work (Moses et al., 2005). 51

Figure 22. Estimated constant for MHD power available for Moses test vehicle. 51

Figure 23. Ragone plot for electrical energy storage systems under consideration. 53

Figure 24. Electrical energy storage system model flowchart. 55

Figure 25. Direct entry power generation profile for Moses test vehicle (Moses et al., 2005). 56

Figure 26. Percent available energy stored for Moses test vehicle direct entry case, mass constrained to 100 kg. 57

Figure 27. SSRP EDL Altitude vs. Mach number of the entry vehicle during EDL. 59

Figure 28. Common methane engine used in the NASA EMC (Percy et al., 2015). 60

Figure 29. Left: Mars Surface ISRU processing module for CO₂ and H₂O to O₂ and CH₄ production. Right: 3 modules with associated excavators and regolith handling provide sufficient capability for MDAV/SSRL refueling powered with 30 kWe SPP units (Kleinhenz, 2017). 61

Figure 30. NIAC Mars Atmospheric Gas Resources Collector Vehicle (RCV) stack concept during an aerobraking CO₂ collection pass in the upper atmosphere.63

Figure 31. Mars atmospheric resource mining stack concept (solid and section views).....64

Figure 32. Typical NASA Cryogenic Propulsion Stage (CPS) concept, LEO to HEO. (Credit: NASA)65

Figure 33. NASA Orion Crew Orbital Vehicle (COV) in development. (Credit: NASA)66

Figure 34. Concept of typical NASA Crew Transit Stage (CTS) with COV docked. (Credit: NASA)66

Figure 35. Concept of NASA EMC Crew Transit Stage (CTS) (Credit: NASA)67

Figure 36. Concept of typical NASA Mars Transport Cryogenic Stage (MTCS) from the EMC. (Percy et al., 2015)68

Figure 37. Resource Collector Vehicle with major systems.69

Figure 38. Cross section side view of RCV compressor cone and RCV.70

Figure 39. General heat shield geometry, defining coordinate system and gas flow angle Φ relative to the vehicle reference (Button et al., 2009).71

Figure 40. Universal heat shield shape with the center of mass as reference and the distance from the CM to the front of the heat shield as the unit length (Button et al., 2009).71

Figure 41. Mars Exploration Rover entry vehicle design with the universal heat shield shape overlaid (Davies & Arcadi, 2006).72

Figure 42. MHD concept design for spacecraft skin mounted on blunt body cone. Isometric view includes optional alkali metal seeding devices to increase plasma conductivity. Side view shows gas flow, magnetic field, and collected current (Steeves, 2007).....73

Figure 43. MHD power generation capability during atmospheric passes.....74

Figure 44. Stowed configuration for launch from Earth.....75

Figure 45. MDAV/SSRL decelerating aerodynamically at Mars with recessed SRP engines (top and bottom isometric views).....76

Figure 46. Configuration for landing at Mars (top and left) and for ascent from Mars after launch (right).77

Figure 47. Comparison of required and available PMF for Hercules SSTO design space.78

TABLES

Table 1. Elements, mass, and origins for the Mars Molniya Atmospheric Resource Mining Architecture.29

Table 2. Results of astrodynamics analysis.....30

Table 3. Departure scenario considerations for human missions to Mars. (Source: NASA DRA 5.0)34

Table 4. Mars atmospheric scooping concept of operations.....36

Table 5. MSR RCV parameters calculated from Mars Atmospheric Resource Mining Model.....37

Table 6. Human mission RCV parameters calculated from Mars Atmospheric Resource Mining Model.....37

Table 7. MSR reference case – on-orbit oxygen production.....45

Table 8. Human mission reference case - on-orbit oxygen production.46

NIAC FY16: Mars Molniya Orbit Atmospheric Resource Mining

Table 9. Martian atmospheric compositions (Mahaffy et al., 2013).....	48
Table 10. Vehicle Parameters for the Moses test vehicle (Moses et al., 2005).....	50
Table 11. Electrical Energy Storage System performance data.....	53
Table 12. Electrical Energy Storage System performance data.....	54
Table 13. Moses test vehicle direct entry electrical energy storage system mass.	56
Table 14. Mass calculations for ISRU and cargo for the completion of the MSR reference mission.....	62
Table 15. Work Plan: Work Breakdown Structure (WBS), Resource Allocation & Schedule	90

ACRONYMS, ABBREVIATIONS, AND UNITS

Δv	delta- v (change in velocity)
AIAA	American Institute of Aeronautics and Astronautics
AMOSS	atmospheric mining in the outer Solar System
AR&D	analytical research and development
CAD	computer-aided design
CEA	Chemical Equilibrium Analysis
CH ₄	methane
CH ₄	methane
ConOps	concept of operations
COV	Crew Orbital Vehicle
CPS	Cryogenic Propulsion Stage
CTC	Crew Transit Vehicle
CTV	Crew Transit Vehicle
d	day
DRA	Design Reference Architecture
DSH	Deep Space Habitat
ED&PL	Entry, Descent, and Precision Landing
EDL	Entry, Descent, and Landing
EES	electrical energy storage
EMC	Evolvable Mars Campaign
ESD	Exploration Systems Development
ESD	Exploration Systems Development (Division)
FAQ	frequently asked questions
FSP	fission surface power
GaTech	Georgia Institute of Technology
GN&C	guidance, navigation, and control
HEEO	high Earth elliptical orbit
HEO	high Earth orbit
HMO	high Mars orbit
IMLEO	initial mass in LEO
Isp	specific impulse
ISRU	<i>in situ</i> resource utilization
ISS	International Space Station
kg	kilogram
km	kilometer
LEO	low Earth orbit
LMO	low Mars orbit
LO ₂	liquid oxygen
m	meter
MAV	Mars Ascent Vehicle
MCL	Mars Crew Lander
MDAV	Mars Descent Ascent Vehicle
MEL	Master Equipment List
MEPAG	Mars Exploration Program Analysis Group

NIAC FY16: Mars Molniya Orbit Atmospheric Resource Mining

MHD	magnetohydrodynamic
MMOM	Mars Molniya orbital mining
MSFC	Marshall Space Flight Center
MSL	Mars Science Lab
MSR	Mars Sample Return
MTCS	Mars Transport Cryogenic Stage
NEP	nuclear electric propulsion
NIAC	NASA Innovative Advanced Concepts
NIAC	NASA Innovative Advanced Concepts
NTP	Notice to Proceed
NTP	nuclear thermal propulsion
PHARO	Propellant Harvesting of Atmospheric Resources in Orbit
POST2	Program to Optimize Simulated Trajectories II
PROFAC	Propulsive Fluid Accumulator (system)
RCV	Resource Collector Vehicle
RPSCL	Robotic Precursor Small Cargo Lander
s	second
SEP	solar electric propulsion
SKG	Strategic Knowledge Gaps
SLS	Space Launch System
SM	Service Module
SOE	solid oxide electrolysis
SOFC	solid oxide fuel cells
SPP	Surface Power Plant
SRP	supersonic retropropulsion
SSRL	Single-Stage Reusable Lander
t	ton
TA	Technology Area
TMI	Trans-Mars Injection
TRL	technology readiness level
vs.	versus
ZBO	zero boiloff

1. INTRODUCTION AND BACKGROUND

Landing on Mars is extremely difficult (Braun & Manning, 2006) and is considered one of NASA's biggest technical challenges on the journey to Mars (NASA OCT, 2010). *Science* magazine (Kerr, 2012) reported the following about the NASA Mars Science Lab (MSL) MISSION:

Not only will NASA have to slow the most massive load ever delivered to another planet's surface from hypervelocity bullet speeds to a dead stop, all in the usual "7 minutes of terror," but NASA is also attempting to deliver Curiosity to the surface of Mars more precisely than any mission before, within a 20-kilometer-long ellipse some 240 million kilometers from Earth. Both feats are essential to NASA's long-term goals at Mars: returning samples of Martian rock and sending humans to the Red Planet.

As a result of the thin Martian atmosphere, this challenge is exacerbated as the payload mass is increased, and landing the propellants needed for a return launch from Mars in a Mars Descent Ascent Vehicle/Single-Stage Reusable Lander (MDAV/SSRL) severely constrains the "up-mass" because of limitations in current entry, descent, and landing (EDL) technologies and the logistics and high cost of transporting propellants from distant Earth. Ideally the MDAV/SSRL would be reusable in order to amortize development, fabrication, and operation costs, to avoid the constraints of Mars launch windows (which typically exist every 26 months) and to provide flexibility in operations. This study investigated a completely new mission architecture for landing large-mass payloads. This is a new concept—using Mars orbital atmospheric resource mining (scooping CO₂ resources outside of the deeper part of the Mars gravity well) to provide propellant for an MDAV/SSRL for routine and repeated transportation from Mars orbit to the surface and back. Such a capability would enable flexible and sustainable activity in the cis-Martian vicinity. In Phase II of this NIAC study, we intend to expand the study to other applications of Mars orbital atmospheric resource mining such as Mars propellant depots, Earth-Mars cyler transportation systems, visits to Phobos and Deimos, and investigations on how relevant cis-Martian activity can support other Solar System activity.

In Phase I of this NIAC project, we demonstrated the integration of advanced *in situ* resource utilization (ISRU) methods into an enabling core component for multiscale mission contexts as part of a larger space exploration architecture and pioneering campaign to sustain a human presence on the planet Mars. We developed an innovative and feasible concept for a reusable Mars space transportation system that, without ever relying on propellant transported from Earth, can repeatedly launch and land on Mars by using propellant and electrical energy generated on orbit via plasma-harnessing, scooping, and ram-compressing the 95% CO₂ Martian atmosphere, and by using indigenous resources on the surface of Mars (CO₂, H₂O). This system can carry four crew members and cargo up to a limit of 20 metric tons (t) of landed mass. With today's EDL technology, landed mass on Mars is limited to approximately 1–2 t. Our new technology and mission concept is scalable, and in NIAC Phase II, the upper feasible limit will be examined. It is anticipated that masses up to 100 t could be landed for Mars colonization efforts.

The proposed mission architecture for the Mars Molniya Orbit Atmospheric Resource Mining concept incorporates a wide range of vehicle classes to make round-trip travel between Earth and

Mars robust, affordable, and ultimately routine for cargo and crew, thereby helping to expand human civilization to Mars.

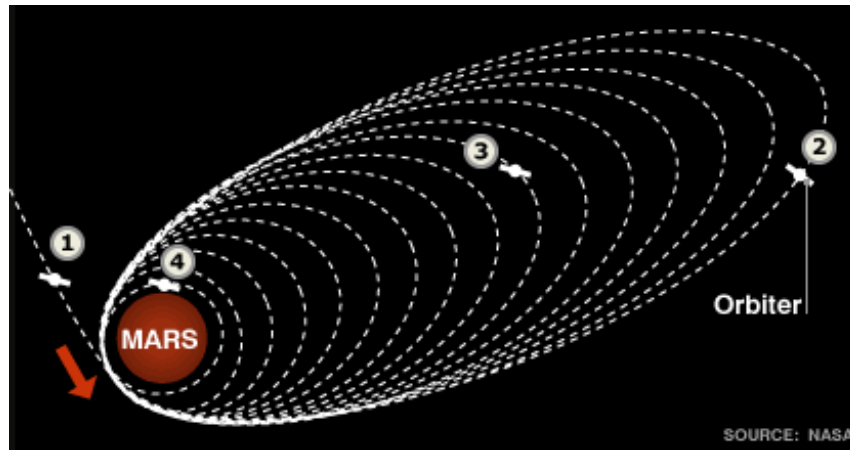


Figure 1. A representative decaying highly elliptical Molniya orbit around Mars.

In situ resource utilization (ISRU) on the surface of Mars has been proposed and studied for making rocket propellants, in order to fuel a Mars Ascent Vehicle (MAV) (Drake, 2010; Zubrin, 1991), but using ISRU in Mars orbit to make propellants for supersonic retropropulsion (SRP)-enabled EDL is a new concept, which creates an unprecedented association of ISRU, including energy harvesting, and EDL. *Molniya* is the Russian word for *lightning*, and in this study, a highly elliptical Mars orbit is referred to as a *Mars Molniya orbit* because of the high velocities encountered at periapsis (Figure 1). Our calculations and modeling indicate that the scooping velocities achieved at periapsis will range from 3.57 km/s to 4.5 km/s. Similar orbits are used in Earth applications, but we are not constraining ourselves to the definition of an Earth Molniya orbit. Typically during aerobraking, kinetic energy is converted into heat energy and wasted, but in our concept, the heat and associated plasma are transformed into magnetohydrodynamic (MHD) electricity generation, heat transfer, and thermal storage for endothermic chemical ISRU solid oxide electrolysis (SOE) processes, and the high velocity of the spacecraft is used for hypersonic ram compression of atmospheric gases for storing and making liquid O₂ oxidizer for SRP-assisted EDL.

From 1956 to 1963, S.T. Demetriades proposed three methods of atmospheric gas accumulation: (1) by means of a satellite moving in a 120 km low Earth orbit, (2) by accumulating propellants on the surface of a planet, or (3) by gathering and exploiting interstellar matter. He called this concept the PROpulsive Fluid ACcumulator system (PROFAC). Wilkes and Klinkman revived the idea at a 2007 AIAA conference (Wilkes, 2007; Capriotti, 2013). In 2007, B. Palaszewski proposed atmospheric mining in the outer solar system (AMOSS) because of the abundance of valuable resources such as hydrogen and helium 3 for potential use in nuclear power and propulsion systems. The primary targets considered by Palaszewski were Uranus and Neptune. Demetriades' proposal was further refined by C. Jones and A. Wilhite in 2010 in the PHARO concept, describing multiple collection vehicles (Figure 2) that would accumulate propellant gases approximately 120 km above Earth, and later transfer them to a higher orbit (Jones, 2010). In 2015, D. Arney et al. published a paper at the AIAA Space Forum titled, "Sustainable Human

presence on Mars Using ISRU and a Reusable Lander,” which defined a Mars SSRL vehicle using O₂ and CH₄ propellants made on the surface of Mars.

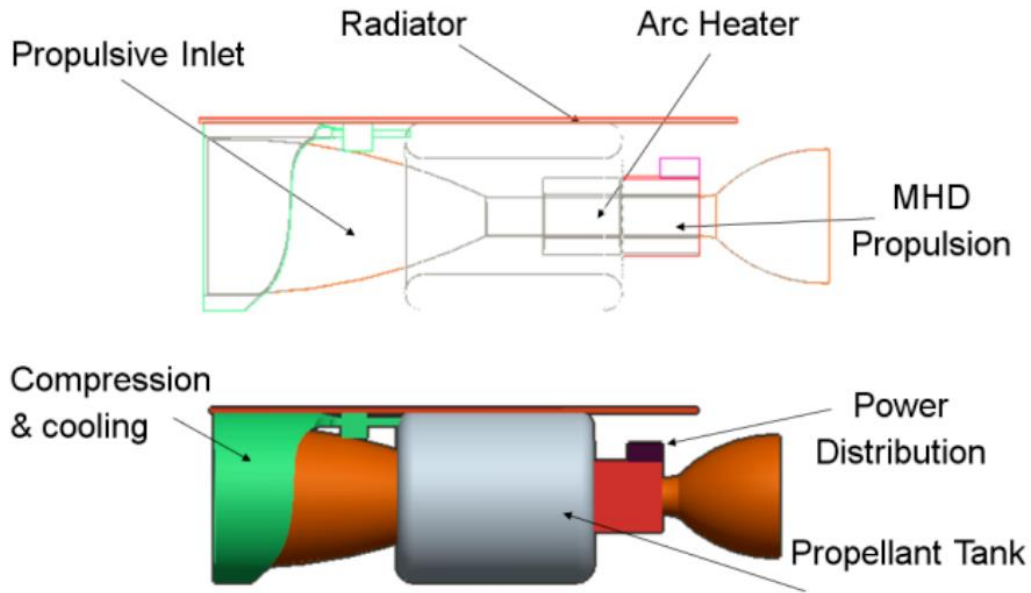


Figure 2. Atmospheric collector design for Earth orbit in the PHARO concept (Jones et al., 2010).

Our NIAC study draws from these previous efforts to show, for the first time, that atmospheric mining of CO₂ and ISRU processing on orbit and on the surface of Mars is a potential solution for developing and operating a large reusable Mars MDAV/SSRL.

While previous studies investigated an MDAV/SSRL in Earth’s orbit, in this study the Mars atmosphere is used to make propellant and no attempt is made to maintain an orbital altitude since a decaying Mars Molniya orbit via aerobraking is useful. Previously, MHD was used with beamed solar power to boost the orbit, but in this study, MHD is used in the opposite way: electric power is generated from plasma and kinetic energy via decaying Molniya scooping orbits. Moses et al. also considered MHD for electrical power generation and proposed generating O₂ from the plasma, but did not generate it using SOE and did not have an application for the resulting oxidizer (Moses et al., 2005). The nozzle used for gas compression and collection is also very different, since the spacecraft in this study operates at 79 km Mars altitude and travels at hypersonic speeds, requiring a different approach to the size and shape of the compressor cone and collection nozzle. While a solar-powered satellite network was required in the Propellant Harvesting of Atmospheric Resources in Orbit (PHARO) study, in our concept electrical power is generated via plasma MHD, which is then stored for subsequent use. The PHARO study analyzed making propellant on Earth for a trans-Mars injection (TMI), whereas this study addressed propellant-making on Mars for an MDAV/SSRL capability. It is conceivable that the two atmospheric mining approaches could be combined into an MDAV/SSRL mission architecture that uses Mars Molniya atmospheric resource mining to make TMI propellant outside the deep Earth gravity well, but the cost, risk, logistics, and scheduling factors of this approach would have to be traded off against those of convention approaches where propellant is made on Earth and launched it into orbit for TMI.

2. DESCRIPTION AND BENEFITS OF THE CONCEPT

2.1 Description of Orbital Resource Mining and Resource Utilization

By using ISRU, propellant and logistics items do not have to be transported from Earth, which makes self-sustainment and independence possible for the pioneering Martian crews.

This Phase I study has expanded the possibilities of ISRU at Mars, not only in using propellant made on the surface, but also in using propellant and electrical energy generated on orbit via plasma-harnessing MHD, scooping, and ram-compressing the 95% CO₂ Martian atmosphere, and by using indigenous resources on the surface of Mars (CO₂, H₂O). This system can carry four crew members and cargo up to 20 metric tons (t) of landed mass.

By combining the atmospheric orbital ISRU with surface ISRU (CO₂ and H₂O), an Earth-independent MDAV/SSRL with large landed-mass payloads is possible, which dramatically changes the possibilities for mission designers and crews operating at Mars. The technical descriptions of the required element concepts and their associated technologies are described in the following sections of this report. This concept is at a technology readiness level (TRL) of TRL 2, which means that substantial work is required to advance it to a higher level. The goal of this study was to establish the architectural and technical feasibility of this concept through ideation, modeling, and analysis.

2.2 Architectural Advantages of Orbital Resource Mining and Resource Utilization

While it is possible to execute a human mission to Mars through using existing technologies and transporting the propellants through the Earth's deep gravity well all the way to the surface of Mars, a substantial penalty is paid for doing so, as the *gear ratio* for landing 1 kg of mass on Mars requires 10.5 kg to 17 kg to be launched to low Earth orbit (LEO) (Rapp, 2008). Under our approach, transporting propellants from Earth is no longer necessary in order to be able to land and launch from the surface of Mars. This results in fewer vehicles being launched from Earth and means that smaller propulsion stages are needed to reach TMI. This produces a substantial recurring cost savings (billions of dollars) and flexibility in scheduling Mars landings and launches, since the propellant does not have to be sent within a constrained launch window (every 26 months). By using the SSRL, multiple Mars launches and landings could be possible within the typical 18-month Mars visit in a conjunction-class mission. In addition, an abort to Mars orbit and operations from orbit would be possible in the event of a catastrophe on the surface.

The method for achieving this derives from harnessing local resources at Mars. NASA has considered the surface component of this approach before, in a study performed in the 2000s and published as the *Mars Design Reference Architecture 5.0* (Drake, 2010). The study considered an ISRU system that would have already been deployed on the surface of Mars, with an estimated mass of 1 t, and 400 kg of imported hydrogen. It was estimated that the surface ISRU plant could produce 25 t of O₂ for an ascent vehicle, 2 t of O₂ for crew consumption, and 133 kg of nitrogen/argon buffer gas, and as a by-product, could produce water for crew use. The power requirements were estimated to be between 24 kWe and 30 kWe.

However, because NASA Mars DRA 5.0 uses disposable landers, a large amount of mass is being transported from Earth on a 26-month cadence at each launch opportunity for a conjunction-class Mars mission. A reference mission is intended to be the best and most realistic design at the moment of release, and a baseline for future variants of it. However, the mission design's default philosophy was to maximize the number of individual expendable vehicles and components, and minimize the amount of redundancy and reusability (Strickland, 2014). In total, the architecture required approximately 850 t of initial mass in LEO (IMLEO) to enable a crew of six to visit Mars for 500 days; any future visits would have required launching another full-up package. Aerocapture was not considered to be the optimum way to enter Mars orbit, and some technologies in the area of aerodynamic decelerators have advanced to a point where this is now believed to be possible for larger payload masses. By comparison, the total mass of the International Space Station (ISS) is 420 t, which required 13 years and approximately \$100 billion to deploy in LEO. A Mars DRA 5.0 mission would cost at least as much as ISS and probably twice the amount, ~\$200 billion, based on mass equivalence, unless new methods, technologies, and business practices are implemented.

By making propellants at Mars and using them for SRP with a deployable aerobrake, it is also possible to scale up the landed mass from the 1 t that is possible today, to 20 t in the future. This would enable human missions that are not possible with existing EDL systems, such as the Mars sky crane system developed by the NASA Jet Propulsion Lab.

Our NIAC Phase I work has shown that it is feasible to use a new Mars EDL and launch system that uses not only surface ISRU (as previously proposed), but also atmospheric ISRU where O₂ is extracted from CO₂. This means that the propellant oxidizer doesn't have to be launched through the Mars gravity well for an MDAV/SSRL as proposed by others (Arney, 2010). This new Mars transportation system is made possible by purposefully infusing energy sources into the architecture. Combining the use of MHD to generate and store large amounts of electrical power in orbit with the use of fission-based power units on the surface is a key innovation that enables the energetic balance to be sustained. In Phase II, the impact of MHD power generation in excess of that needed for O₂ production will be studied as a potential means to produce fuel on the RCV and to power a hybrid MHD/solar electric propulsion (SEP) system for orbital boosting of the RCV stack. The integration of MHD in the architecture also opens the possibilities of using system components to create a magnetoshell that would serve as a reusable entry shield for the MDAV/SSRL.

Preliminary estimates indicate that the launch mass of an RCV could pay for itself in two descent/ascent missions in terms of the O₂ propellant produced. All missions after that provide net gains in O₂ propellant by avoiding the requirement for transportation of O₂ propellant from Earth or the Mars surface. Further work is needed in Phase II to work out specifics, and our team will use the following three published architectures to benchmark and compare our results:

- *Human Exploration of Mars, NASA Design Reference Architecture 5.0* (Drake, 2010)
- Jet Propulsion Lab, *A Minimal Architecture for Human Journeys to Mars* (Price, 2015)
- NASA Langley Research Center, *Sustaining Human Presence on Mars Using ISRU and a Reusable Lander* (Arney, 2015)

NIAC FY16: Mars Molniya Orbit Atmospheric Resource Mining

This NIAC Phase II proposal is a viable enabling component for the following NASA Space Technology Thrust Areas: High Performance Space Propulsion; Advanced Life Support & Resource Utilization; and Entry, Descent & Landing Systems. In addition, this proposal also meets the objectives of the following NASA roadmaps: Technology Area (TA) 02 In-Space Propulsion, TA 03 Space Power & Energy Storage, TA 07 Human Exploration Destination Systems, and TA 09 EDL Systems.

This study addresses the following NASA Mars Strategic Knowledge Gaps (SKG) identified by the Mars Exploration Program Analysis Group (MEPAG):

Relevant Mars Strategic Knowledge Gaps (SKG)	
A4	Technology to/from Mars System:
A4-1	Autonomous rendezvous and docking demo
A4-2	Optical Comm. Tech demo
A4-3	Aerocapture demo
A4-4	Auto systems tech demo
B1	Entry, Descent & Landing / Launch (EDLL)
B1-4	EDL profiles
B1-6	EDL demo
B1-7	Ascent demo
B6	Atmospheric ISRU:
B6-3	Trace gas abundances
B6-4	Lower Atmosphere
D2	Tech: Sustained Presence:
D2-1	Repeatedly land
D2-2	Sustain humans
D2-3	Reduce logistical support

3. STUDY APPROACH

In Phase I of this NIAC study, two major applications for Mars Molniya Orbit Atmospheric Mining mission architecture were studied. Both mission concepts are aligned with NASA’s top priorities for Mars exploration in the next three decades:

- a. A path for further architecture and technology development and eventual implementation is proposed by proving this technology as part of an **ISRU/Mars Sample Return (MSR) demonstration mission**.
- b. The eventual goal for this revolutionary and breakthrough space mission architecture is to enable **landing humans (4 crew) on the surface of Mars with all associated equipment** needed to allow them to survive and thrive. This will require landing very large vehicles, from 20 t to 60 t in mass. A breakthrough method is required to make this technically and economically feasible.

Other solar system destinations and related space transportation systems have been deferred to Phase II of the study. It is likely that the same orbital resource mining architecture being developed for Mars in this study could also be viable at outer Solar System destinations.

3.1 Phase I Study Work Plan

Task	Key Milestone or Accomplishment
0.0	Start NIAC Phase I project – Notice to Proceed (NTP)
1.0	Define Mars Molniya ISRU Architecture
1.1	Define Architecture & Mission Goals, Ground Rules & Assumptions
1.2	Develop Concept of Operations
1.3	Develop Requirements
1.4	Develop Arch. Concepts for trades
2.0	Assess Feasibility of Architectural Concepts
2.1	Develop Atmospheric ISRU Model (Swamp Works)
2.2	Develop Astrodynamics Model (GaTech)
2.3	Develop Magneto-Hydrodynamic Model (GaTech)
2.4	Develop Spacecraft concepts and Models (Swamp Works & GaTech)
2.5	Develop Mars Surface ISRU Model (Swamp Works)
3.0	Perform Architectural Trade Studies and Sensitivity Analysis
3.1	Integrate 2.1-2.5 Models into a Dashboard
3.2	Trade Studies of 1.4 concepts
3.3	Sensitivity Analysis of 1.4 concepts
4.0	Final Reporting
4.1	Develop a CAD concept spacecraft model
4.2	Generate concept graphics and data visualization
4.3	Write, Deliver, Present Final Phase I Report

3.2 Study Objectives

3.2.1 Objective 1: Examine Architecture Concepts

A Mars sample return mission and a human-class Mars surface mission were chosen as the two case studies because they showed a credible evolutionary path towards achieving a feasible and viable Mars campaign capability that would result in a pioneering approach to settling the Red Planet. By doing an MSR mission, all the technologies needed for a human-scale mission can be proven at a smaller scale in a mission to Mars with existing expendable launch vehicles. The resulting reduction in risk gained from the MSR paves the way for a scaled-up version of the same technologies with a higher degree of confidence. The large 100 kg sample would have compelling science value, and it would also allow us to examine hazards that are potentially harmful to humans, such as dust and perchlorates thought to be in the regolith.

In order to determine the mission element requirements, the team made a substantial effort to develop various mission architectures and associated concepts of operations. Since architectural feasibility is critical to overall concept feasibility, trades against these candidate mission architectures were performed throughout the study until the analysis revealed the best options, which we then designated as our baseline concept of operations in order to proceed with the element concept design. These concepts are discussed in Section 4.

Transportation ΔV s determined the sizing of the propellant tanks, and orbital mechanics dictated the selection of the departure point: high Earth orbit (HEO) as well as Mars capture into a highly elliptical Mars Molniya orbit and subsequent aerobraking to low Mars orbit (LMO).

3.2.2 Objective 2: Establish Feasibility of Mars Molniya Atmospheric Resource Mining

While Mars missions have been proposed and studied many times since Wernher von Braun proposed “das Marsprojekt” in 1948, the novelty of this NIAC Phase I study hinged on the feasibility of being able to scoop, compress, and capture CO₂ from the atmosphere with a spacecraft that could be launched and operated successfully within the means of existing technology. The payload was limited to 20 t landed mass since existing launch vehicles are constrained by mass and volume. Future launch vehicles may allow much larger versions; or deployable large-diameter scooping nozzles, which will be examined in Phase II, could be used.

A series of models were developed to link aerobraking with scooping and compressing gas. The nozzle diameter, mass of the Resource Collector Vehicle (RCV) stack, and orbital periapsis altitude were the critical variables that determined how many passes were required in order to make sufficient O₂ to support a landing on Mars using SRP. In addition, aerobraking is required because it greatly benefits velocity reduction through a low propellant-mass penalty. An integrated concept was developed for an SSRL that could fly with the RCV, receive O₂ from the RCV in a transfer operation through a mutual interface, and then land safely. Packaging and system design were major challenges that were overcome via computer-aided design (CAD) modeling and the use of existing blunt body physics and aerodynamics at hypersonic speeds to design a compressor cone and nozzle system. These concepts are detailed in Section 0.

3.2.3 Objective 3: Develop Systems Models and Apply Iterative Design

Once the basic feasibility of Mars Molniya Atmospheric Resource Mining had been established, the team focused on developing a series of required computer code models. A MHD model was written in Matlab to assess performance and the required configuration. MHD is at TRL 2 and has never been considered before for this type of application. Most of the issues that were encountered are doctoral-thesis-level topics that will be addressed by our team member Hisham Ali in his upcoming PhD research work at Georgia Tech. One unexpected benefit from the preliminary modeling is that we expect a large surplus of electrical power to be available on orbit.

The entry, descent, and landing sequence was simulated using the NASA Program to Optimize Simulated Trajectories II (POST2). This work was performed by Keir Gonyea, who is a graduate student with substantial expertise in running POST2. Keir and Hisham developed the RCV scooping code together in Matlab, which is able to calculate the oxidizer mass capture and MHD energy generated from atmospheric passes during the aerobraking maneuver.

The MDAV/SSRL launch mass from the Martian surface to low Mars orbit (LMO) was a critical parameter since it dictated the size of the MDAV/SSRL. An MDAV/SSRL launch code was developed in Matlab and benchmarked against Mars Ascent Vehicle (MAV) studies from the NASA Evolvable Mars Campaign (EMC) studies of 2015 and 2016. This code produced ΔV s that allowed the vehicle propellants and mass fraction to be calculated.

After the MDAV/SSRL vehicle mass and volume had been established, it was assumed that the total payload would be 20 t for a human mission, but the smaller payload for the MSR version needed to be calculated as well. The feasibility of delivering surface systems in 20 t packages was also examined.

A surface ISRU model with EMC heritage was customized to calculate the payload mass, volume, and power, which informed the MDAV/SSRL size so that the EDL and aerobraking/scooping parameters could be calculated. Details on all the modeling efforts can be found in Section 5.

By running multiple iterations of the computer models listed above, all the elements in the mission architecture were examined, traded, sized, and defined to fit into a feasible system.

The engineering challenge for the RCV and MDAV/SSRL was to create a CAD model and systems Master Equipment List (MEL) that satisfied the modeling results for scooping, SRP, surface ISRU, and Mars ascent. For example, the diameter of the nozzle was constrained by the shroud size of the launch vehicle and was also determined by the density of the atmosphere at various periapse altitudes. Another consideration was momentum exchange for compression and gas acquisition, which affected the desired RCV stack configuration and overall mass. Momentum exchange was driven by the amount of propellant needed to use the SRP for EDL of the MDAV/SSRL, which in turn was driven by the amount needed for surface ISRU and the eventual Mars launch propellant mass fraction. Many innovative ideas were incorporated, culminating in the concepts that are explained in Section 6.

3.2.4 Objective 4: Develop a Technology Roadmap

The work performed in Phase I revealed numerous technical challenges that would need to be addressed in order to use Mars Molniya Atmospheric Resource Mining in conjunction with an MDAV/SSRL at Mars. A roadmap was developed to guide future work and activities associated with this concept. The roadmap is available in Section 7.

4. MISSION ARCHITECTURE AND CONCEPTS OF OPERATION

4.1 Ground Rules and Assumptions

The overarching goal of the mission architecture—which provides context to this study—is to enable multiple landings of large payloads and crew vehicles (>20 t payloads) on the surface of Mars to sustain the long-term presence of humans on the planet. The objective achieved in Phase I was to provide a system-level technical solution toward the goal of using the acquisition of Mars atmospheric CO₂ during orbital operations and processing the CO₂ into propellant for the landing phase. Two case studies were done: one was an unmanned Mars Sample Return (MSR) and the other was a reference four-crew surface mission. The use of ISRU in orbital operations at Mars provides a potential way to obtain propellant for the EDL of large vehicles at Mars. By successfully using ISRU, we can decrease the launch mass required from Earth and contribute to the sustainability of human exploration of Mars. Ultimately, making optimal use of accessible resources within the Mars planetary system will lead to Mars missions becoming logistically independent from Earth.

Ground Rules – The team adopted the overall ground rule that the solution would leverage any assets currently in use by NASA or in development by NASA’s Exploration Systems Development (ESD) Division for the Evolvable Mars Campaign and other campaign architectures, as well as those developed by academic institutions and private space companies whose aim is to land large vehicles on Mars. New concepts and systems were developed to meet the NIAC Phase I objective. This ground rule aims at maximizing compatibility of the mission concept with existing NASA assets and engage participation of non-NASA developers and stakeholders.

The scope of the Phase I NIAC mission concept was focused on the operations in the Mars system that enable four crew members to descend to the Mars surface, ascend from the Mars surface, and rendezvous with an Earth-Mars transportation system. This focus enabled us to study solutions based on new paradigms in the Mars system while adopting reasonable assumptions for the architecture of the system for transportation from Earth launch to arrival in the vicinity of Mars. Robotic precursor missions such as MSR were included to test capabilities and validate technologies at the destination before launching a crew in order to reduce the risk in reliance on these systems.

Assumptions – The mission architecture is founded on the following assumptions.

The current NASA Mars timeline for sending humans to Mars system and return them safely to Earth by the mid-2030s was adopted. It is based on the 2010 National Space Policy of the United

States of America. In Phase II, we intend to perform a timeline trade with the use of SpaceX Red Dragon-based mission architecture if enough data can be obtained on this system.

The Space Launch System is used as the baseline for Earth launches with cadences adopted by EMC studies: 1 per year from 2021 through 2027, then 2 per year starting in 2028. The transition between the 105 t payload capability of SLS Block 1B to the 130 t capability of SLS Block 2B is assumed to be set for 2028. In Phase II, we propose to examine the potential use of other heavy-lift launch vehicles for transporting cargo and unmanned spacecraft to the Mars system.

The launch vehicle stacks for the Mars missions will be assembled in HEO for rendezvous with the crew vehicles and additional required elements (e.g., limited life in-space propulsion orbital elements) based on EMC studies showing that HEO is an appropriate location for departure and return in an efficient trans-Mars injection orbit.

Our mission architecture uses Orion, the vehicle that NASA plans to use for performing tasks such as delivering a crew from Earth to the HEO staging area and returning the crew from the staging area to Earth at mission end. Because Orion was selected for such tasks independent of architecture or trajectory, in Phase II we intend to perform a system trade with commercial or partner crew excursion vehicles (e.g., SpaceX), if enough data is available, to verify that this is the optimal selection for this specific mission architecture.

The in-space transportation system used for crew travel between Earth and Mars will be based on chemical propulsion to reduce the transit time for crew and make in-space transportation compatible with emerging concepts of propellant depots in the Earth-Moon system. Only conjunction-class trajectories between Earth and Mars are considered, and a maximum round-trip duration of 1100 days is assumed, including a 300-day surface stay. In Phase II, we intend to perform a system trade between chemical propulsion, solar-electric propulsion, and nuclear propulsion from Earth to Mars to assess costs, development timelines, and synergistic impacts on the architecture.

In the Mars vicinity, the architecture will use a Mars 1-Sol orbit ($\sim 250 \times 33,000$ km) as a waypoint in route to other orbital and surface destinations because it supports arrivals and departures for Earth-Mars trajectories. Low Mars orbit (LMO) is defined as a 250 km circular orbit. In Phase II, we intend to trade the 1-Sol option with 5-Sol orbits ($\sim 200 \times 60,000$ km) for timeline efficiency and overall capability. A single long-duration surface site located within $\pm 30^\circ$ of the Martian equator will be targeted so that the infrastructure required for a sustained human presence can be efficiently put into place. The delivered infrastructure will include modular 10 kWe nuclear power systems for continuous high-specific power generation.

4.1.1 Mission Design/ConOps

The concepts of operation for trade studies have been developed as follows:

- a. ISRU/Mars Sample Return demonstration mission – 100 kg delivered to Earth
 - (1) All propellants are brought from Earth – reference case without ISRU

NIAC FY16: Mars Molniya Orbit Atmospheric Resource Mining

- (2) Mars surface ISRU is used to make propellants for an expendable Mars Ascent Vehicle (MAV) – no orbital atmospheric mining is used. Supersonic retropropulsion (SRP) is proven while landing the ISRU equipment and MAV.
 - (3) Mars Molniya Orbit Atmospheric Mining is used (and proven) to acquire carbon dioxide and make oxygen for SRP lander propulsion, and surface ISRU is used to make propellants for the MAV.
- b. Mission architecture for landing human crews on the surface of Mars
- (1) All propellants are brought from Earth – reference case without ISRU
 - (2) Mars surface ISRU is used to make propellants for a reusable MDAV/SSRL – no orbital atmospheric mining is used.
 - (3) Mars Molniya Orbit Atmospheric Mining is used to acquire carbon dioxide and make oxygen for lander propulsion, and surface ISRU is used to make propellants (LO₂/ CH₄) for the MDAV/SSRL. The MDAV/SSRL carries enough CH₄ fuel into orbit to enable landing on Mars again from a high Mars orbit (HMO) – which has a period of 1 Sol and is a highly elliptical orbit.

4.1.2 ConOps

4.1.2.1 Mission Architecture Elements

**Mars Sample Return
Architecture Elements**



◆ SLS.....
(100 t to LEO)



◆ Evolved Expendable Launch Vehicle (EELV).....
(30 t to LEO)



◆ Science payload.....



◆ Surface Power Plant (SPP) & ISRU Cargo



◆ Cryogenic Propulsion Stage (CPS)



◆ Crew Orbital Vehicle (COV)



◆ Mars Transit Cryogenic Stage (MTCS).....



◆ Mars Cargo Lander (MCL).....



◆ Robotic Precursor Small Cargo Lander (RPSCL)...



◆ Resource Capture Vehicle (RCV)



◆ Sample Collection Rover (SCR).....



Figure 3. Mars sample mission architecture elements.

Human Mars Mission Architecture Elements



- ◆ SLS
(105 t – 130 t to LEO) 
- ◆ Surface Power Plant (SPP) & ISRU Cargo 
- ◆ Cryogenic Propulsion Stage (CPS) 
- ◆ Crew Transit Vehicle CTV (MTCS + DSH) 
- ◆ Crew Orbital Vehicle (COV) & Service Module (SM) 
- ◆ Deep Space Hab (DSH) 
- ◆ Mars Transit Cryogenic Stage (MTCS)..... 
- ◆ Mars Cargo Lander (MCL) 
- ◆ Mars Descent & Ascent Vehicle (MDAV) 
- ◆ Resource Capture Vehicle (RCV) 
- ◆ Solar Electric Propulsion (SEP) 

Figure 4. Human Mars mission architecture elements.

4.1.2.2 Sample Return Mission

Reference Case 3: Mars Sample Return & Tech Demo
Earth Departure – Chemical Propulsion

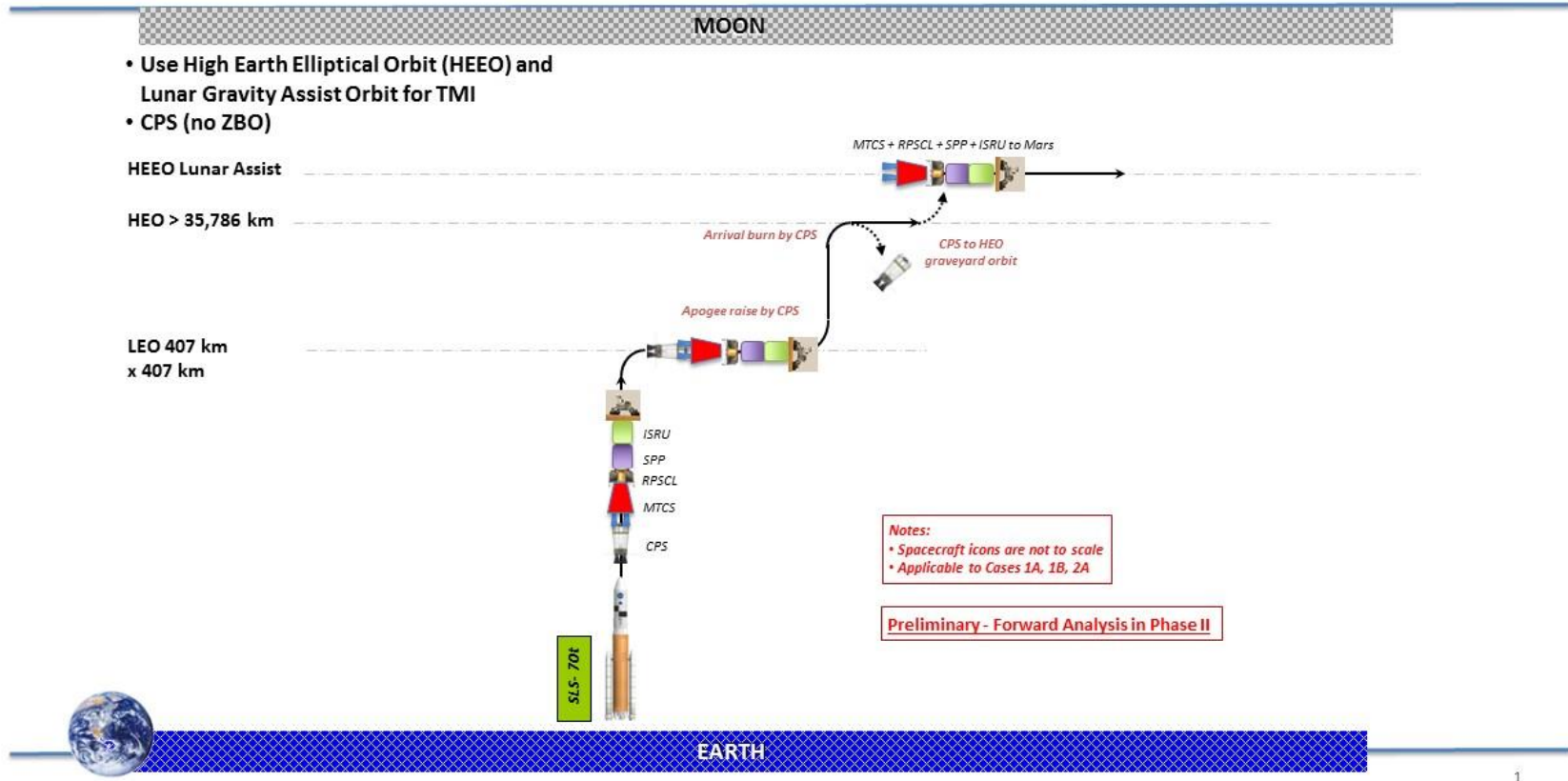


Figure 5. Mars Sample Return mission – Earth departure, chemical propulsion.

Reference Case 3: Mars Sample Return & Tech Demo
 Mars Molniya Orbital Mining (MMOM) Enabled, Surface ISRU

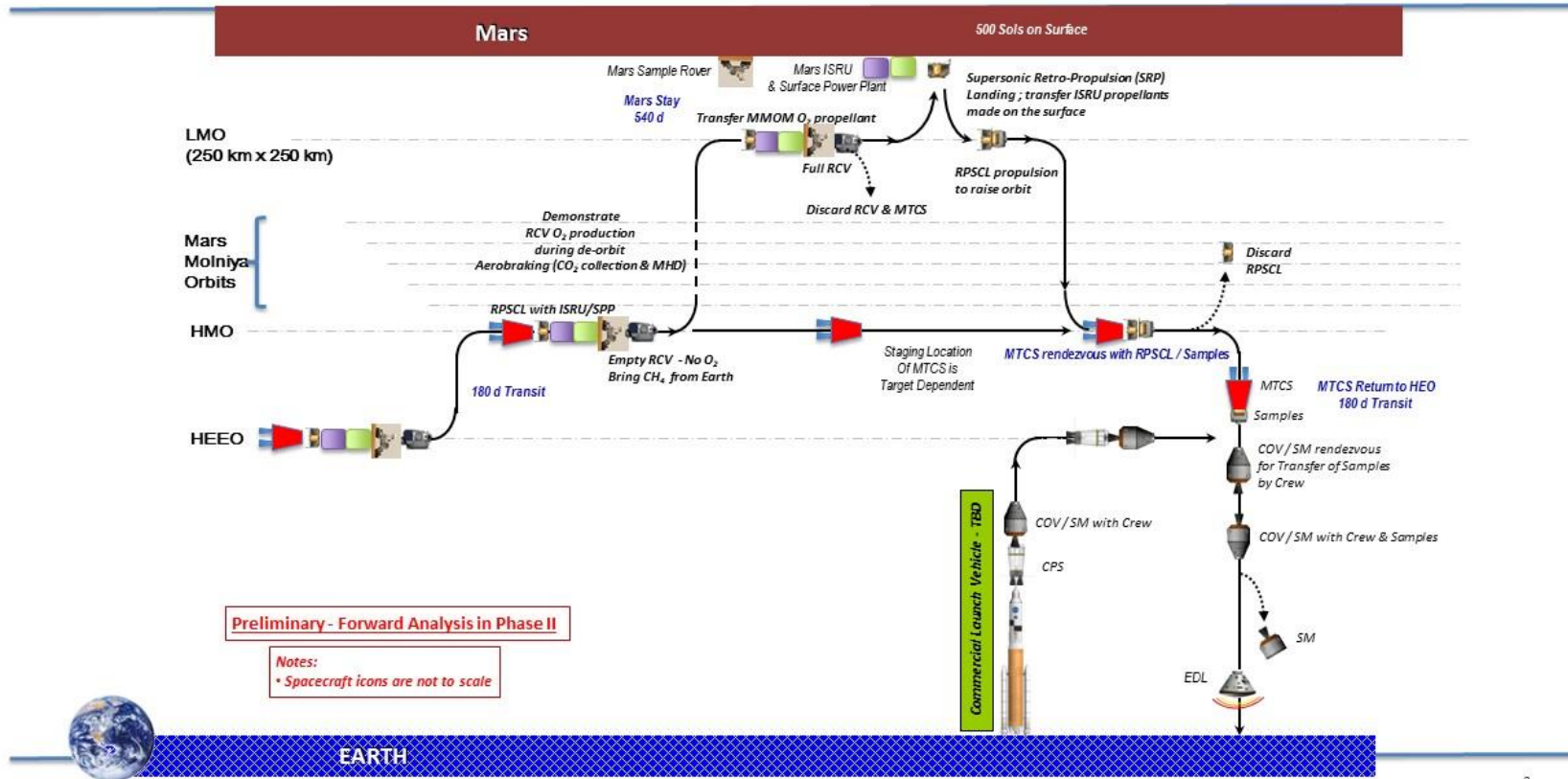
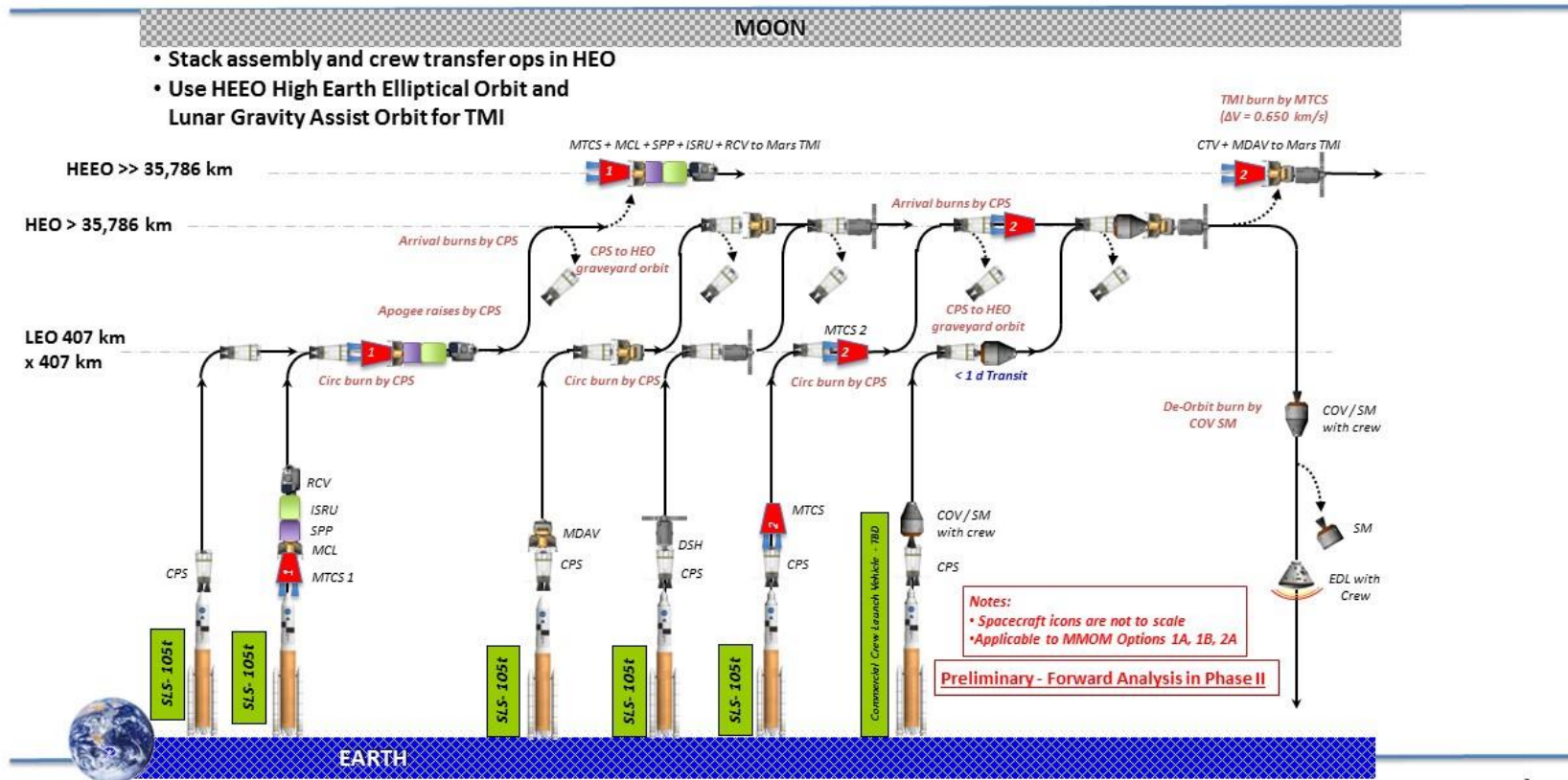


Figure 6. Mars Sample Return – MMOM and surface ISRU.

4.1.2.3 Human-Crewed Mission to Mars

Reference Case 3a: Mars Crewed Mission (Baseline)
 Earth Departure – Chemical Propulsion Option, MMOM-Enabled



3

Figure 7. Mars Crewed Mission reference case concept of operations – Earth departure phase.

NIAC FY17: Mars Molniya Orbit Atmospheric Resource Mining

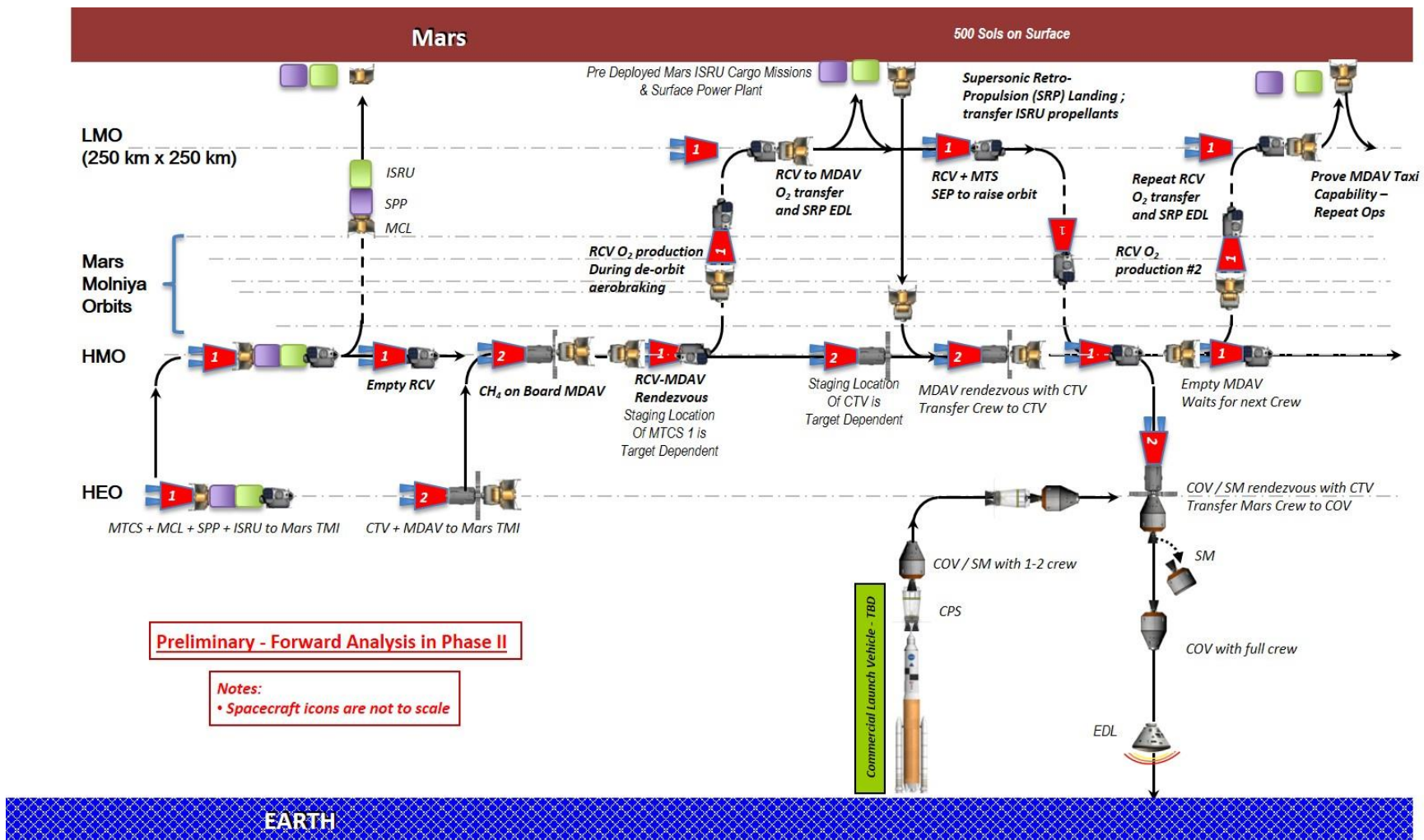


Figure 8. Mars Crewed Mission – Mars ops, surface ISRU, MMOM, RCV+MDAV docked.during Aerobraking/Scoping

NIAC FY17: Mars Molniya Orbit Atmospheric Resource Mining

The masses in Table 1 were used to inform the reference case concepts of operations shown in Figure 5 through Figure 8, based on parametric design, analysis, NASA missions, studies, and reference papers.

Table 1. Elements, mass, and origins for the Mars Molniya Atmospheric Resource Mining Architecture.

Element	Mass (t)	Notes
CPS – Cryogenic Propulsion Stage	10	Dry mass, parametric design
CTV – Crew Transit Vehicle (MTCS + DSH)	47	Dry mass, EMC
MDAV/SSRL	22	MCL with crew cabin, parametric design, Ref: Hercules
COV with SM	25.8	EMC/Orion
DSH – Deep Space Habitat	43	EMC
MTCS – Mars Transit Cryogenic Stage	4	Dry mass, parametric design
MCL – Mars Cargo Lander	18.1	Ref: Hercules Lander (Arney et al.)
SPP – Surface Power Plant, 10 kWe unit	1.5	EMC
ISRU – 1 module	0.6	EMC
SP – Science Payload	0.1	MSR mission
RPSCL – Robotic Precursor Small Cargo Lander	1.9	MSR mission
RCV – Resource Collector Vehicle stack (Human)	84	RCV+MDAV+MTCS dry mass
RCV – Resource Collector Vehicle (Human)	58	Dry mass, atm. mining model
RCV – Resource Collector Vehicle stack (MSR)	21	RCV+ RPSCL+Payload dry mass
RCV – Resource Collector Vehicle (MSR)	12.4	Dry mass, atm. mining model
SCR – Sample Collection Rover	1	MSR mission
COV SM – Service Module	15.5	EMC/Orion
Mars Samples	0.1	MSR mission
Total Payload RPSCL	6.4	MSR mission

5. ANALYSIS METHODS AND MODELING

This section explains the analytic computer models that were developed according to our work plan. The modeling and associated results are described in detail below. The work was divided between all the team members by subject matter expertise. The advanced nature of this work benefited greatly from the government and academic alliance that was formed between NASA and Georgia Tech graduate researchers. Engineering simulations based on physics principals, in addition to proven NASA computer models, were used to ensure an accurate assessment of the component performance within the uncertainty of the low TRL level. The emphasis was on determining the critical variables, their relationships, sensitivity, and ultimately, the feasibility of the concept. Closing the mission case for an MDAV/SSRL using ISRU on orbit and on the surface was the primary goal of Phase I. Other orbital resource mining applications and simulations were deferred to Phase II.

5.1 Astrodynamics Model

The astrodynamics of all architectural spacecraft was modeled by using fundamental physics equations modeled in Matlab. The fundamental laws of astrodynamics—Newton’s law of universal gravitation, Newton’s laws of motion, and Kepler’s laws—were used to determine the required change in velocity (ΔV) while Tsiolkovsky’s rocket equation was used to determine propellant masses required. Subsequently, parametric modeling with typical existing spacecraft mass fractions (80%–90% propellant) was used to determine the propulsive stages estimated masses. This data was then used to inform our mission architecture concepts of operations (ConOps), including generating launch vehicle payload stacks and launch manifests. The calculated ΔV is summarized in Table 2 for each mission segment.

Table 2. Results of astrodynamics analysis.

Mission Segment	ΔV (km/s)	Propellant Required (t) per event	Notes
LEO to HEO	2.46	29-94	CPS H ₂ /O ₂ , Highly Elliptical Orbit 407 × >40,000 km
Dock Elements	0.1	1.2	CH ₄ /O ₂
TMI	0.65	17.2	CH ₄ /O ₂ , Depart from HEO, TMI burn at perigee
Mars Aerocapture	0.9	Negligible – Aerocapture	Heat Shield RCV & MDAV/SSRL
Mars Aerobraking	1.3	Negligible – Aerobrake	Heat Shield RCV
Raise Periapsis	0.01	Negligible	Raise orbit out of atmosphere
Mars EDL & SRP	4.0	8.5	SSRL Aero decel. & CH ₄ /O ₂ SRP
Mars Ascent to LMO	4.2	110.9	CH ₄ /O ₂ , MDAV + CH ₄ for EDL
Mars LMO to HMO	1.32	11.3	CH ₄ /O ₂ , MDAV + CH ₄ for EDL
TEI	1.45	21.9	CH ₄ /O ₂
Earth Capture to HEO	0.80	10.9	CH ₄ /O ₂
Dock with CTV	0.1	1.2	CH ₄ /O ₂
HEO orient and burn for EDL	.092	0.7	Orion

The launch-to-LMO mission segment required special attention due to various parameters that are unique to Mars, and it was benchmarked against work done by NASA in Mars DRA 5.0, the Evolvable Mars Campaign (EMC) at Marshall Space Flight Center (MSFC) and available literature (Arney et al., 2015).

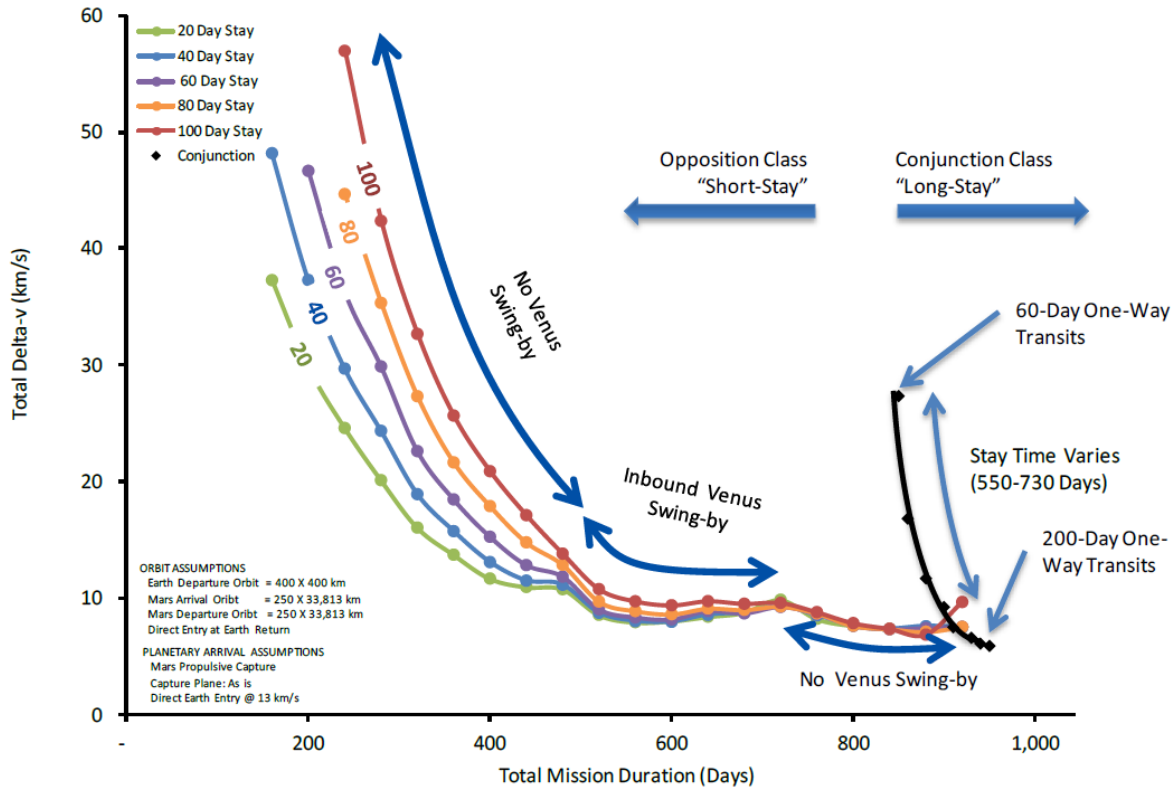


Figure 9. Example round trip ΔV as a function of total mission duration. (Source: NASA DRA 5.0)

There are many ways to travel to Mars, but as shown in Figure 9, a ΔV penalty must be paid for decreasing the total mission duration from the period given in the NASA Mars DRA 5.0 study.

Most studies for human missions have concluded that two options are viable for human spaceflight to Mars: opposition-class missions and conjunction-class missions (see Figure 10).

NIAC FY16: Mars Molniya Orbit Atmospheric Resource Mining

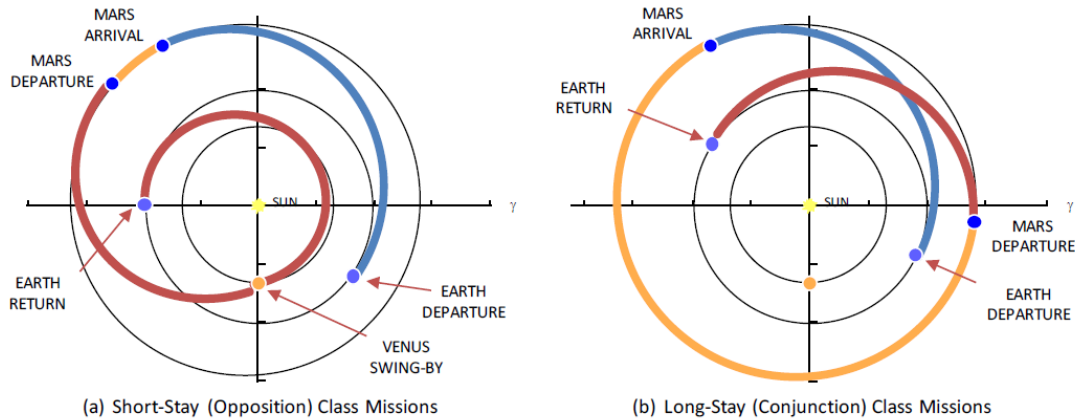


Figure 10. Representative mission profiles for the major classes for human Mars missions. (Source: NASA Mars DRA 5.0)

A conjunction-class Mars mission was assumed since the goal of this NIAC Mars mission architecture is to enable a human pioneering campaign for the settlement of Mars. The conjunction-class mission provides longer surface stays and shorter flight times than the alternative opposition-class mission typically considered in Mars studies (see Figure 11).

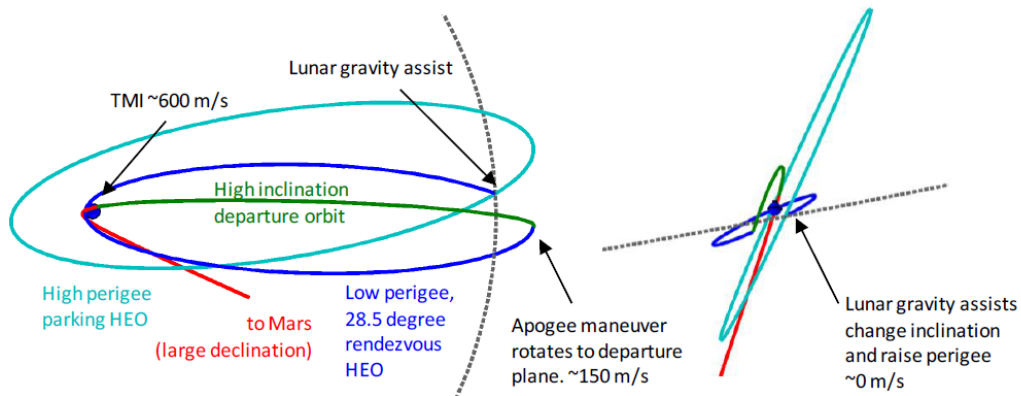


Figure 11. Lunar gravity assists and maneuvers near apogee shape HEO for efficient departures (source: NASA DRA 5.0).

The purpose of this NIAC study was to investigate the orbital resource mining at Mars, so the transportation to Mars was selected by referencing Mars DRA 5.0 which states:

High-Earth orbit is characterized by a low perigee at a few hundred kilometers altitude and an apogee that crosses lunar orbit, resulting in an eccentric 10- to 14-day period orbit. This orbit spends at most 1% of the time passing through the van Allen belts. Should this belt passage prove to be unacceptable, the perigee can be raised above the belts for approximately 300 m/s or via lunar gravity assist for negligible Delta-V. In contrast to the L2 and high-lunar orbit staging nodes, the inclination of the staging orbit is constrained by the inclination of the launch orbit. Ideally, HEO would have a 28.5

degree inclination for launches from Florida, or 51.6 degrees for transfers from Space Station orbit. (Though transfers from the Space Station itself add an extra constraint on HEO to match the node of the station's orbit.) However, Earth-Mars transfers with large declinations (e.g., 2033) are expensive to reach when the inclination is less than the (absolute magnitude of) declination. An efficient method to overcome this limitation is to rotate the orbit along the line of apsides (the "apo-twist" maneuver⁴) into a plane that shares the departure asymptote. An example sequence is depicted in [Figure 12]. High departure declinations may be achieved propulsively from HEO, whereas these declinations are more easily achieved via the Moon's gravity for the L2 and high-lunar orbit locations (Drake, 2014).

By using the analysis previously done by NASA in Mars DRA 5.0, this study concluded that a good average value for TMI ΔV is 650 m/s as shown in the figures below. Since this study uses aerocapture and subsequent aerobraking, propulsive ΔV for Mars capture is not included.

Mars aerocapture results in large propellant savings because atmospheric drag is used to perform over 95% of the orbit insertion ΔV . This allows the use of smaller, less expensive launch vehicles, faster travel times, or increased payloads, but it requires the addition of heat shields. In Phase II, we will trade aerocapture at Mars vs. propulsive capture to determine the net benefit on a human-mission scale. Since our RCV stack and the MDAV/SSRL both have heat shields, this may be possible.

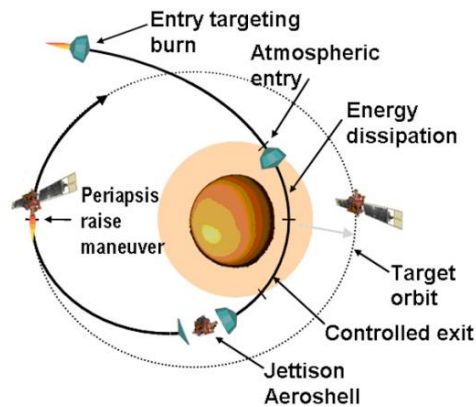


Figure 12. The aerocapture maneuver is accomplished in a single atmospheric pass to eliminate propellant. (Image: NASA)

The NASA DRA 5.0 architecture studies showed that aerocapture is of high value to a human Mars architecture. Approximately 200 t IMLEO was avoided in that study by using aerocapture, which provides a significant cost, risk, and logistics savings.

NIAC FY16: Mars Molniya Orbit Atmospheric Resource Mining

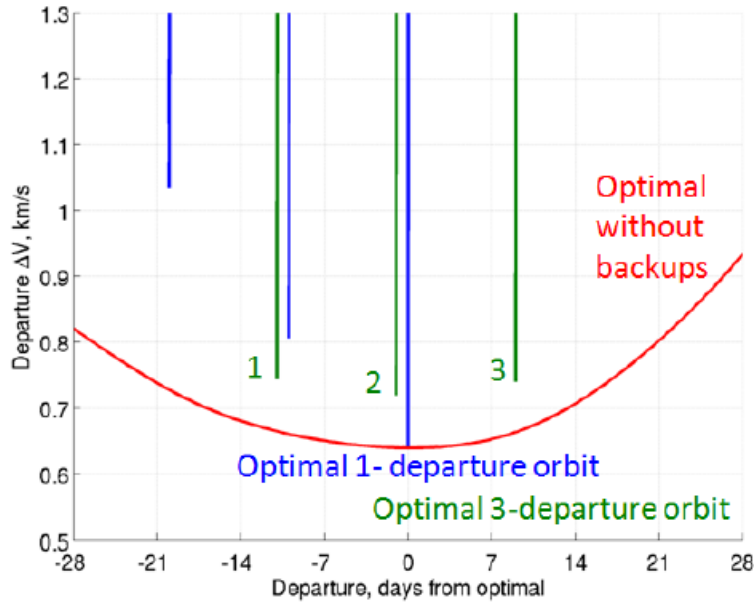


Figure 13. 2035 Mars departure opportunity. (Source: NASA DRA 5.0)

Table 3. Departure scenario considerations for human missions to Mars. (Source: NASA DRA 5.0)

Aggregation Location	L ₂ Halo	Lunar Orbit	10-d HEO	Low Earth Orbit
Crew to rend. location (from LEO)	3450 m/s, 8 d	3300 m/s, 4 d	3100 m/s, 1 d	0 m/s, 0 d
Departure 2033 (51.6 deg LEO)	1050-1200 m/s	900-1200 m/s	600-650 m/s	3600 m/s
Departure 2033 (28.5 deg LEO)	1050-1200 m/s	900-1200 m/s	750-850 m/s	3750-3800 m/s
Departure 2035 (28.5 deg LEO)	1000-1300 m/s	900-1300 m/s	650-750 m/s	3650-3950 m/s
Total DV through TMI	4450-4750 m/s	4200-4600 m/s	3650-3950 m/s	3600-3950 m/s
Trans-Mars Departure Window Length # TMI Opportunities	3-4 days 1-2 Opportunities	2.5-3.5 days 1-2 Opportunities	20 days 1-3 Opportunities	For Dec=Inc (e.g. 2033) 5-10 days, 75-100 opp. For Dec<Inc. (e.g. 2035) 0-56 days, 1-2 opp.
Crew Critical Maneuvers	Depart LEO Lunar Flyby Out/In L2 Halo Arr./Dep. TMI	Depart LEO Lunar orbit arrival Lunar orbit departure TMI	Depart LEO HEO arrival TMI	LEO arrival TMI
Crew Contingency Return	350 m/s, 8 d	200 m/s, 4 d	<25 m/s, 4 d	100 m/s, 0 d

The NASA DRA 5.0, Addendum 2 study also states:

When considering the overall magnitude, number, and timing of escape maneuvers, L2 and high-lunar orbit are very similar both energetically and operationally. High-Earth orbit requires less ΔV and few maneuvers, but the maneuver timing is driven by perigee passages. High-Earth orbit provides additional versatility with a wide range of

inclinations, periods, and perigees that are achievable via lunar gravity assists. Backup opportunities for trans-Mars injection are available for any of the departure options with an intermediate high-Earth orbit. Low-Earth orbit is distinct from other options because it has no intermediate staging node, and requires fewer maneuvers to depart. Indirect departures with large declinations to Mars are available via a reorientation maneuver at apogee on an intermediate HEO. Departures from LEO generally require the lowest ΔV , but could require more mass if efficiencies such as solar electric propulsion and deep-space-vehicle reuse are available with the other staging locations (Drake, 2014).

5.2 Mars Atmospheric Resource Mining Model

5.2.1 Aerobraking and Atmospheric Resource Mining Simulation Algorithm

An aerobraking simulation was developed to assess the effects of the Resource Collector Vehicle (RCV) design on the oxidizer ingestion during the aerobraking campaign. This simulation, along with the EDL and ISRU simulations, was used to determine closure of the overall vehicle architecture.

The aerobraking simulation is composed of two parts, an atmospheric trajectory calculator that determines the state parameters during a single pass through the atmosphere and a wrapper function which propagates and tabulates the orbit and vehicle state between successive passes, starting from the initial highly elliptical orbit and ending with the circular parking orbit.

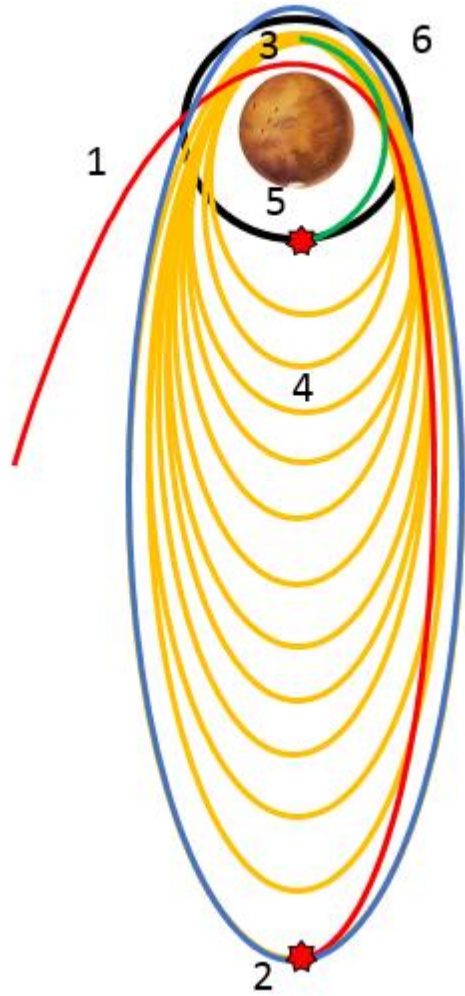
For a given atmospheric periapsis target, which is assumed to be constant for each pass, and atmospheric interface altitude, a geometric trajectory was constructed in order to determine the average altitude during the atmospheric pass. This geometric trajectory started at the atmospheric interface, passed through the periapsis altitude at its closest approach, and proceeded symmetrically back to the atmospheric interface altitude. The approximate average pass altitude and distance traveled during the pass were determined from the trajectory. The calculation of the approximate average altitude and distance traveled therefore neglected the effects of drag and changing inertia throughout the pass. A second calculation was performed to determine the minimum velocity necessary at the periapsis altitude to attain the final circular orbit altitude. These two parameters were used in the atmospheric trajectory calculator and trajectory propagating functions.

The atmospheric trajectory calculator assumes that the entire pass occurs at the average altitude and with a constant vehicle state. Therefore, all atmospheric parameters, vehicle mass, and vehicle velocity are constant throughout the maneuver. The CO₂ mass flux, MHD power generated, and drag force are all determined by the average altitude, and vehicle and entry state and are integrated based on the atmospheric pass distance to determine total CO₂ ingestion mass, MHD energy available, and change in velocity. The trajectory propagator takes the output from the atmospheric trajectory calculator and applies the vehicle and trajectory state updates, including the added vehicle mass and reduction in velocity, approximating the pass as occurring instantaneously at the trajectory periapsis. The subsequent orbit is calculated based on the updated velocity and the trajectory is propagated to the next pass. When the updated periapsis velocity drops below the velocity required to reach the terminal circular orbit, the simulation

stops. Total CO₂ capture is converted to equivalent oxidizer capture based on the overall conversion efficiency of 20% by mass. Total MHD energy stored is based on the MHD power profile and the battery storage system power and energy density.

Table 4. Mars atmospheric scooping concept of operations.

Mission Phase	Action
1. RCV stack enters initial orbit	Systems checkout; initial aerobrake orbit entered.
2. Periapsis-lowering burn	Use thruster to lower periapsis to target altitude.
3. Scooping drag near periapsis	With each pass through the atmosphere, the scooping drag reduces the orbit energy and lowers the orbit apoapsis.
4. Apoapsis burns to control periapsis	Apoapsis burns will be made as necessary to adjust periapsis altitude to counter secular orbit disturbances and maintain periapsis altitude within the target window (~79 km).
5. Periapsis-raising burns	As the apoapsis altitude nears the desired level, several apoapsis burns will raise the periapsis out of the atmosphere, therefore stopping the aerobraking (~250 km).
6. Final circular orbit	Thruster burns will now set the RCV stack at the desired orbital parameters (250 km × 250 km).



5.2.2 Mars Sample Return Mission RCV Modeling Parameters

Table 5. MSR RCV parameters calculated from Mars Atmospheric Resource Mining Model.

Parameter	Value	Notes
Aerobraking target altitude (h_periapsis)	80 km	Optimized to enable max CO ₂ ingestion
Inlet area (A _{in})	24 m ²	Adjusted to meet oxidizer ingestion requirements
RCV stack mass (mVeh)	21 t	Based on sizing requirements of vehicle and subsystems, also adjusted to meet ingestion requirements
Hypersonic drag coefficient (C _d)	1.6	Based on heritage data
RCV diameter (Dia)	5.5 m	Based on subsystem packaging requirements and rocket shroud packaging requirements
Atmospheric interface altitude (h _{atm})	120 km	Standard value used in Mars EDL modeling

5.2.3 Human Mars Mission RCV Modeling Parameters

Table 6. Human mission RCV parameters calculated from Mars Atmospheric Resource Mining Model.

Parameter	Value	Description
Aerobraking target altitude (h_periapsis)	79 km	Optimized to enable max CO ₂ ingestion
Inlet area (A _{in})	80 m ²	Adjusted to meet oxidizer ingestion requirements
RCV stack mass (mVeh)	84 t	Based on sizing requirements of vehicle and subsystems, also adjusted to meet ingestion requirements
Hypersonic drag coefficient (C _d)	1.6	Based on heritage data
RCV diameter (Dia)	10 m	Based on subsystem packaging requirements and rocket shroud packaging requirements
Atmospheric interface altitude (h _{atm})	120 km	Standard value used in Mars EDL modeling

5.2.4 Assumptions

The following assumptions were used for the modeling algorithm:

- a. Passes behave as discrete events.
- b. Atmospheric pass parameters calculated are based on the average aerobraking altitude; all are constant during a single pass.
- c. Average aerobraking altitude calculations are based on a symmetric entry/exit profile (no deceleration during pass).
- d. All atmospheric pass effects are calculated, summed, and applied instantaneously at the orbit periapsis.
- e. Start is in a highly elliptic orbit.
- f. End is in a circular orbit.
- g. 20% efficiency converting mass CO₂ to mass O₂
- h. Atmosphere model: MarsGRAM at median density state
<https://software.nasa.gov/software/MFS-33158-1>
- i. Initial orbit:
250 km altitude (periapsis) × 33,793 km altitude (apoapsis)
- j. Final orbit:
250 km altitude, circular

5.2.5 Algorithm Characteristics

All parameter updates (velocity, CO₂ mass ingested, vehicle mass, MHD energy stored) are assumed to act instantaneously at the periapsis altitude, and subsequent orbit is determined based on new velocity. When subsequent periapsis velocity after the pass is less than the required velocity for the circular orbit, integration is stopped at the previous iteration.

The total atmospheric CO₂ oxidizer feedstock capture mass is determined based on 20% conversion efficiency of CO₂ ingestion mass as calculated by using SOE chemistry and a multiplicative efficiency stack up. The MHD energy storage battery mass and percent energy storage is determined based on MHD power profile and energy/power density of different storage options.

5.2.6 Discussion

Many simulation parameters are a function of the initial and final orbits and, as a result, are fixed. Analysis indicated that four parameters primarily affect the oxidizer ingestion: *the periapsis altitude, inlet area of scooping nozzle, RCV total mass, and RCV diameter.*

Through various studies and iterative modeling, the inlet area was found to be the dominant factor contributing to oxidizer acquisition and storage capability. This was found to be true as

long as the inlet diameter is less than the vehicle diameter; however, for an inlet area greater than the vehicle diameter, the increased drag (and shorter trajectory) negates instantaneous collection benefits. This also was linked to a constraint imposed by the diameter of the launch vehicle shroud. For this study, a maximum heavy-lift launch vehicle diameter of 10 meters (m) was assumed, which coincided with optimal atmospheric scooping characteristics. Some concepts under consideration had inflatable scooping nozzles that exceeded a 10 m RCV bus diameter, but the modeling indicated that this was not desirable because of excessive drag.

If the inlet area and the RCV bus diameter are jointly varied, it does not significantly impact oxidizer ingestion because the improved collection is balanced by increased drag. The RCV bus diameter is limited on the low end by subsystem packaging and on the high end by packaging in a launch vehicle fairing.

The periapsis altitude of the Molniya orbital resource mining scooping passes has the following effects on ingested CO₂:

- a. A higher altitude results in less drag and increased number of passes.
- b. A lower altitude results in higher atmospheric density and more CO₂ oxidizer feedstock collected per pass.
- c. These competing effects result in the existence of an altitude of maximum collection potential.

The RCV stack mass affects CO₂ ingestion because of the effects of momentum transfer: A higher stack mass decreases deceleration because of atmospheric drag and CO₂ ingestion and allows for a longer trajectory through the atmosphere.

For the MSR case, the RPSCL lander required the production of 1.78 t of O₂, which meant that, with efficiency considerations, 8.76 t of CO₂ would have to be ingested during the scooping passes through the atmosphere. The periapsis of the decaying elliptical orbits was set at 80 km altitude for optimum atmospheric density, and a periapsis raise maneuver resulted in a 250 km × 250 km circular LMO staging orbit prior to EDL. The RCV stack in the MSR case consisted of the RPSCL, ISRU, SPP, SCR, and RCV weighing 21 t, which was required for atmospheric momentum exchange for scooping and compression of the atmospheric gases.

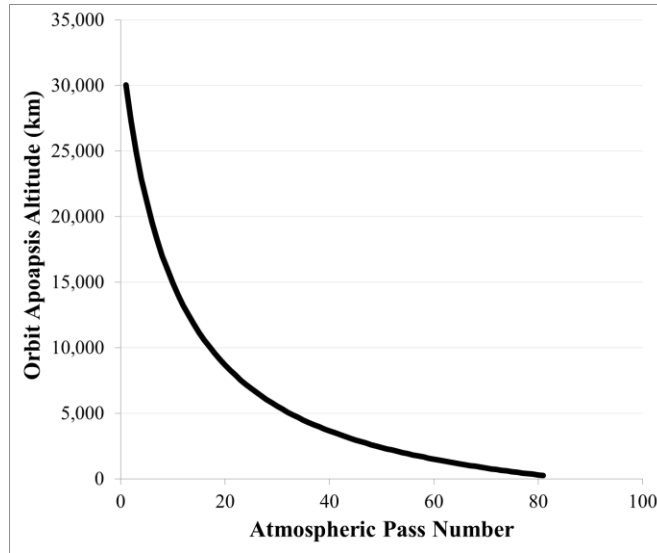


Figure 14. Decaying elliptical orbits during aerobraking maneuver. (Target is a final altitude of 250 km.)

The modeling and simulation results were also used to determine the configuration and design of the human mission RCV stack element concepts. The RCV stack consists of the RCV, MDAV/SSRL, and MTCS stages. Although the team initially tried to reduce the size of the stack in an alternative ConOps, the modeling indicated that a higher mass was needed to achieve efficient momentum exchange. As a result, the MDAV/SSRL and MTCS are not demated prior to orbital scooping passes. Higher mass can also be achieved by putting more electrical storage capacity on board, which provides a convenient and useful variable for achieving any required RCV stack mass. This stack scooping method provides several benefits, including eliminating separate MDAV/SSRL aerobraking, and avoiding a rendezvous and docking operation between the RCV and the MDAV/SSRL in circular Mars orbit. The O₂ that is made on orbit can be directly transferred from the mated RCV to the MDAV/SSRL prior to separation for EDL.

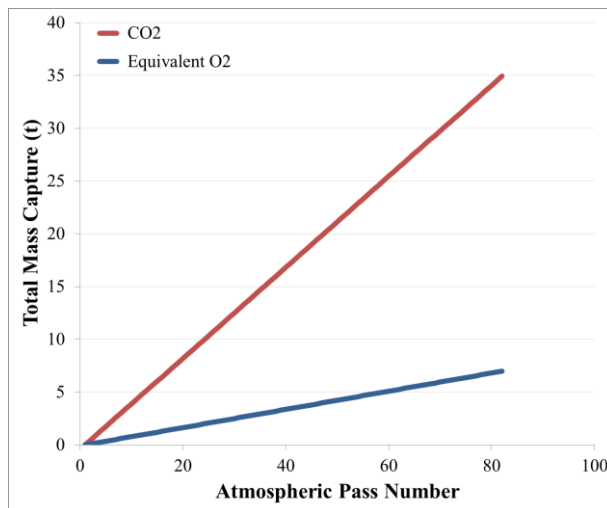


Figure 15. Mars orbital resource mining capability.

After 80 periapsis scooping passes, the full-scale human mission version of the RCV has captured ~35 t of CO₂, which will then be processed via SOE in circular LMO to produce ~7 t of O₂ for EDL propulsion use.

A risk that must be considered is the seasonal fluctuations and overall uncertainty in the Mars atmosphere. These variations are attributed to many factors, including dust storms and other weather phenomena, and may cause unexpected conditions that must be compensated for. Our team used the state-of-the-art Mars atmosphere database (MarsGRAM), which has been used by NASA when designing Mars missions, to best account for these considerations in the scooping calculations.

5.2.7 Mars Atmospheric Orbital ISRU Model

One of the primary innovations of this NIAC concept is that it features the production of O₂ on orbit to be used as oxidizer by the SSRL vehicle during its EDL phase to the Mars surface under supersonic retropropulsion (SRP). This production is made possible by capturing atmospheric CO₂ via ram compression during successive orbital flight passes in the upper Martian atmosphere between the altitudes of 120 km (entry point) and 80 km (periapsis.) The acquired gas feedstock can be processed into O₂ on board the RCV by a limited number of chemical methods applicable according to the availability of certain reagents, and an energy source. Thermochemical splitting of CO₂ (thermolysis) was considered since the following simple reaction (Equation 1) can be potentially performed by concentrated sunlight, which can be obtained readily in space operations.

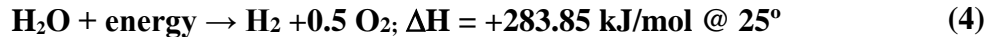


Potentially, the CO produced can be used to produce hydrogen (H₂) as another rocket engine fuel by steam reforming as follows:



with the forward reaction being exothermic ($\Delta H = -41$ kJ/mol) when water is available on board. However, water is a precious commodity during space travel supporting life of the crew and possibly providing radiation shielding. It is possible to use a portion of this water at the end of the Earth-Mars journey but it requires its transport from Earth at great cost and would only apply to crew missions since robotic missions would not require it on board. Practical engineering constraints led to downgrading this technique in our trade studies; state-of-the-art CO₂ thermolysis (Equation 1) proceeds at ultra-high temperatures in excess of 1000 °C and requires metal oxide substrates such as ferrite stabilized by a high-temperature ceramic matrix such as zirconia or yttria-stabilized zirconia (YSZ), (Miller, 2009). These substrates operate as oxygen absorbers when O₂ saturates the material to its fully oxidized state. This scheme devised for the production of CO rather than O₂ is impractical in our case since it sequesters O₂ in a solid-state matrix, which we require to use as rocket engine oxidizer.

The well-known Sabatier reaction is another possibility, which requires available H₂ to react with CO₂ as follows, then electrolyze the water to obtain O₂:



The hydrogen produced is then recycled in the methanation reaction (Equation 3).

The use of the Sabatier process is attractive since it produces both CH₄ fuel as well as O₂ oxidizer on orbit for the SRP engines of the lander but the requirement to import H₂, and the additional complexity and required system mass to store and transfer it resulted in a lower rating in our trade study analysis. In this study, it was concluded that O₂ could be made on orbit by solid oxide electrolysis (SOE), but CH₄ has to be made on the Mars surface and brought to orbit for EDL propulsion with an SSRL. Fortunately, the rocket engines currently planned to be used within NASA and by others have an O₂:CH₄ mass ratio of 3.5:1 so that only 22% of the total EDL SSRP propellant must be launched from the surface to orbit, thereby reducing the size and mass of the SSRL substantially when using orbital resource mining as proposed here. By using ISRU, the transportation of propellant from Earth for SSRP EDL is completely eliminated, with a much better SSRL mass fraction than has been previously proposed (Arney, 2015.)

The use of aqueous catalytic electroreduction of CO₂ was also considered (Gattrell, 2006; Chen, 2012) for its potential in performing multiple reactions of interest for Mars ISRU namely CO₂ reduction to CO and O₂, and water splitting into H₂ and O₂ or performing the synthesis of hydrocarbons such as methane (CH₄) in one cell using copper electrodes. While the pursuit of such promising reaction holds great potential for ISRU, our preliminary trade studies ranked the technique lower than solid oxide electrolysis (SOE) for orbital operations because of its use of liquid water cells requiring yet unknown engineering solutions for microgravity operations and it also requires the import of water from Earth already addressed. These cells do offer very attractive features and their recent performance tests as the SOE-Embedded Sabatier Reactor (SOE-ESR) combined technology are promising (Iacomini, 2015.)

5.2.7.1 Solid-Oxide Electrolysis (SOE)

The on-board generation of electrical energy by MHD on the RCV led to the selection of SOE as a method of oxygen production since it relies exclusively on electrical energy to achieve the conversion of CO₂ collected from the upper Martian atmosphere into O₂ according to reaction (Equation 5):



Other technologies require the use of chemical reducing agents such as hydrogen (Sabatier process) in addition to electrolysis. The solid oxide electrolysis cell (SOEC) technology has also advanced significantly and has been modeled and developed experimentally for Mars surface mission demonstrations such as the MIP experiment initially planned on the Mars Phoenix lander in 2001 (TRL 8) and more recently the Mars Atmosphere Resource Verification In Situ (MARVIN) experiment (Sanders, 2014) and the Mars Oxygen ISRU Experiment (MOXIE) experiment for the NASA Mars 2020 mission. In Phase I, we adapted a modeling tool based on SOEC technology (Fig. 1-1) developed since 2001 by K. Araghi and others to estimate cell performance parameters (Sanders, 2014.)

• **OXYGEN GENERATION TECHNIQUE:**

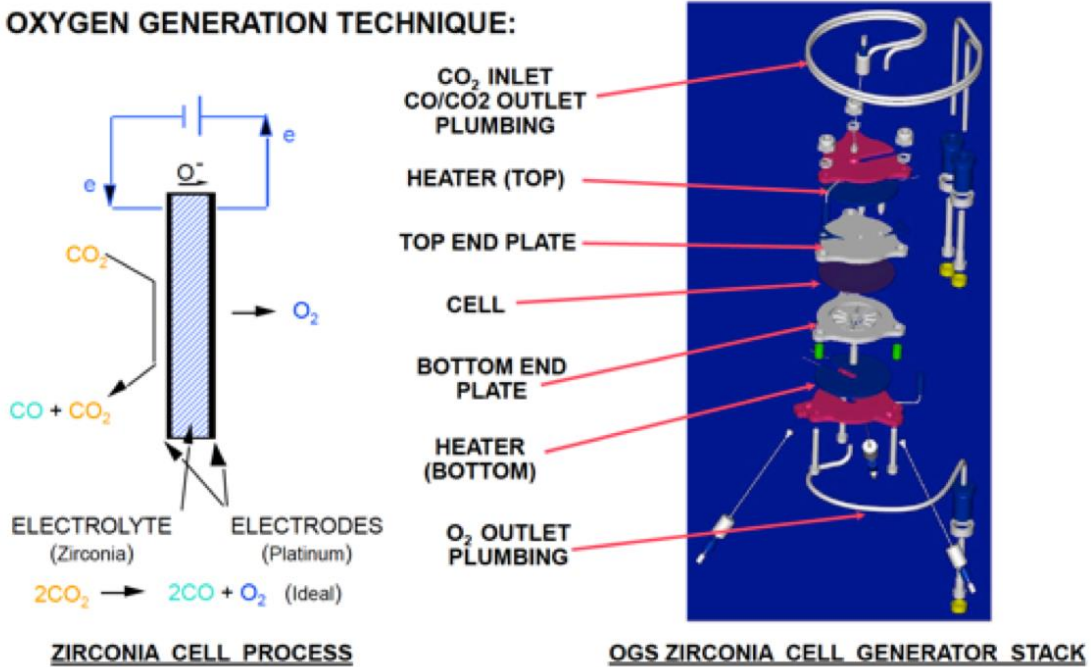


Figure 16. SOEC cell design for MIP experiment (2001).

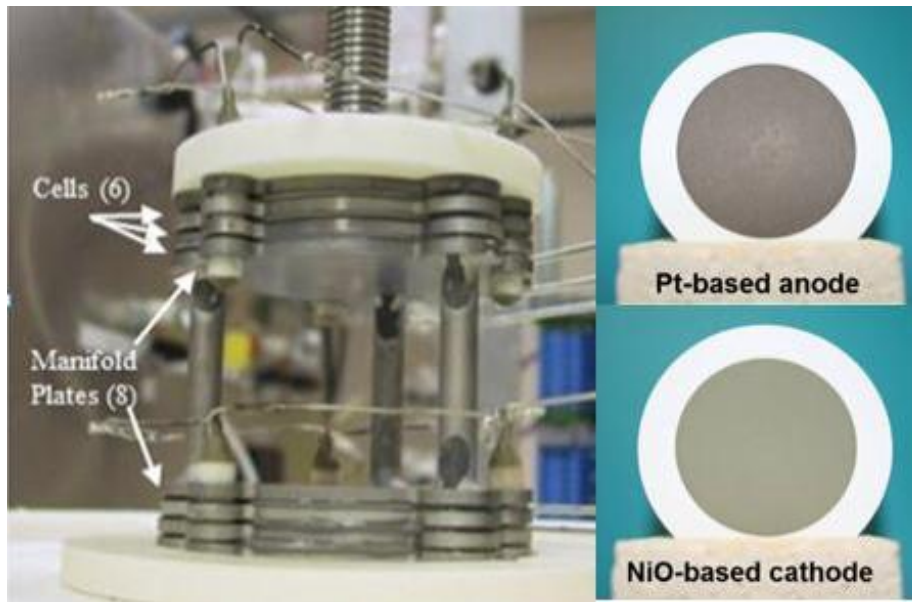


Figure 17. SOE-ESR Dual Stack (l); 10 cm² electrodes on 8YSZ electrolyte designed for proposed use on Mars 2020 mission (Sanders, 2014).

Because SOE-ESR technology (Figure 17) uses a cell and stack approach similar to fuel cells, production operations are easily scalable to different production rates. A SOE cell uses an electrolyte made of a nonporous ceramic oxide, such as YSZ, which conducts oxygen ions at elevated temperatures (750 °C to 850 °C). Electrically-conducting porous cathodes and anodes attached on opposite sides of the electrolyte facilitate gas/electron transport and act as catalysts.

At the cathode, an oxygen atom is liberated from CO₂, via an endothermic reaction. The oxygen atom receives two electrons from the cathode to become a doubly charged oxygen ion, O²⁻. A voltage applied to the electrodes drives the oxygen ion through vacancies in the crystal lattice of the nonporous electrolyte, and when the ion reaches the other side of the cell it releases the electrons to the anode and combines with another oxygen atom to form an O₂ molecule. The voltage applied across the cells in the SOE stack in conjunction with the CO₂ supply rate drive the O₂ production rate. A SOE stack can also generate O₂ from H₂O vapor via the exact same process but instead of producing CO, it produces H₂ in the cathode exhaust. Besides electrolyzing CO₂ and H₂O, with proper selection of the electrode catalyst, the CO and H₂ byproducts can be converted into CH₄ at a lower temperature, a reaction that is performed in a second SOE-ESR stack in series with the first electrolysis stack.

Figures 28 and 29 illustrate the operation and systems of the RCV. The high altitude atmospheric CO₂ is ingested during the high-velocity periapsis passes via ram compression, and then a staged approach is used to further compress it to a state of liquefaction in another tank. The capture tank is isolated with a valve after the CO₂ has been transferred into the storage tank and it is evacuated to be ready for the next periapsis scooping pass. The target production of O₂ on board the RCV was used in the MSR (1.78t O₂) and the human mission (6.98t O₂) reference cases to calculate the power and mass budgets of the processing system and to conceptualize a timeline of production consistent with the energy generation system (see MHD in section 5.3) and the electrical energy storage (EES) system (see section 5.4).

5.2.7.1.1 MSR Reference Case – On-Orbit O₂ Production

Two concepts of operation were traded: (1) the totality of collected CO₂ is processed into O₂ during each orbital period, and (2) CO₂ is collected during each atmospheric pass at a periapsis of 80 km and stored in a buffer tank which continuously feeds the SOE system for an extended production period equal or longer than the total duration of the Molniya collection period (16.3 days; 84 passes). The amount of MHD power generated during each 5- to 7-minute-long atmospheric pass is on the order of 2-9 MW for a RCV vehicle stack of 21 t per our model described in Section 5.2. This large amount of power is far greater than what is needed for the O₂ production (see Table 7), but our preliminary analysis concluded that significant uncertainties exist in the charge-discharge cycles and the frequency of such cycles for the EES coupled with MHD. This led us to selecting the second concept of increased production time to operate within large enough margins before more is known through in-depth analysis in Phase II work. The calculated results summarized in Table 7 show that an increase in the O₂ production time to twice the duration of the Molniya collection period (32.6 days) would lessen the demand on the EES, the SOEC, and the liquefaction systems. This would result in less stringent requirements on the discharge rates from the EES and allow for losses in the charging rates.

Table 7. MSR reference case – on-orbit oxygen production.

RCV on-board ISRU – Mars Sample Return Reference Case			
	Mass (kg)	Power (kW)	Duration
O ₂ Production Target	1,780		
CO ₂ Collection total	8,764		
Average collection pass (CO ₂)	104.3		5.2–7 min
Processing Time			32.6 days
SOE System (283 cells)	86	17	
O ₂ Liquefaction	47	2.9	
Thermal (54 m ² Cu radiators)	216.5		

This first analysis shows that the modeled SOE cell technology is marginally adapted to this production rate but the total number of SOEC (283 cells) could be reduced by lengthening the processing time or by opting for a larger-scale design to reduce risks of cell failures. Additional power is required for the CO₂ capture and storage/delivery system, and liquid oxygen (LOX) conditioning system (ZBO) and will be calculated in Phase II as part of a design adapted to scale.

In the HMO Molniya orbit period, which decays from 21.1 to 1.8 hours for the MSR case, some of the stored CO₂ gas is processed to O₂ gas on the way to and from apoapsis by using SOE on orbit. Later on, the remaining stored CO₂ is processed in a LMO circular orbit (250 × 250 km). The power requirements for SOE are mostly derived from the need to maintain the solid oxide membranes at operating temperatures between 750 °C and 900 °C. The atmospheric friction experienced by the spacecraft during CO₂ harvesting is expected to generate large amounts of radiative heat as the post-shock temperatures in the plasma reach 2240–2500 K (1966–2317 °C). This represents thermal energy that can be channeled to the SOE modules via an onboard thermal phase-change material heat sink and possibly heat pipes, to passively satisfy the thermal requirements for gaseous oxygen production without consumption of onboard electrical power. While in LMO, stored electrical energy from MHD in the EES must be used to make the remaining O₂. Liquefaction and pumping of the collected CO₂ and the produced O₂ will require the onboard electrical power to cryogenically store it in tanks for the landing phase. In phase II of this project, zero boiloff storage will be traded vs allowing boiloff. The EDL SSRP fuel consists of methane (CH₄) that is brought from Earth on the first mission, but for subsequent missions it can be made on the Mars surface using atmospheric CO₂ and water (H₂O) from hydrated minerals or excavated water ice, which is buried underneath the regolith at higher Mars latitudes.

SOE is simpler, lighter and has also been selected by NASA as a technology demonstration payload on the Mars 2020 mission *Moxie* payload. However, it does require high amounts of thermal energy and is harder to scale up in production quantities. On the Mars surface, the SOE-ESR technology is proposed to produce both CH₄ and O₂. CH₄ must be produced for the ascent phase, and additional methane can be transported to HMO in the fuel tanks and later used for the descent. In Phase II we will investigate these issues of scalability and power. Since there is a lot of thermal heating during scooping the in-situ thermal heat energy can be used to avoid heat generation from stored electrical energy.

5.2.7.1.2 Human Mission Reference Case – On-Orbit O₂ Production

The mass of the RCV vehicle stack performing the atmospheric passes is on the order of 84 t, which allows more CO₂ to be collected on board and more MHD energy to be generated while the orbital period decays similarly from 21.1 to 1.8 hours in 81 orbits for a total of 16.35 days.

Table 8. Human mission reference case - on-orbit oxygen production.

RCV on-board ISRU – Human Mission Reference Case			
	Mass (kg)	Power (kW)	Duration
O ₂ Production Target	6,985		
CO ₂ Collection total	34,929		
Average collection pass (CO ₂)	431.2		5.2 – 7 min
Processing Time			49 days
SOE System (779 cells)	236	46.7	
O ₂ Liquefaction	120	8.1	
Thermal (148 m ² Cu radiators)	592		

The results of a ConOps option trade similar to that of the MSR case led to the selection of a total processing time of 49 days, equivalent to 3 times the Molniya collection duration of 16.3 days. This ConOps would leave the RCV stack in LMO for ~33 days to complete the production of liquid O₂ prior to transfer to the MDAV/SSRL. The analysis shows that the SOEC technology as modeled would require 779 cells (Table 8) and would need to be scaled-up to match a smaller number of cells to the production rate at higher power efficiencies and less risk of failures. In Phase II, the SOEC system will be modeled using larger scale technologies in development for larger energy systems, such as pilot-plant scale hydrogen production.

5.3 Magneto-Hydrodynamic (MHD) Model

MHD offers a very innovative feature to this NIAC concept. The CO₂ that is acquired during orbital mining scooping requires an energy source to convert it into O₂ via SOE processing. The SOE electrical power requirements are quite high (46.7 kW), but the modeling explained in the following section indicates that MHD electrical energy generation in a very high velocity Mars Molniya periapsis creates a surplus of energy (MW scale), creating many possibilities if the energy can be rapidly stored during an approximately 5- to 8-minute periapsis atmospheric scooping pass.

5.3.1 General MHD Energy Generation, Faraday Type Flow Through

- From first principles, estimate maximum power available for MHD Energy generation for Faraday type generator

- From Ohm's Law

$$\bar{j} = \sigma(\bar{E} + \bar{u} \times \bar{B})$$

$$j_y = \sigma(E_y - uB)$$

- Define a Loading Parameter, K (0 for Short Circuit, 1, for Open Circuit)

$$K \equiv \frac{E_y}{uB} \quad 0 \leq K \leq 1$$

$$j_y = -\sigma uB(1 - K)$$

- Calculate Power Per Unit Volume

$$P = \bar{j} \cdot \bar{E}$$

$$P = -\sigma u^2 B^2 K(1 - K)$$

- Calculate Maximum Power Available

$$P_{max} = \frac{\sigma u^2 B^2}{4} A_i L_i$$

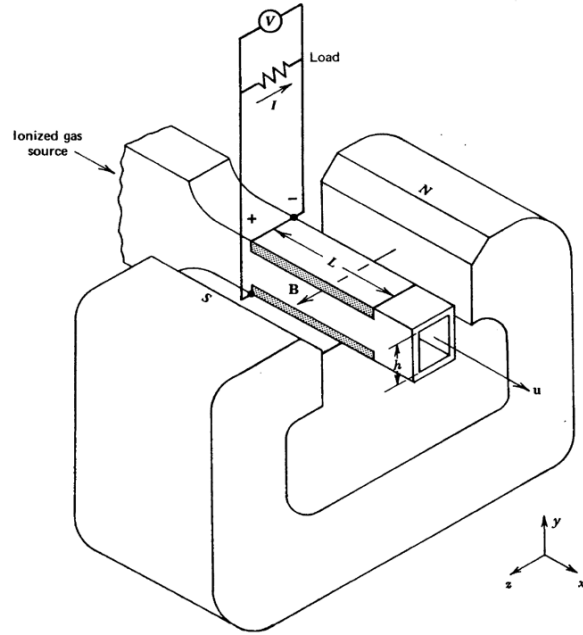


Figure 18. First principles analysis of MHD energy generation.

5.3.2 Determining the Power Available for MHD Energy Generation During Aerobraking

The total energy available via MHD energy generation is the integration of the power available for an MHD generator along a given trajectory. To calculate this power generation profile, it is necessary to identify the relevant physical interactions occurring along a given trajectory. These interactions are the gravitational interaction between planetary body and spacecraft, the aerodynamic interaction between planetary atmosphere and spacecraft, and the thermochemical interaction within the atmosphere as the spacecraft decelerates at hypersonic speed. The superimposed effects of these three physical interactions allow for the definition of the position state, velocity state, and electron number density. These states define the total power that can be generated by MHD energy conversion. For a Faraday-type MHD generator, the generated power behaves according to the following scaling law (Moses et al., 2005):

$$P \propto \sigma_e u^2 B^2 A_c L_i \quad (6)$$

Where P is the generator power output, σ_e is the scalar electrical conductivity, u is the local flow velocity, B is the magnetic field strength, A_c is the generator interaction area, and L_i is the generator length. In reality, an open channel Faraday-type MHD energy generator may be unsuitable for planetary entry applications because of the necessity of allowing the high temperature entry plasma to flow through the vehicle. However, the basic physics of Equation 6

apply to a non-flow through MHD energy generator design applicable to planetary entry vehicles and thus may be used in this analysis (Steeves et al., 2007).

For the purposes of this analysis, the magnetic field strength will be assumed in all cases to be a constant 0.2 Tesla as studied in previous investigations (Macheret et al., 2004; Steeves et al., 2007). The generator area is assumed to be 1 square meter in all cases, with a characteristic length of 1 meter. As a result, the above scaling law can be reduced to a function of electrical conductivity and velocity only, given as Equation 7:

$$P \propto \sigma_e u^2 \quad (7)$$

To calculate the electrical conductivity, the atmospheric properties and composition after passing through a shock wave must be calculated. Since the ambient density, pressure, and temperature can be calculated as functions of altitude, and ambient atmospheric species composition is known and assumed to be constant, the addition of velocity fully specifies the postshock state. A chemical equilibrium solver, in this case NASA's Chemical Equilibrium Analysis (CEA) code, is then used to calculate the postshock state by solving the equilibrium one-dimensional normal shock problem with chemistry (Gordon and McBride, 1994).

Table 9. Martian atmospheric compositions (Mahaffy et al., 2013).

Constituent	Relative Abundance
CO ₂	96.0%
Ar	1.9%
N ₂	1.9%
O ₂	0.14%
CO	0.06%

Martian atmospheric constituents and their abundances are presented in Table 9 in order of relative abundance (Mahaffy et al., 2013). Postshock species include the following: Ar, C, N, O, C₂, N₂, O₂, CN, CO, NO, CO₂, NCO, Ar⁺, C⁺, C₂⁺, N⁺, N₂⁺, O⁺, O₂⁺, CN⁺, CO⁺, NO⁺, and e⁻. In the case of seeding, K⁺ will also be present in the postshock species. Our study does not use the seeding option, to avoid using consumables. Using these data in conjunction with the atmospheric properties as a function of altitude, the postshock temperature, pressure, and species composition can be calculated as a function of velocity.

Once the species composition, temperature, and pressure are known, the scalar electrical conductivity in the shock layer can be calculated. The scalar electrical conductivity behind the shock is based on the electron number density and electron mobility, determined by the frequency of all electron-ion and electron-neutral collisions. The resulting expression is given below as Equation 8 (first principles analysis of MHD energy generation) (Kim and Boyd, 2012).

$$\sigma = \frac{n_e e^2}{m_e \sum_{s \neq e} \nu_{e,s}^m} \quad (8)$$

where n_e is the electron number density, e is the elementary charge, m_e is the mass of an electron, and $\nu_{e,s}^m$ is the collision frequency of electrons with a chemical species s . True

calculation of the collision frequencies involves knowledge of the temperatures for each species, the collision cross sections, as well as the number density of each species. For simplicity and computational expediency; however, the electrical conductivity model for the Martian atmosphere suggested by Macheret et al. (2004), given below as Equation 9.

$$\sigma = 2.7 \times 10^5 \frac{n_e}{n} \left(\frac{1}{\Omega m} \right) \quad (9)$$

where n_e is the postshock overall number density and $\frac{1}{\Omega m}$ is the unit of electrical conductivity.

The scalar electrical conductivity is calculated using Equation 9 and the output of NASA’s CEA code solution to the postshock thermochemistry problem. Inputs are the freestream velocity, atmospheric composition, ambient atmospheric pressure, and ambient temperature. The ambient pressure and temperature can be generalized as functions of altitude for each planetary atmosphere, such that the shock layer electrical conductivity is essentially a function of altitude and velocity only. In order to expedite computation for multiple runs, lookup tables for electrical conductivity as a function of altitude and velocity are generated, with altitude varying from 15 to 125 km in 1 km increments and velocity varying from 2500–13500 m/s in 100 m/s increments. These values cover the range of conditions and velocities relevant to MHD energy generation, with final postshock properties such as electrical conductivity linearly interpolated based on the table values. Figure 19 is an example of the output of this postshock thermochemistry model.

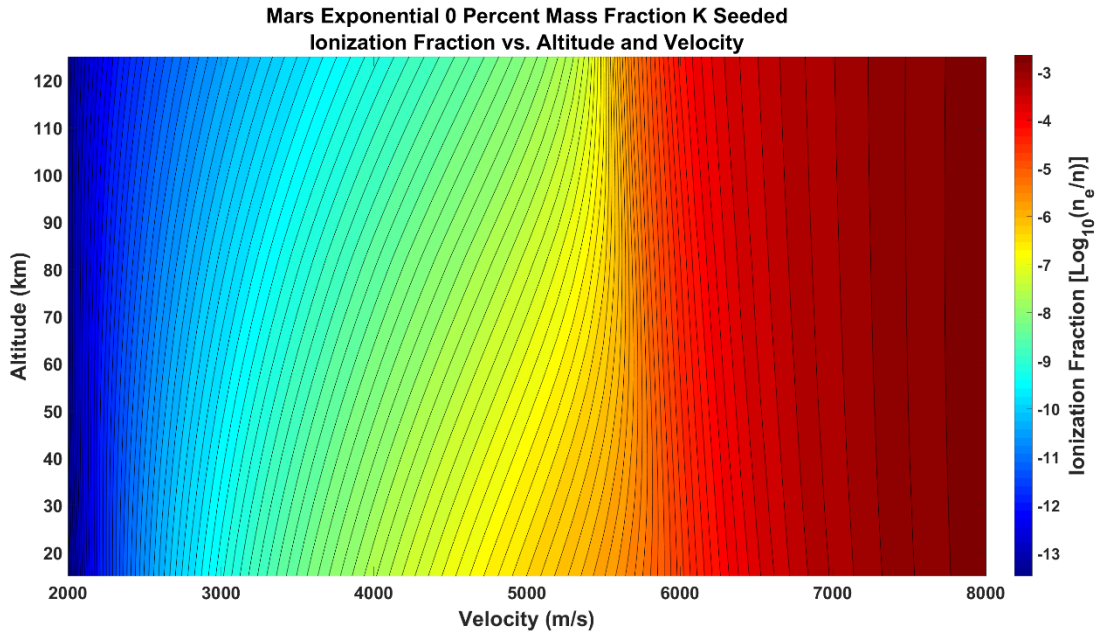


Figure 19. 0% K seed postshock ionization fraction as a function of altitude and freestream velocity.

These values then define the power available for MHD energy generation as represented by Equation 10.

$$P = C \sigma_e u^2 B^2 \quad (10)$$

where C is a constant of proportionality to be determined from either detailed numerical results or previous work. In this case, the constant was determined from previous work (Moses et al., 2005) for demonstrative purposes. However, since electrical conductivity is a function of both altitude and velocity, the altitude history of the trajectory simulation shown in Figure 20 has been reconstructed.

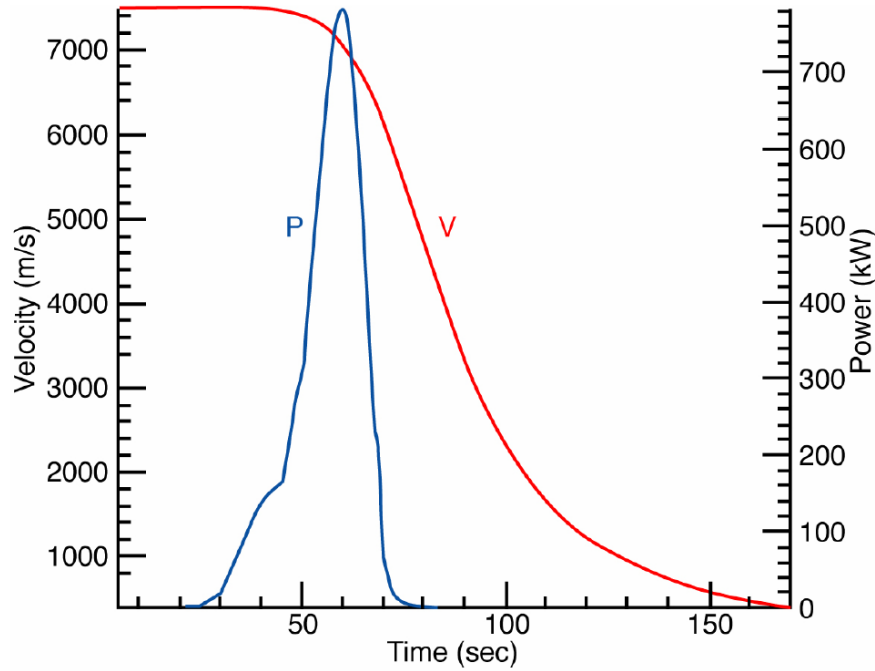


Figure 20. Sample power vs. time and velocity vs. time from previous work (Moses et al., 2005).

The vehicle parameters for the results presented in Figure 20 are given as Table 10.

Table 10. Vehicle Parameters for the Moses test vehicle (Moses et al., 2005).

Vehicle Name	Vehicle Mass (kg)	Vehicle Diameter (m)	Vehicle C_D
Moses Test Vehicle	1000	3.37	0.4

Based on the velocity profile in Figure 20, the knowledge that the vehicle followed a ballistic trajectory in the Martian atmosphere, and the vehicle parameters provided in Table 10, an altitude velocity history for the test vehicle is constructed, presented as Figure 21.

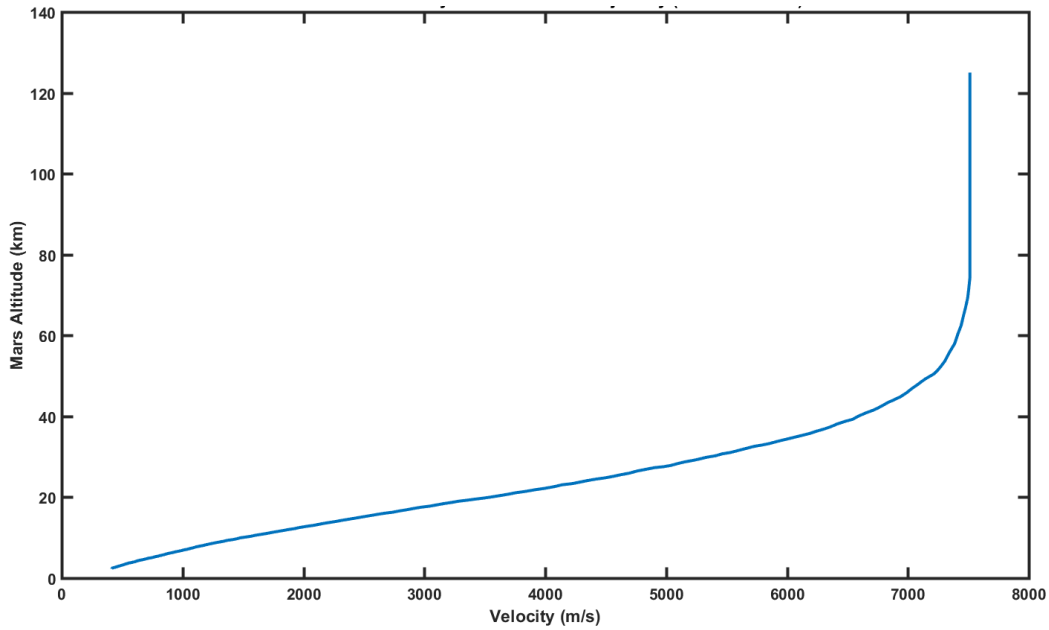


Figure 21. Reconstructed altitude velocity history for vehicle studied in previous work (Moses et al., 2005).

Based on this reconstructed trajectory, and taking the interaction area as 1 m^2 , the values necessary to determine the constant C in Equation 5 were calculated using a linear regression, given as Figure 22.

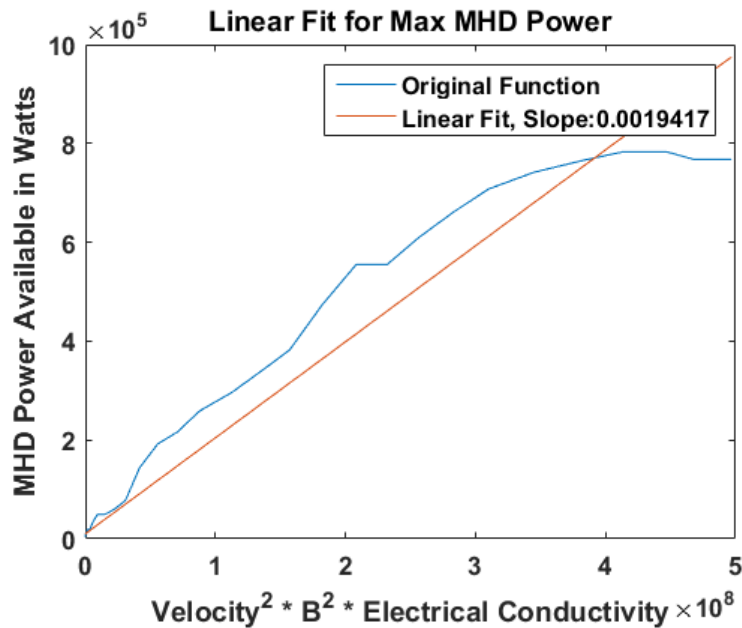


Figure 22. Estimated constant for MHD power available for Moses test vehicle.

Noting that the magnetic field strength was taken as 0.2 T in the previous study (Moses et al., 2005), the constant C has a value of **0.001947** for power available in watts, allowing for

analysis across multiple entry vehicles, planetary bodies, and entry conditions. In practice, this constant can be recomputed using a more detailed numerical simulation that accounts for the specific geometry of the generator as well as the full flow field and chemical kinetics surrounding the entry vehicle. However, for the analysis presented herein, this value for C is used in all simulations in order to provide a reference demonstration for the methodology.

After the numerical integration has been done to calculate the trajectory and obtain the velocity and altitude, the scalar electrical conductivity at each point in the trajectory is calculated using the method described above. Then, the power generated can be calculated for each point, giving a power vs. time curve that defines the amount of energy available for that trajectory. This curve is then ready for analysis by the electrical energy storage system model.

5.4 Electrical Energy Storage Systems

Electrical energy storage (EES) systems are extremely diverse in their mechanisms and applications. These systems can be mechanical, chemical, and electrodynamic in mechanism, or a combination of these elements. Applications for electrical energy storage systems range from mobile devices to large water retention ponds capable of powering entire cities for long periods of time (Chen et al., 2009). With such a diversity in mechanisms and applications, it is challenging to develop appropriate performance objectives upon which to evaluate electrical energy storage systems. This problem is particularly troublesome for systems under development that may have an ill-defined application profile.

Examples of common electrical energy storage system performance parameters include mass, endurance, power capacity, longevity, and heat generation. The application being presently considered is a flight application, and thus mass is expected to play an extremely important role in the suitability of an energy storage technology. In addition, although electrical energy storage system parameters such as longevity and heat generation are important, the assessment of their impact requires detailed system design information that is outside the scope of this analysis and typically not known without precise knowledge of the energy usage loads and flight system geometry. The total amount of electrical energy generated will allow for estimation of the size of energy storage device needed; however, as mentioned earlier the electrical energy generation for this application may occur at a relatively high rate that will place requirements on system power capacity as well (Chen et al., 2009).

Thus, for the purposes of this analysis, total electrical energy storage system mass is determined to be the most important parameter. Mass and energy requirements can be calculated for a given total amount of energy to be generated at a certain rate. Both total energy storage capacity and discharge power capacity for an electrical energy storage system can be related to system mass by defining mass specific versions of each of these properties. Typical units are watt hours per kg and watts per kg for specific energy storage and power discharge capacity. Although electrical energy storage systems for a given type may vary in their values for the aforementioned parameters, there is typically a range for each parameter that is considered appropriate for a given technology. These values are determined experimentally and continually evolve as new developments in energy storage techniques come to fruition. These ranges can be used to define a best, average, and worst-case scenario for a given technology.

The electrical energy storage systems categories that will be considered in this analysis are batteries, capacitors, and miscellaneous devices such as flywheels and super conducting magnetic energy storage. For the present application of power generation and energy storage, charge power capacity and discharge power capacity are assumed to be roughly equal, simplifying the analysis. One way in which to visualize the performance of these systems is to plot the specific power vs. the specific energy storage capacity. Such a plot is termed a Ragone plot, and such a plot generated using the values employed for this analysis is given as Figure 23. For the application being considered, good choices generally lie to the top right of the chart, while poorer choices lie to the bottom left.

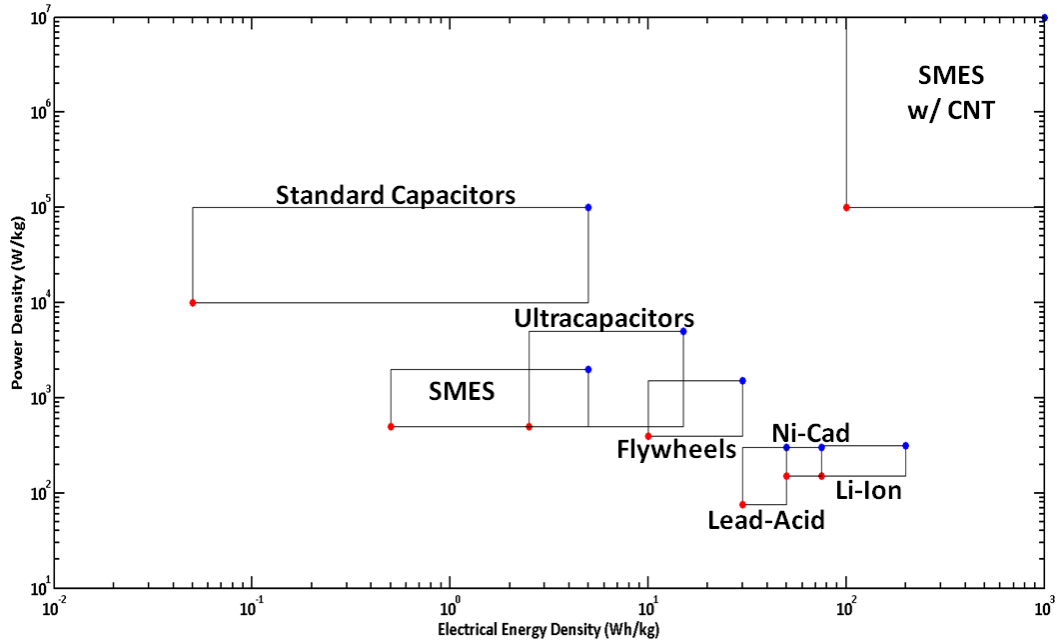


Figure 23. Ragone plot for electrical energy storage systems under consideration.

The plot presented as Figure 23 includes highlights of best and worst case scenarios, as represented by the red and blue dots respectively. Numerically, they are summarized along with an estimate of their technology readiness level (TRL) in Table 11.

Table 11. Electrical Energy Storage System performance data.

EES System	Minimum Wh/kg	Maximum Wh/kg	Minimum W/kg	Maximum W/kg	Technology Readiness Level
Lead Acid	30	50	75	300	High
Nickel Cadmium	50	75	150	300	High
Lithium Ion	75	200	150	315	High
Capacitors	0.05	5	10,000	100,000	Medium
Ultracapacitors	2.5	15	500	5,000	Medium
SMES	0.5	5	500	2,000	Low
SMES w/ CNT*	100	1,000	100,000	10,000,000	Low
Flywheels	10	30	400	1,500	Low

* Superconducting Magnetic Energy Storage with Carbon Nano tubes (SMES w/CNT)

The values given in this table provide the necessary information to calculate electrical energy storage system mass for a power vs. time profile for a given technology. In addition, it may prove useful to characterize electrical energy storage system performance by technology readiness level (TRL). This characterization is done by taking the best overall performer in each of the three TRL categories as representative of that category. The resulting average values for each TRL are presented in Table 12.

Table 12. Electrical Energy Storage System performance data.

EES System TRL	Average Specific Energy (Wh/kg)	Average Specific Power (W/kg)
High (Lithium-Ion)	137.5	232.5
Medium (Ultracapacitors)	8.75	2750
Low (SMES w/ CNT)	550	5,050,000

A model has been created that calculates the electrical energy storage system mass for a given power generation profile and energy storage system type. It does so by integrating the power generation vs. time profile curve to calculate the total energy available for storage while also noting the peak energy generation power. As shown in Figure 23 and Table 12, both power and energy requirements define energy storage system mass. Thus, there are two possibilities, power capacity driven mass, and energy generation driven mass. Both approaches must be taken, and the final stored energy is assessed relative to the initial amount of energy. From the system mass and relative energy conversion metrics, an educated assessment can be made with regards to what energy storage system mass is most advantageous for a given technology.

The minimum and maximum pairs for specific energy and power in Table 12 define worst and best cases respectively. In addition, an average case for specific energy and power is generated for each technology. Thus, three distinct performance cases for each technology are selectable within the model by the user. The end result is to generate specific values for power and energy density given selections for energy storage system type and performance scenario. The process for doing so is described in Figure 24.

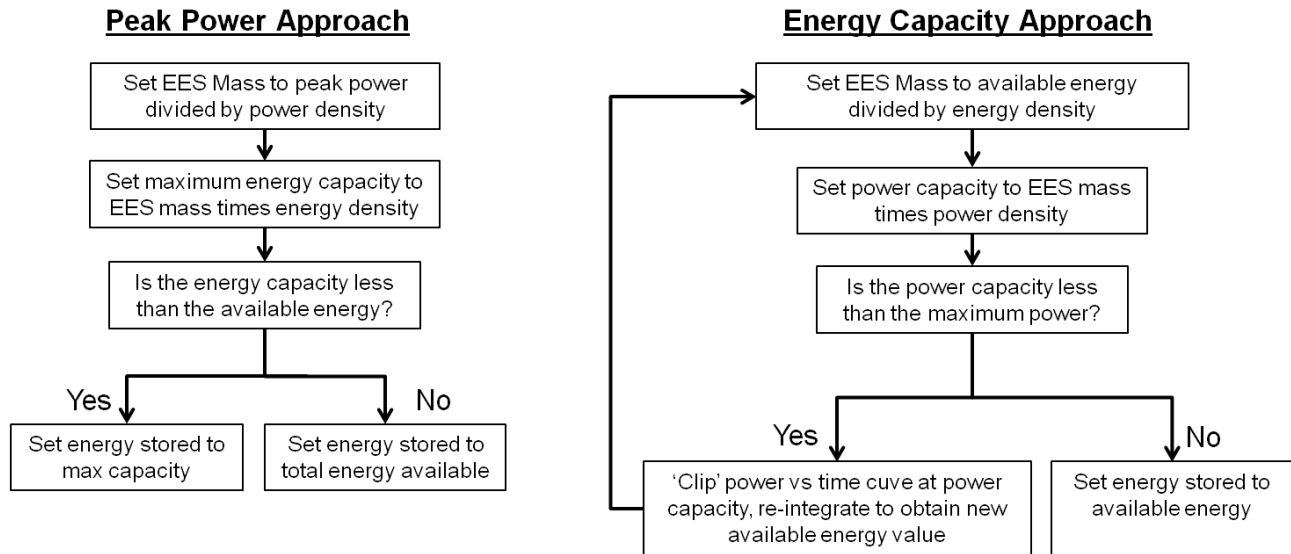


Figure 24. Electrical energy storage system model flowchart.

As shown in Figure 24, there are two approaches to finding energy storage system mass. The reason for taking both approaches is to find an energy storage system mass that is capable of storing all available energy at the rate it is generated. The first approach, termed the *Peak Power Approach*, involves defining system power capacity as equal to the maximum energy generation rate from the given power profile. Dividing this system power capacity by the specific power capacity for the technology under consideration results in the system mass. Total stored energy is calculated by multiplying this mass by the specific energy capacity of the technology under consideration, and this value is compared with the total energy available. Depending on the technology, this approach may generate a very high or very low mass and very high or very low percent available energy stored.

The second approach, termed the *Energy Capacity Approach*, involves using the total available energy to drive system mass. An initial guess for the system mass is set by dividing total available energy by specific energy capacity for the technology in question. This initial guess for system mass is then used to calculate the power capacity of this system. If the power capacity is above the maximum power for the power profile, no further action is taken, otherwise, the power generation profile must be *clipped* at the maximum power capacity rate for the system. Thus, a new power profile curve and associated total energy is generated, requiring that the initial guess for the mass be modified. This process must be completed iteratively until a converged value for energy storage mass is found. At the completion of the process, the final mass determines the amount of energy stored, and it can be compared with the original amount of energy available from the power generation profile.

At the conclusion of this process, the model outputs the system mass and converted energy using both approaches in addition to the total energy available for conversion. Different technologies may result in one or the other sizing approach being better than the other. For this analysis, the highest percent energy retained is chosen. Finally, there is an option to limit the total energy storage system mass to some predefined value, which is also useful in assessing energy storage technological requirements.

A digitized power generation profile for the Moses Entry Vehicle direct entry case from previous work is shown in Figure 25 (Moses et al., 2005).

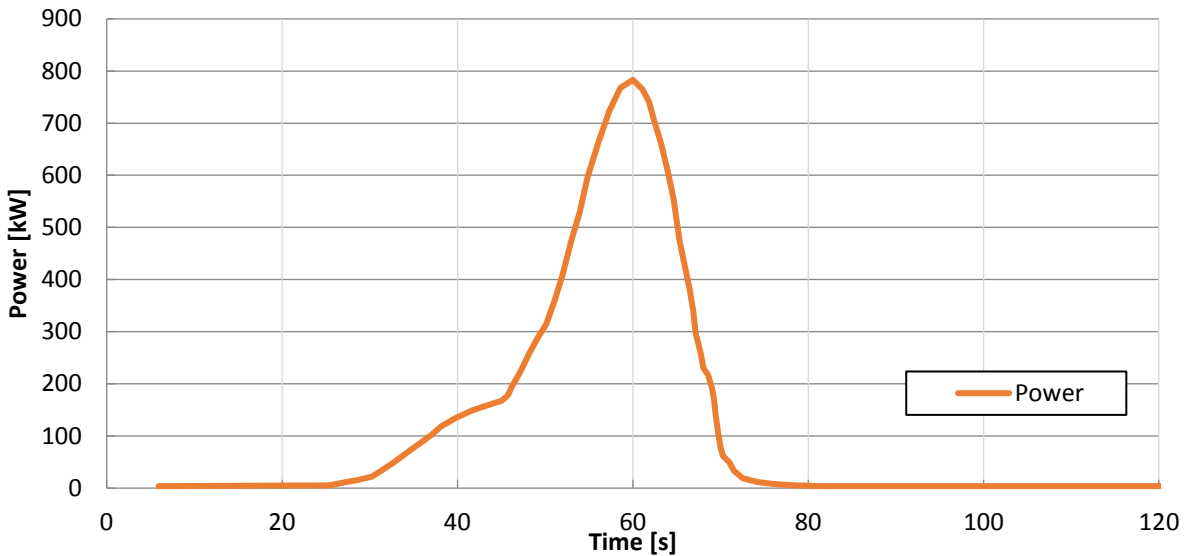


Figure 25. Direct entry power generation profile for Moses test vehicle (Moses et al., 2005).

Table 13 presents the energy storage system masses that were determined from an analysis of the aforementioned power profile, assuming no constraints on energy storage mass, each energy storage technology’s average performance case for specific energy and power, and requiring that all available energy be stored.

Table 13. Moses test vehicle direct entry electrical energy storage system mass.

EES Technology	Mass (kg)	Calculation Method
Li-Ion	3368	Peak power
Lead Acid	4176	Peak power
NiCad	3480	Peak power
Capacitor	1551	Max energy
Ultra-capacitor	447.5	Max energy
SMES	1424	Max energy
SMES w/ CNT	7.120	Max energy
Flywheel	824.2	Peak power

Many of the energy storage system masses in Table 13 are above the original vehicle mass of 1000 kg. In many cases, the mass is very high because of the limited input power capacity in comparison to the total energy stored capacity or vice versa. Since the energy storage system mass is a function of only two parameters, power density and energy density, a surface plot of the total energy stored while constraining total energy storage system mass to 10% of overall vehicle mass (100 kg) can be generated, given as Figure 26.

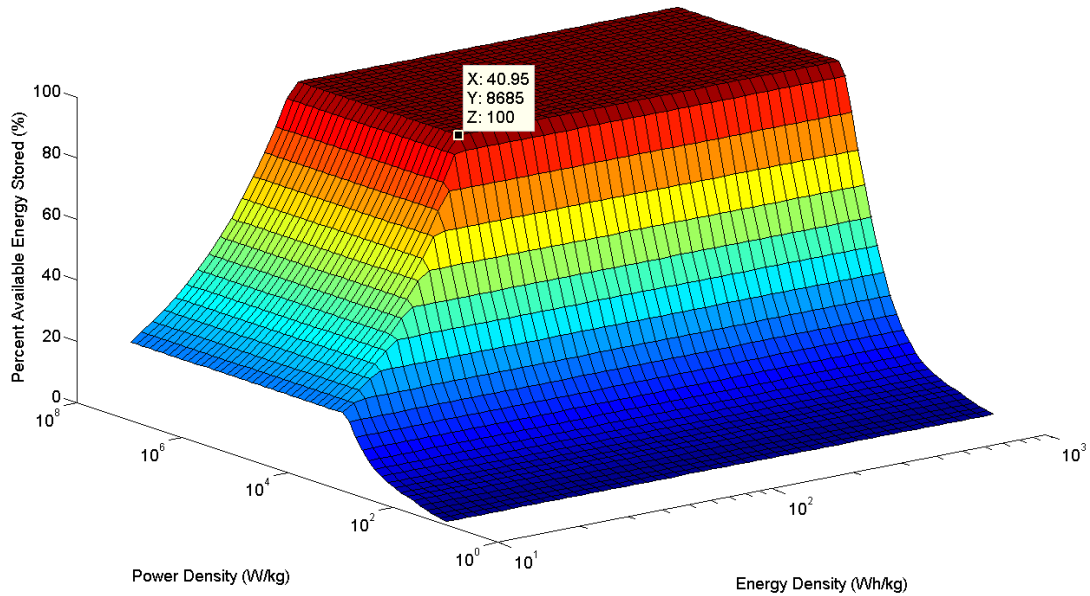


Figure 26. Percent available energy stored for Moses test vehicle direct entry case, mass constrained to 100 kg.

As Figure 26 shows, the energy storage system is incapable of storing all the available energy up to a certain performance point. This is marked with a data cursor highlighting a required specific energy of 40.95 Wh/kg and specific power of 8685 W/kg. This point is of interest because it defines the minimum performance characteristics necessary for an energy storage system to satisfy a certain mass constraint and store all of the available energy at the rate that it is generated.

Similar methods will be used to analyze the RCV energy storage system in our study, but this work was deferred to Phase II.

5.5 Entry, Descent & Landing (EDL) Model

5.5.1 EDL Simulation

The EDL concept used in this study consists of a blunt body aerodynamic deceleration vehicle that enters following a deorbit burn from the circular 250 km × 250 km LMO. Since it would be prohibitive, in terms of propellant required, to do a full propulsive deceleration burn to the Mars surface, aerodynamic deceleration must be used. The diameter of the aerodynamic decelerator directly affects the performance of the vehicle's EDL characteristics. A larger area decelerator will allow for lower peak heat rate and peak deceleration. Analysis and a literature review indicated that typical Mars entry vehicles employ a blunt body, sphere-cone forebody ranging in diameter from 12 to 20 m. Since a large, heavy lift rocket is not anticipated to be more than 10 to 12 m in diameter, a deployable decelerator must be used. Although an inflatable heat shield is an option in single-use vehicles, reusability considerations indicate that a deployable and furling decelerator system poses less risk. Such a system is presented in section 6.3. In this study, a 21 m

diameter deployable heat shield was used in the modeling analysis described in the following paragraphs.

A trajectory simulation was developed to calculate the entry, descent, and landing (EDL) sequence of the MDAV/SSRL. A three-degree-of-freedom trajectory was implemented in the NASA software, Program to Optimize Simulated Trajectories 2 (POST2), which integrates the equations of motion starting from initial atmospheric interface through hypersonic aerodynamic deceleration and propulsive descent and landing (<https://post2.larc.nasa.gov/>). As stated by NASA:

The Program to Optimize Simulated Trajectories 2 (POST2) is a generalized point mass, discrete parameter targeting and optimization program. POST2 provides the capability to target and optimize point mass trajectories for multiple powered or unpowered vehicles near an arbitrary rotating, oblate planet. POST2 has been used successfully to solve a wide variety of atmospheric ascent and entry problems, as well as exoatmospheric orbital transfer problems. The generality of the program is evidenced by its multiple phase simulation capability which features generalized planet and vehicle models. This flexible simulation capability is augmented by an efficient discrete parameter optimization capability that includes equality and inequality constraints. POST2 supports NASA's Strategic Goal to expand the frontiers of knowledge, capability, and opportunity in space by directly contributing to expanding our human and robotic presence into the solar system and to the surface of Mars as well as other planetary bodies. (<https://post2.larc.nasa.gov/>).

The RCV aerodynamic and propulsive performance parameters are based off literature values of a blunt body entry vehicle with liquid methane—liquid oxygen propulsion (Arney et al., 2015; Price et al., 2015). During hypersonic deceleration, bank angle modulation is used to control the lifting trajectory until propulsive initiation. Upon propulsive initiation, the vehicle flies a powered, ballistic trajectory at full thrust until the planet-relative velocity is nullified. Propellant mass is converged upon to ensure the entry vehicle is able to thrust for the entire powered descent phase and land with no residual propellant. The structural mass of the vehicle is not determined a priori and instead scales with the propellant mass based on sizing ratios derived from literature data (Arney et al., 2015). The propulsive initiation conditions are also optimized to achieve a soft landing, attaining 0 m/s relative velocity at 0 m altitude. Favorable propulsive initiation conditions, which minimize the required propellant mass, are found through adjustment of the hypersonic bank angle profile within a genetic algorithm optimizer. The bank profile is subject to certain constraints, which reject trajectories that exceed the maximum g -force limits for human payloads. Figure 27 is an example of the EDL trajectory.

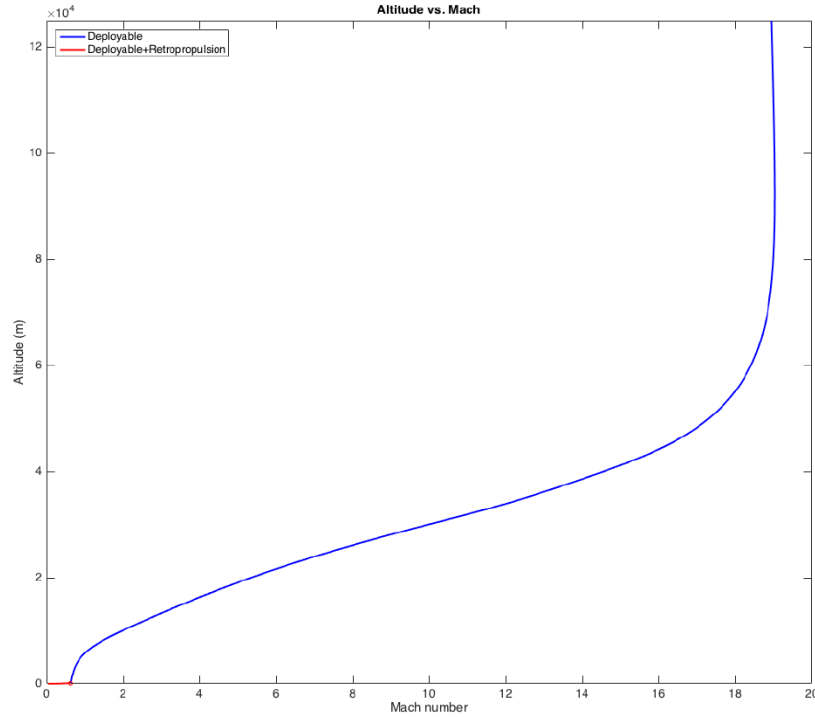


Figure 27. SSRP EDL Altitude vs. Mach number of the entry vehicle during EDL.

Through iterative analysis methods, a feasible MDAV/SSRL configuration with a landed payload mass of 20 t was achieved. This vehicle used a 21 m diameter deployable/furling decelerator during the hypersonic deceleration phases in order to reach valid propulsive initiation conditions, which is explained in Section 6. Closure may be possible with smaller diameter decelerators, which will be the subject of further investigation and analysis in Phase II.

Since parachutes do not scale to the large lander sizes required for human-class missions, retropropulsion is used in the final stages of the EDL sequence, all propellants being produced at Mars. The CH₄ fuel is made on the surface and transported to orbit in the MDAV/SSRL and the O₂ oxidizer is made on orbit in the RCV and subsequently transferred to the MDAV/SSRL. A reusable propulsion system must be developed that is able to deep throttle while also attaining a long life cycle without required maintenance. Such an engine does not exist today and must be developed. Concepts are being studied by NASA, an example of which is shown in Figure 28. This concept is a 100 kN thrust variant.

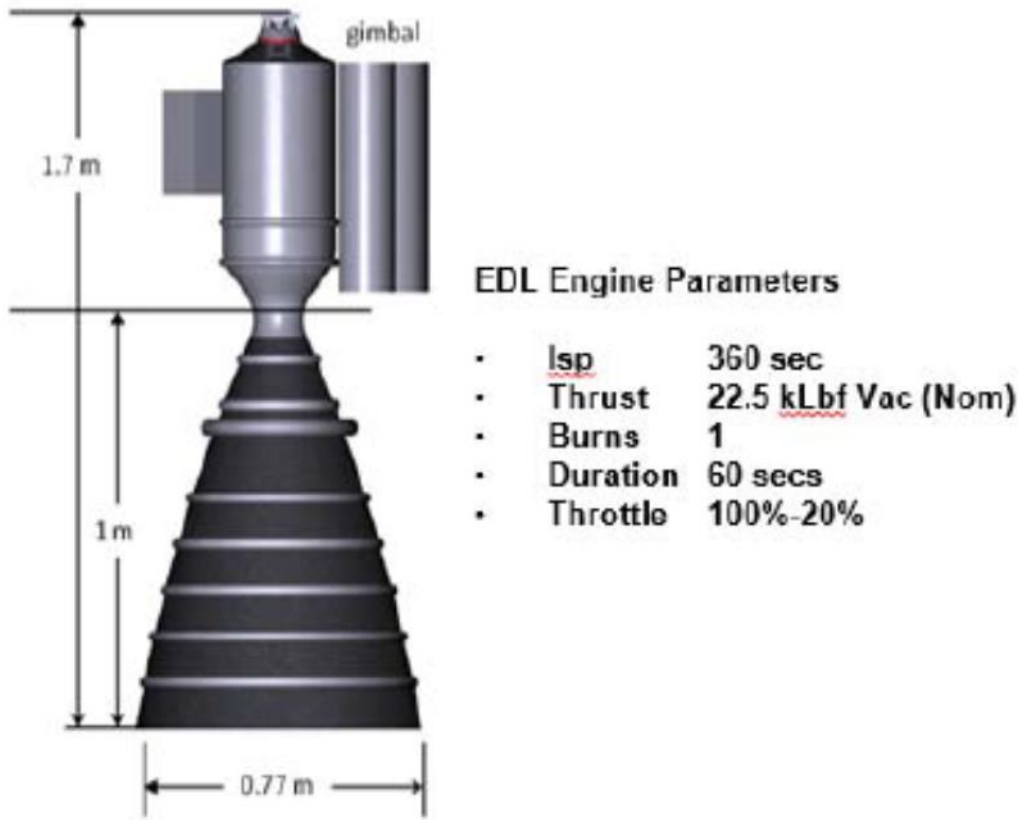


Figure 28. Common methane engine used in the NASA EMC (Percy et al., 2015).

With a projected MDAV/SSRL mass of 38 t (including 20 t of payload) and approximately 8.5 t of propellant required for EDL, the total MDAV/SSRL mass during EDL is 46.5 t. Engine thrust for retropropulsive descent and landing is based on a 3 Earth G's thrust-to-weight. This is planned to be accomplished with four 353 kN rocket engines—3.3 times larger than the concept shown in Figure 28. The engines must be throttled to 10 % at landing, which would require some further technology development.

5.6 Mars Surface ISRU Model

The ISRU surface infrastructure is comprised of all systems needed for the production of the MDAV/SSRL fuel CH_4 and oxidizer O_2 during a predefined production time of 500 days in our Phase I work. These system elements were modeled based on previous work done for the EMC coordinated and led by one of the authors of this study, R. Mueller (Kleinhenz, 2017). These systems are the following and are depicted in Figure 29:

1. Small and lightweight modular surface excavators have been tested at Kennedy Space Center Swamp Works to provide performance data included in our model. These excavators, called RASSOR (for Regolith Advanced Surface Systems Operations Robot), are designed for water-rich regolith handling and hauling. The model describes the performance of RASSOR 2.0.

2. Regolith sorters and conveyor/dryers, demonstrated in laboratory tests (TRL 3-4)
3. Separate SOE, Sabatier, and water electrolysis modules, selected in this model because of the available master equipment list (MEL) that describes them and their TRL 4. The modeling of an SOE-ESR module sized to the production target is planned for Phase II work to realize anticipated gains of mass and power.
4. In addition, the electrical energy needed to power the ISRU systems comes from a set of 10 kWe fission power units called Surface Power Plants (SPP) whose number can be adjusted as needed. The SPP concept has been developed by NASA for Mars studies. One SPP was found to be needed for the production of propellants for the Robotic Precursor Small Cargo Lander (RPSCL) tasked to lift off the Martian surface with samples during the Mars Sample Return (MSR) mission. Our modeling found that 3 SPP units were needed for the propellant production of a human-mission MDAV/SSRL.

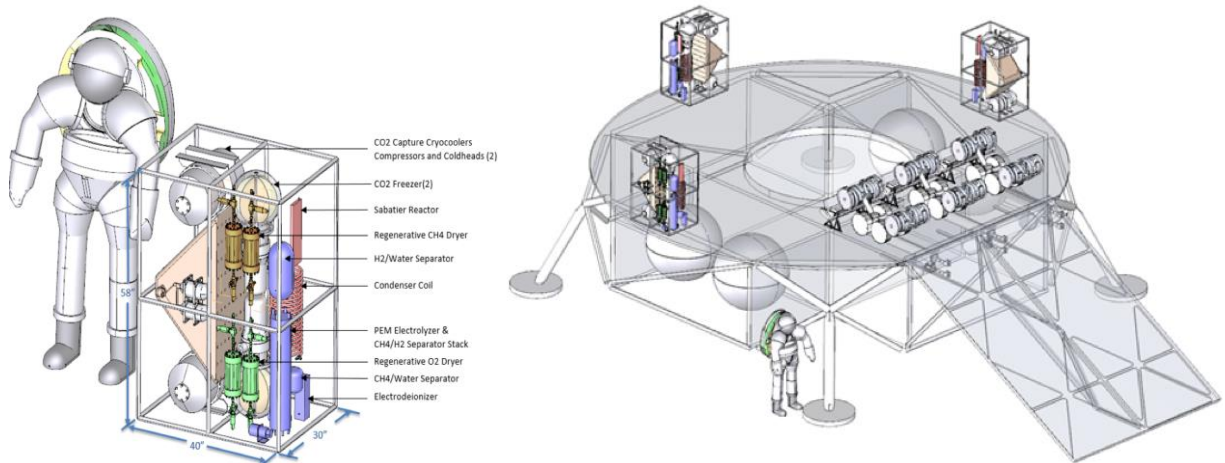


Figure 29. Left: Mars Surface ISRU processing module for CO₂ and H₂O to O₂ and CH₄ production. Right: 3 modules with associated excavators and regolith handling provide sufficient capability for MDAV/SSRL refueling powered with 30 kWe SPP units (Kleinhenz, 2017).

The concept of operations of the surface ISRU is identical in both the MSR and the human mission case. A cargo lander delivers the ISRU and the SPP units with the needed deployment system. During MSR, this cargo lander is the RPSCL and is then scaled up to be the Mars Cargo Lander (MCL) for the human mission. The RASSOR excavators are designed to acquire 80 kg batches of water-rich regolith and haul their load, multiple times, over loose terrain travel to a resource field within 500 m of the landing site. Three excavators are delivered to the surface as depicted on the front end of the lander at the top of the ramp in Figure 29. The triple capability ensures continuous operations during charging times of the batteries at the SPP and provides redundancy in case of failure. Regolith-size sorters and dryer conveyors are located under deck on the lander to facilitate delivery of the regolith by RASSOR and distribution of the extracted water to the processing modules. The same rationale described for the number of excavators applies to the number of processing modules. In addition, each module is designed to function nominally at a production rate equal to 40% of the total production target of CH₄. In nominal operations, this means that 120% of the target is achieved at the end of production time while the

margin contributes success assurance. The calculated results of the ISRU systems and additional cargo for the MSR reference case are displayed in Table 3.

Table 14. Mass calculations for ISRU and cargo for the completion of the MSR reference mission.

Mars Sample Return – Payloads	Mass (kg)	Source
ISRU production systems	429	Model
Excavator (RASSOR x1)	100	Model
Surface Power Plant	3340	EMC
Rover & Cargo deployment system	1200	EMC
Rover Sampling mechanism	100	MSL
Rover Science Instruments	75	MSL
Sample Container	30	Estimate
Samples collected	100	Estimate
Total	5274	
20% Margin	1054.8	
Total w/margin	6428.8	

The MSR case is designed to be a demonstration and validation mission, with one ISRU module being placed on the surface of Mars to be operated for 500 days. In the subsequent human mission, three ISRU modules will be sent

Our Phase II work will focus on advancing these ISRU models to include reliability factors and ISRU development costs using state-of-the-art systems performance data. The ConOps will be optimized for the fueling of the MDAV/SSRL in order to investigate gains and losses in energy efficiency.

5.7 Spacecraft Concepts and CAD Models

The results from all mission architectural trades and technical analysis was used to develop concepts for propulsive transfer stages, mission spacecraft and surface payloads. The focus of this study was on the Mars segment of the missions. In Phase I, standard and available propulsion technology was assumed for Earth-to-Mars transportation. In Phase II, other more exotic propulsion stages may be considered such as nuclear thermal propulsion (NTP) and/or dual mode NTP with nuclear electric propulsion (NEP). Other examples of options are hybrid solar electric propulsion (SEP).

The modeling work and associated mission simulations pointed toward a large stack for the RCV of 10 m diameter with a mass of 84 t operating at 79 km periapsis scooping altitude to achieve the propellant oxidizer requirements for a human-mission class with an MDAV/SSRL having a 20 t landed payload capacity. The RCV stack artistic concept is shown in Figure 30. Note that

the stack consists of the RCV at the front, with the MDAV/SSRL docked to it and an alignment and structural interface cylinder acting as an aerodynamic fairing as well.

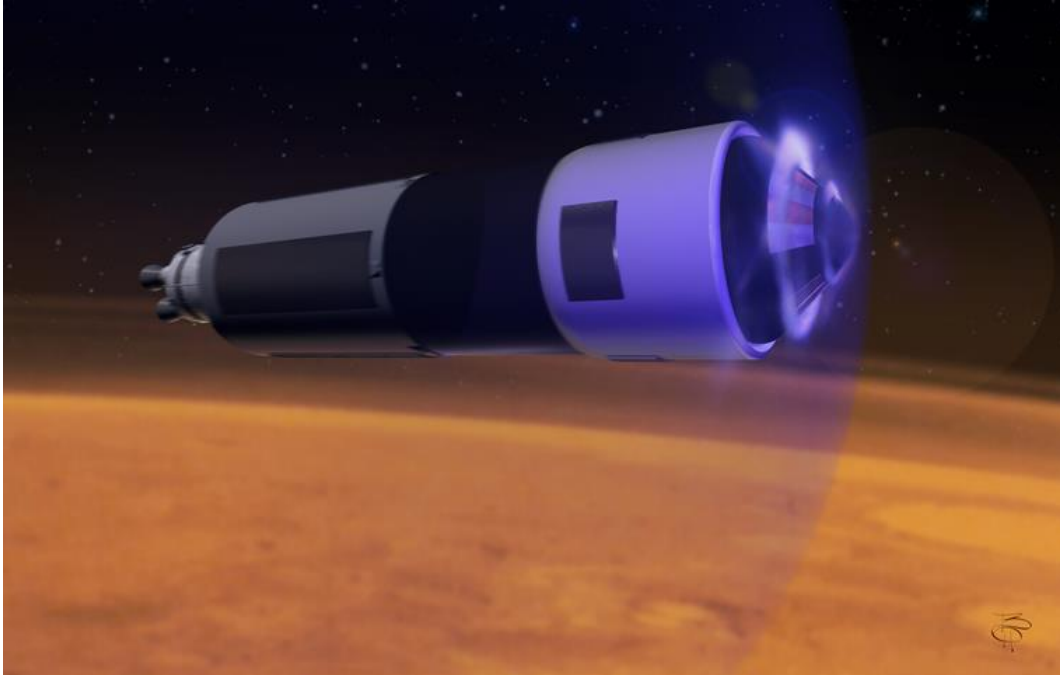


Figure 30. NIAC Mars Atmospheric Gas Resources Collector Vehicle (RCV) stack concept during an aerobraking CO₂ collection pass in the upper atmosphere.

Behind the MDAV/SSRL, an MTCS pushes the stack with propellants for TMI and Mars EDL brought from Earth in the first mission. In subsequent missions, no propellant is needed (other than for the RCS), since it is only used as ballast to achieve the mass required for orbital resource mining. After the surface mission has been completed, the MDAV/SSRL launches the crew directly to HMO into a Mars Molniya orbit to restart the Conops sequence. Propellants for this launch are made on the surface of Mars via the ISRU methods previously described in section 5.5.

Further descriptions and technical details of the mission elements are provided in Section 6.0.

6. CONCEPT TECHNOLOGY DESCRIPTIONS AND TECHNICAL DETAILS TO SUPPORT FEASIBILITY

In Phase I, two mission case studies were evaluated: a demonstrator Mars sample return (MSR) vehicle and a full-scale human MDAV/SSRL capable of transporting a crew of four to the surface and back to LMO. The amount of propellant required to perform retropropulsive EDL was calculated for both cases. The MSR mission has a landed payload mass of 6.4 t, consisting of ISRU equipment, fission power plants, an excavator and a sample collection rover, which requires 1.8 t of O₂ produced on orbit for EDL. The human-scale mission has a landed payload mass of 20 t per lander, consisting of a crew cabin with cargo in one lander version, and just cargo in the other version, while using the same lander platform and EDL system. The transportation system was analyzed to assess the functional allocations, interfaces, and element

divisions to enable in-orbit O₂ production. Our assessment of the concept of operations concluded that the RCV will be mated with the MDAV/SSRL during orbital collection of CO₂ and O₂ production, then transfer the O₂ to the MDAV/SSRL prior to its separation and departure for a Mars surface taxi trip, while the RCV remains in orbit. The concept evolved to include the Mars Transport Cryogenic Stage (MTCS), which propels mission elements between Earth and Mars via the Atmospheric Mining stack, as shown in Figure 31. This evolution was driven by the requirement for the high momentum exchange needed for the collection vehicle to achieve a number of atmospheric passes sufficient to collect enough CO₂ and generate onboard electrical power. In Phase II, the stack concept will be evaluated in detail in terms of operational limits, risks, and viability of the associated technologies.

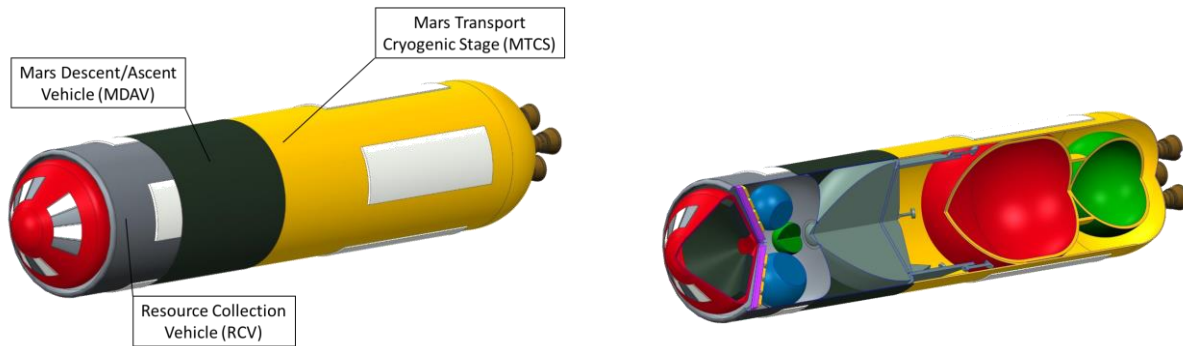


Figure 31. Mars atmospheric resource mining stack concept (solid and section views).

Once the spacecraft oxidizer (and possibly fuel) have been made on orbit and stored, then it becomes possible to use retropropulsion to decelerate the spacecraft, even at supersonic speeds (Morring, 2014), thereby replacing conventional parachutes in the EDL, which do not scale on Mars when the landed mass is above approximately 1,000 to 2,000 kg. The *in situ* production of sufficient propellants that do not have to be transported from Earth enables the descent to be controlled by MDAV/SSRL aerodynamic deceleration (shown in section 6.3), followed by supersonic retropropulsion to enable a precision landing.

This innovative Mars transportation system will allow all the elements to be deployed in a pioneering Mars station without sending a new lander from Earth each time, resulting in cost savings, independence, and mission flexibility.

6.1 In-Space Transportation

Since the main goal of this NIAC study is to investigate feasibility of “Mars Molniya Orbital Atmospheric Mining” and its benefits, we have focused our efforts on transportation in the Mars vicinity. However, in order to assess the complete concept of operations and launch manifests, some existing element concepts developed by NASA in the Evolvable Mars Campaign (EMC) studies have been used. The Space Launch System (SLS) in the 70–105 t launch capacity range and 10 m fairing diameter, cryogenic propulsion stage (CPS), Mars Transport Cryogenic Stage (MTCS), Crew Transit Vehicle (CTV) and the Crew Orbital Vehicle (COV) have all been repurposed to provide linkage and credibility with existing NASA planning and technology development. Commercial equivalent elements may be substituted for these elements. Advanced

in-space propulsion methods, such as Nuclear Thermal Propulsion (NTP) for crew journey and SEP tugs for cargo delivery, would be welcomed as an enhancement to this architecture. Such trades will be considered in Phase II.



Figure 32. Typical NASA Cryogenic Propulsion Stage (CPS) concept, LEO to HEO. (Credit: NASA)

The CPS concept in our ConOps is used to transport the TMI stacks from LEO to HEO. Since high performance is desired and the propellant comes from Earth, H_2/O_2 propellants are used with a mass fraction of 88%. Passive thermal control of propellants is used with 0.52% per day H_2 boiloff (11 days) and 0.02% per day O_2 boiloff (11 days); while the CPS is loitering on orbit, a 6.0 meter UltraFlex array (2 kW total power) is used for keep-alive power. It is discarded at HEO when the rest of the stack performs a TMI burn. The CPS is sized to carry approximately 94 t of cryogenic H_2/O_2 propellant with an Isp of 453 s since this propellant is all Earth-based and provides maximum performance.

The chosen Crew Orbital Vehicle (COV) for this Mars architecture is the NASA Orion capsule with service module. Orion will serve as the exploration vehicle that will carry the crew to space, provide an emergency abort capability prior to TMI, and provide safe reentry with HEO return velocities. Orion will be launched on NASA's new heavy-lift rocket, the Space Launch System. The crew module can transport four crew members beyond LEO, providing a safe habitat from launch through landing and recovery. The service module provides support to the crew module from launch through crew module separation prior to reentry. It provides an in-space propulsion capability for orbital transfer, attitude control, and high-altitude ascent aborts. While mated with the crew module, the service module also provides water, oxygen, and nitrogen to support the crew module's living environment; generates and stores power while in space; and provides primary thermal control. In addition, the service module also has the capability to accommodate

unpressurized cargo. The Orion capsule mass is 10.3 t and the service module mass 15.5 t, for a total COV mass of 25.8 t. The service module propellant mass is 9.3 t.



Figure 33. NASA Orion Crew Orbital Vehicle (COV) in development. (Credit: NASA)



Figure 34. Concept of typical NASA Crew Transit Stage (CTS) with COV docked. (Credit: NASA)

The crew of four will transfer from the COV to the CTS in HEO for the approximately 6-month journey to Mars orbit. It is sized to provide a pressurized volume of 273 m³ for 1100 days of habitation with an additional contingency. It includes an external airlock for EVA capability for twelve 6.5-hour extravehicular activity (EVA) events and it can dock to the COV for crew

transfer. It is pressurized at 101 kPa and 21% oxygen. The length is 7.45 m and the diameter is 7.2 m. The target gross mass is 43 t.

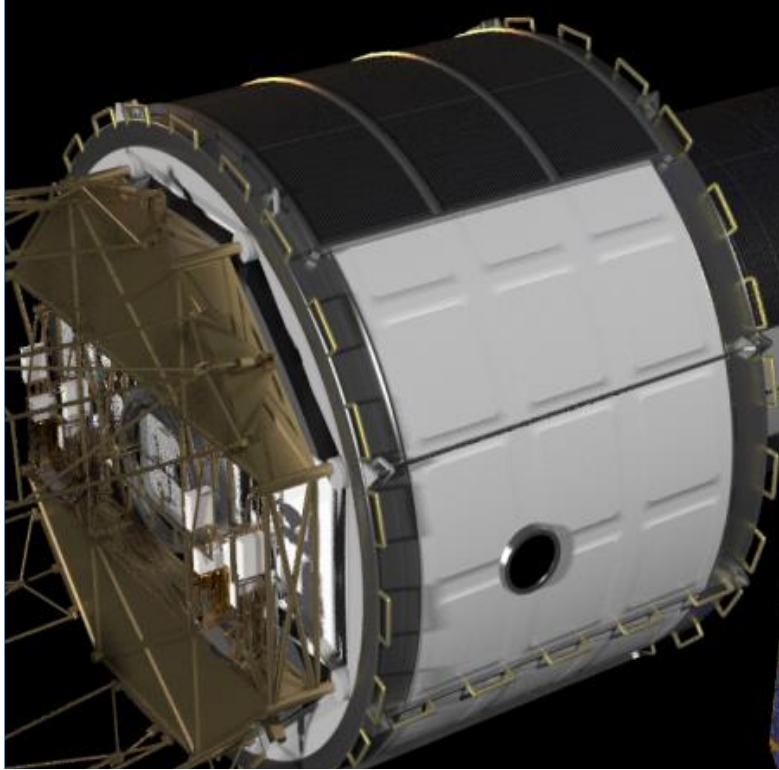


Figure 35. Concept of NASA EMC Crew Transit Stage (CTS) (Credit: NASA)

The MTCS will provide the thrust for the TMI burn and subsequent maneuvers. It is used for all stacks sent to Mars and uses CH_4/O_2 for propellants since that will provide an option to use the empty stages at Mars for potential refueling with ISRU propellants. This was not studied in Phase I but is a consideration for Phase II. The MTCS is also required in the RCV stack in order to provide ballast during scooping operations. After reaching LMO, the MTCS is subsequently boosted up to HMO by the RCV via SEP in order to repeat the atmosphere-scooping operations. Another MTCS is also used for the return journey from Mars to Earth, so it must loiter for 1.5 years in HMO. This implies zero boiloff of the cryogenic propellants, which is easier to achieve with CH_4/O_2 than H_2/O_2 . In Phase I, this was not considered in detail; and more work will be done in Phase II to define solutions to the performance needs.

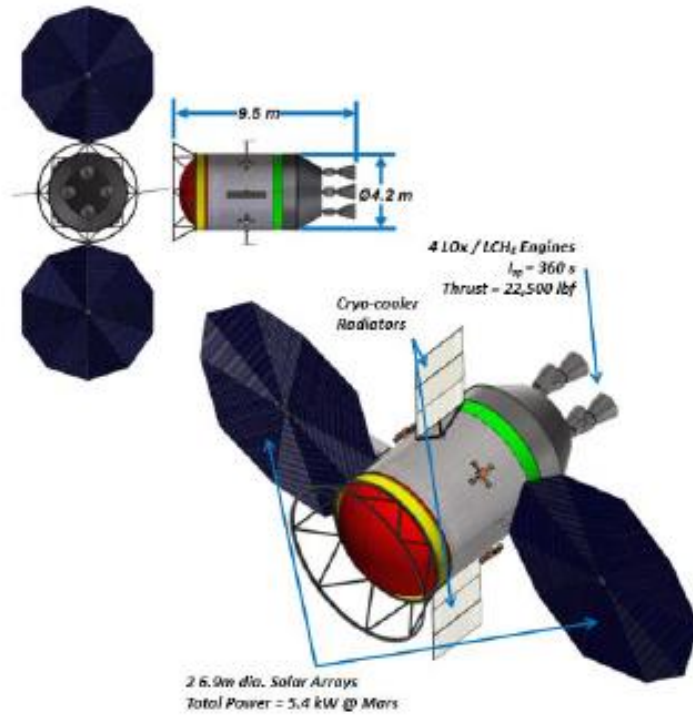


Figure 36. Concept of typical NASA Mars Transport Cryogenic Stage (MTCS) from the EMC. (Percy et al., 2015)

6.2 Resource Collector Vehicle (RCV)

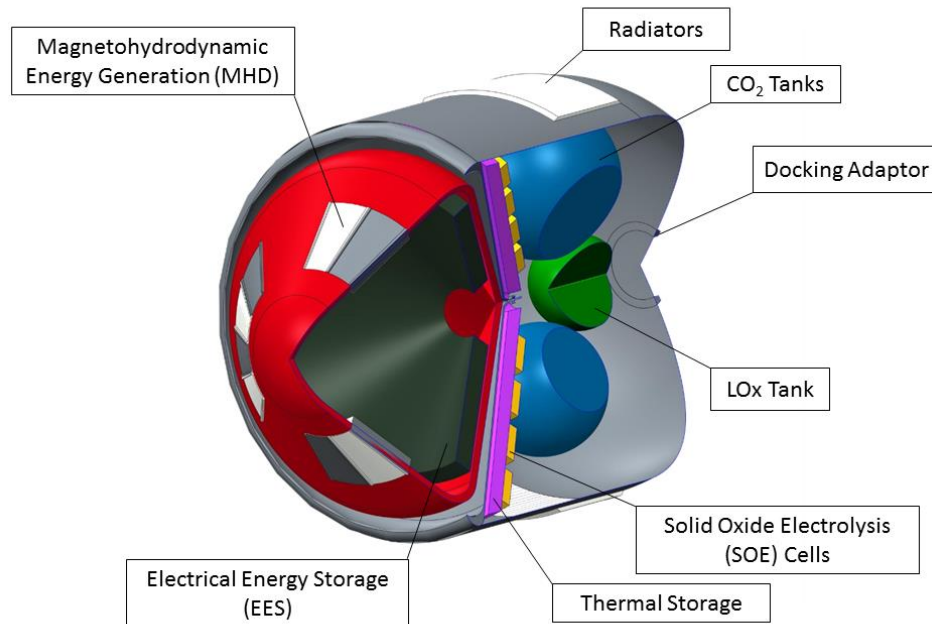


Figure 37. Resource Collector Vehicle with major systems.

6.2.1 Spacecraft Systems and Operations

The RCV is designed to make use of the upper Martian atmosphere to produce two critical products: electrical energy and oxygen for EDL SRP. In Phase I, the RCV concept vehicle was studied for use in two mission scenarios: an unmanned Mars Sample Return (MSR) mission and a reference human landing mission.

The spacecraft systems are designed to achieve the collection and compression of CO₂ atmospheric gases at high Mars altitude (79 km) and high velocities at periapsis ranging from 3.57 km/s to 4.5 km/s. In addition, it is capable of the generation of electrical energy (MHD) and its storage (EES), the storage and use of CO₂ in SOE to produce oxygen, and the liquefaction, storage, and delivery of oxygen to the MDAV/SSRL vehicle docked with the RCV (Fig. 39) The MDAV/SSRL vehicle uses the oxidizer to perform EDL with SRP. The RCV also has a deployable augmented SEP system using solar power and the ESS which boosts itself and the MTCS back to HMO for a re-set of orbital mining operations.

6.2.2 Hypersonic Aeroshell Coupled with CO₂ Collection

The collection of gas and MHD energy occurs at hypersonic speeds within the continuum regime, requiring design guidance from hypersonic heat shield profiles with collection adaptations. Consequently, the critical aerodynamic heating loads can be reduced by using shapes with higher pressure drag and a blunted design (Allen, 1958). Likewise, to maintain a

controlled aerobraking and atmospheric dipping maneuver, the vehicle profile should also act to stabilize the spacecraft as it transitions from a free molecular to continuum flow regime (Button, 2009).

The Viking mission pioneered the use of the 70° sphere-cone to handle the hypersonic entry conditions at Mars. All subsequent missions to Mars have used sphere-cone designs (Prabhu, 2012), with cone half-angles between 45° and 70° to accommodate requirements for packaging, heating, drag, and stability (Tauber, 2008). The Deep Space 2 mission used a 45° sphere-cone, because of a desire for reduced drag (Braun, 1997) and a higher entry velocity. Our design aims to take advantage of this heritage geometry—a sphere-cone design that is guided by hypersonic aerodynamics. Furthermore, a desire for reduced drag has influenced the choice for a steeper half-angle, similar to that used for the Deep Space 2 mission vehicle. In Phase II, detailed analysis of vehicle aerodynamics will serve to further refine this design to accommodate the heating and structural constraints, while achieving our desired aerobraking maneuver objectives. The high-temperature boundary layer will also inform the specific geometry of the flow capture inlet in the detailed design.

6.2.3 RCV Geometry Justification

The resource collection vehicle has the objective of generating oxidizer from CO₂ collected in the Martian atmosphere using electrical energy supplied by MHD generation. The collection of gas and MHD energy occur at hypersonic speeds within the continuum regime, placing specific requirements on the shape of the aeroshell of the vehicle to endure thermal and structural loading. Considering these extreme conditions, the design of the collection structure must be guided by hypersonic heat shield profiles with adaptations for CO₂ gas and MHD collection. Under these conditions, the aerodynamic heating can be reduced by using shapes with higher pressure drag and a blunted design (Allen & Eggers Jr, 1958).

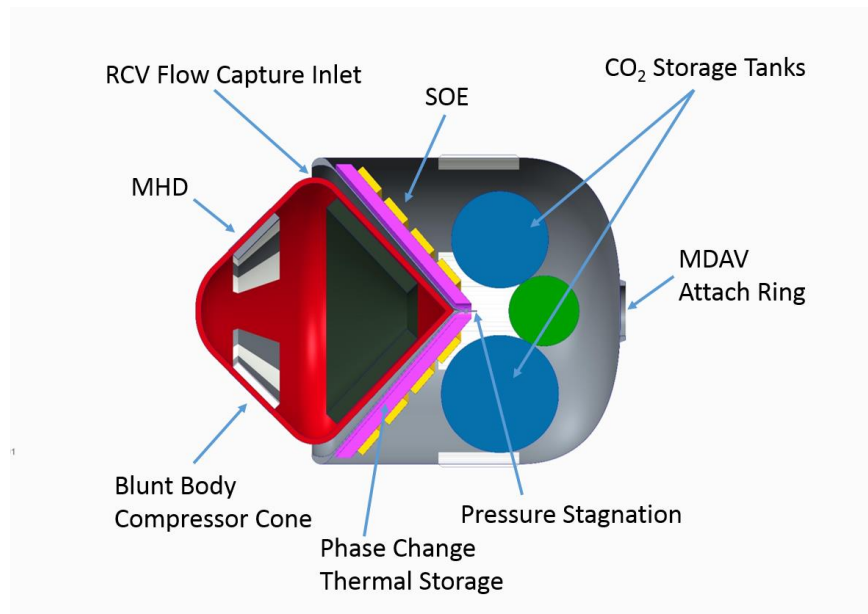


Figure 38. Cross section side view of RCV compressor cone and RCV.

Previous Mars entry vehicles have used sphere-cone designs with cone half-angles between 45° and 70° to accommodate requirements for packaging, heating, drag, and stability (Tauber and Wright, 2008). In order to maintain a controlled aerobraking and atmospheric dipping maneuver, the torque of the flow should also act to stabilize the spacecraft as it transitions from a free molecular to the continuum flow regime (Button et al., 2009). Following the derivation provided by Button et al. (2009), the torque imparted on the vehicle in both regimes can be approximated for the generalized heat shield shape depicted in Figure 39 in polar coordinates, represented by the function $r = f(\theta)$. The angle of attack, Φ , presumed to be small, is used in derivations of the torque, using Newtonian impact theory and free molecular theory (Regan et al., 1993) for both continuum flow and FM flow, respectively. Using calculus of variations yields an equation for the profile of the heat shield, which is invariant in torque for small angles of attack. This universal shape is depicted, as a numerical solution to the detailed equation, in Figure 40.

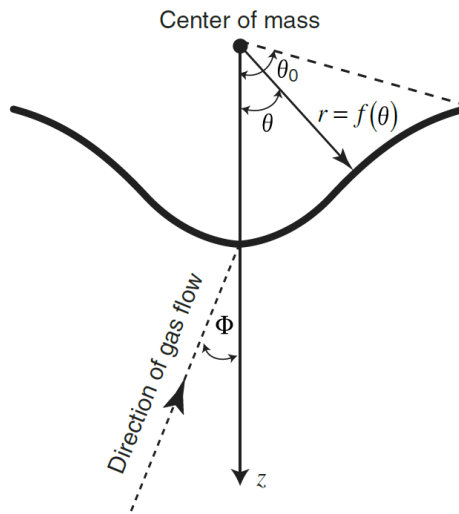


Figure 39. General heat shield geometry, defining coordinate system and gas flow angle Φ relative to the vehicle reference (Button et al., 2009).

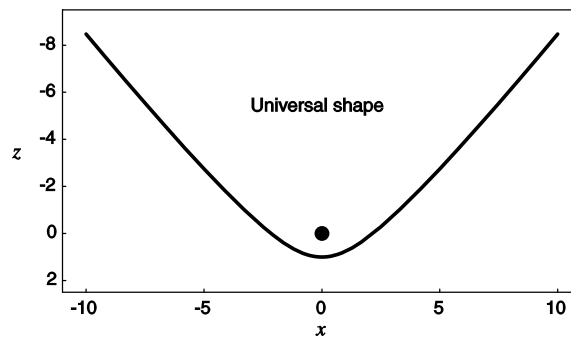


Figure 40. Universal heat shield shape with the center of mass as reference and the distance from the CM to the front of the heat shield as the unit length (Button et al., 2009).

Depending on the chosen nose radius, this shape can be approximated by a sphere-cone shape as used in previous atmospheric entry vehicles. The entry vehicle for the Mars Exploration Rover

missions used a 70° sphere-cone shield as shown in Figure 41, with the universal curve overlaid.

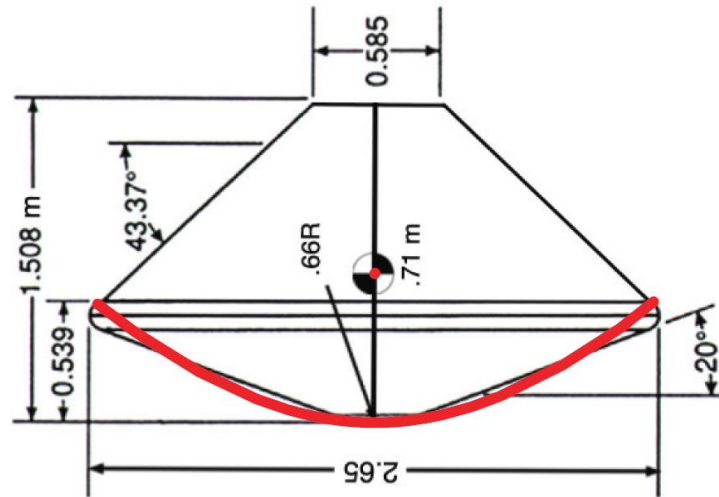


Figure 41. Mars Exploration Rover entry vehicle design with the universal heat shield shape overlaid (Davies & Arcadi, 2006).

The Viking mission pioneered the use of the 70° sphere-cone to handle the hypersonic entry conditions at Mars. All subsequent missions to Mars have used this design (Prabhu and Sanders, 2012), except for the Deep Space 2 mission, because of the desire for reduced drag (Braun et al., 1997) and a higher entry velocity. Our design aims to take advantage of this heritage geometry of a sphere-cone design that is guided by hypersonic aerodynamics. Furthermore, a desire for reduced drag has influenced the choice for a steeper half-angle, similar to the Deep Space 2 mission vehicle.

Detailed analysis of vehicle aerodynamics will serve to further refine this design for the heating and structural constraints, while achieving our desired aerobraking maneuver objectives. The high-temperature boundary layer will also inform the specific geometry of the flow capture inlet in the detailed design.

6.2.4 RCV Flow Capture Inlet

The concept for the RCV flow capture inlet (FCI) is that there is an annular gap between the outer edge of the sphere-cone heat shield/aeroshell and the inner edge of the RCV bus fairing. The aerodynamics of the blunt body create a shock wave and associated gas and plasma flow that will be channeled into the FCI at supersonic velocity. A converging annular cone cavity will further compress the incoming gases through momentum exchange from the high speed/high mass of the RCV stack. At the apex of the FCI cone cavity, a stagnation pressure will occur, at which point a check valve captures the high pressure CO₂ atmosphere gases in a previously evacuated capture tank. Subsequently the CO₂ is pumped into a storage tank, liquefied and the capture tank is reset with vacuum for the next scoping pass. As a point of reference, storing this carbon dioxide in liquid form would require approximately 1.5 megajoules per kilogram (Moses et al., 2005), so with our large surplus of MHD energy this seems very feasible. This design is a

concept and further work is required to validate it, including computational fluid dynamics (CFD) modeling and other analysis such as structural, thermal, and mechanical considerations.

6.2.5 Heat Transfer and Storage

Because the kinetic energy interaction with the atmosphere creates frictional heat, and large amounts of energy are converted into heat because of friction with the Mars atmosphere, there is an opportunity to use this heat for beneficial applications. The SOE system needs to run at 800–900 °C, but most of the SOE processing will happen after the scooping operations. In order to avoid the inefficiencies of converting heat energy to electrical, storing it in batteries and then converting it back to heat while in a circular LMO, the heat is stored in a phase-changing material such as a molten salt or liquid metal in order to release it for SOE operations in LMO. The phase-changing material can be packaged at the bottom of the blunt body sphere, which will be next to the SOE stacks that can be mounted on a bulkhead for a direct conduction path to the SOE stacks via conductive metal plates. The heat can be channeled from the front of the blunt body to the phase-changing material via heat pipes. By storing heat energy in this way, heat from the electrical battery system will be off-loaded and overall system efficiencies will increase. Further work is required in Phase II to validate and expand on this concept.

6.2.6 Magnetohydrodynamic (MHD) Energy Generation

The high kinetic energy of a spacecraft entering an atmosphere, which is traditionally converted into the heat of reentry during friction with the atmosphere, constitutes an energy resource. This rapid deceleration at hypersonic speeds results in the thermal ionization of the atmospheric gas in the shock layer. Numerous free electrons created in this process can be subjected to a magnetic field and their sustained collective motion used to generate an electric field. MHD systems are designed to create the magnetic field and collect the electrical energy generated (Figure 42).

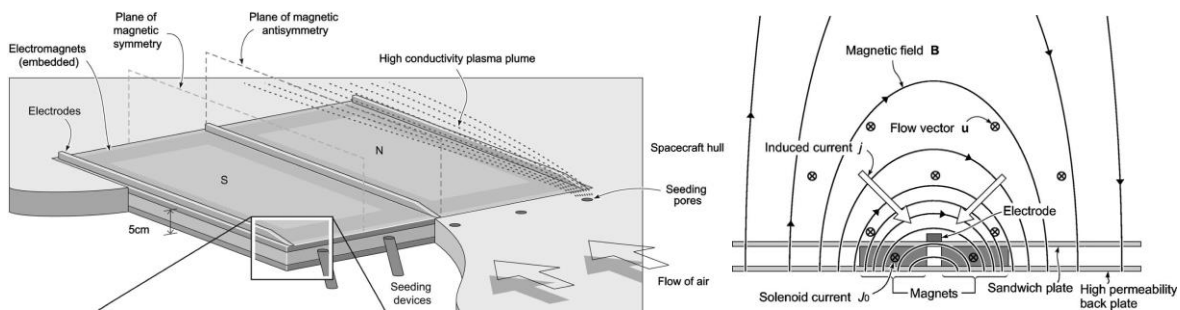


Figure 42. MHD concept design for spacecraft skin mounted on blunt body cone. Isometric view includes optional alkali metal seeding devices to increase plasma conductivity. Side view shows gas flow, magnetic field, and collected current (Steeves, 2007).

In Phase I, the energy produced by MHD was calculated using a model tool developed by Ali et al. (Ali, 2015 and 2016) to determine the values of key variables during each orbital pass through the Martian atmosphere. The total energy available via MHD energy generation is the integration of the power available for an MHD generator along a given trajectory. To calculate this power generation profile, it is necessary to identify the relevant physical interactions occurring along a given trajectory.

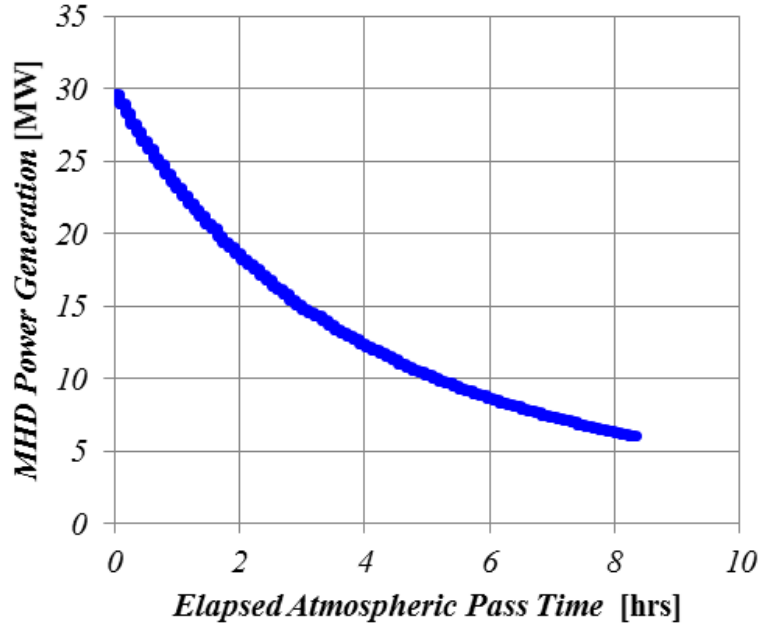


Figure 43. MHD power generation capability during atmospheric passes.

For a Faraday-type MHD generator, the generated power behaves according to the following scaling law:

$$P \propto \sigma_e u^2 B^2 A_c L_i \quad (11)$$

Where P is the generator power output, σ_e is the scalar electrical conductivity, u is the local flow velocity, B is the magnetic field strength, A_c is the generator interaction area, and L_i is the generator length (Moses, 2005.)

In reality, an open-channel Faraday-type MHD energy generator may be unsuitable for planetary entry applications because of the need to allow the high-temperature entry plasma to flow through the vehicle. However, the basic physics of Equation 11 applies to a non-flow through external MHD energy generator design applicable to planetary entry vehicles and thus may be used in this analysis (Steeves et al., 2007). For the purposes of this analysis, the magnetic field strength will be assumed in all cases to be a constant 0.2 T as studied in previous investigations (Steeves et al., 2007; Macheret et al., 2004.) The generator area is assumed to be 1 square meter in all cases, with a characteristic length of 1 meter in order to change its scale up and down in the model. These MHD external generator plates are mounted on the front of the blunt body cone section where a high plasma flow field is expected. In Phase II, our NIAC project will work synergistically with H. Ali’s doctoral research at Georgia Tech on experimental performance assessments of MHD energy generation for planetary entry applications. Our work will advance the state-of-the-art of MHD modeling to evaluate its practical limits in our application. We will also perform a mass and power trade between the integration of one fission surface power (FSP) equivalent unit on board an RCV vs. the MHD + electrical storage. Risks and costs will be evaluated for both systems, including radiation shielding requirements needed on board in proximity to the MDAV/SSRL.

All RCV technologies were derived from the first-order principle and evaluated for feasibility: heat storage phase-change material, RAM compression, CO₂ liquefaction, O₂ liquefaction and storage, propellant transfer, automated AR&D, high-temperature non-ablating materials, GN&C, control authority, and reusability. More work is required in Phase II to increase fidelity of the analysis and related conclusions

6.3 Mars Descent & Ascent Vehicle/Single-Stage Reusable Lander

6.3.1 Spacecraft Systems and Operations

The MDAV/SSRL is designed to execute multiple landings and launches at Mars during a given campaign; it is intended to serve as a safe and reliable Mars transportation element to ferry cargo and crew to and from the Mars surface. The MDAV/SSRL is initially docked with the RCV in the atmospheric mining stack through a docking hatch at top of the MDAV/SSRL ogive fairing. The docking port also provides a propellant-transfer capability from the RCV via umbilical plate connectors. The ogive structure is designed to perform as a launch fairing during a Mars launch as well as an Earth launch on a heavy-lift launcher payload stack.

In principle, the spacecraft systems are designed to achieve maximum reusability through the use of a deployable carbon-fiber polymer matrix composite material aerodynamic deceleration non-ablating system, followed by SRP. An accordion-style webbing is deployed between aerobrake petals made from high-temperature carbon fiber as a 3D woven cloth with battens (Figure 45).



Figure 44. Stowed configuration for launch from Earth.

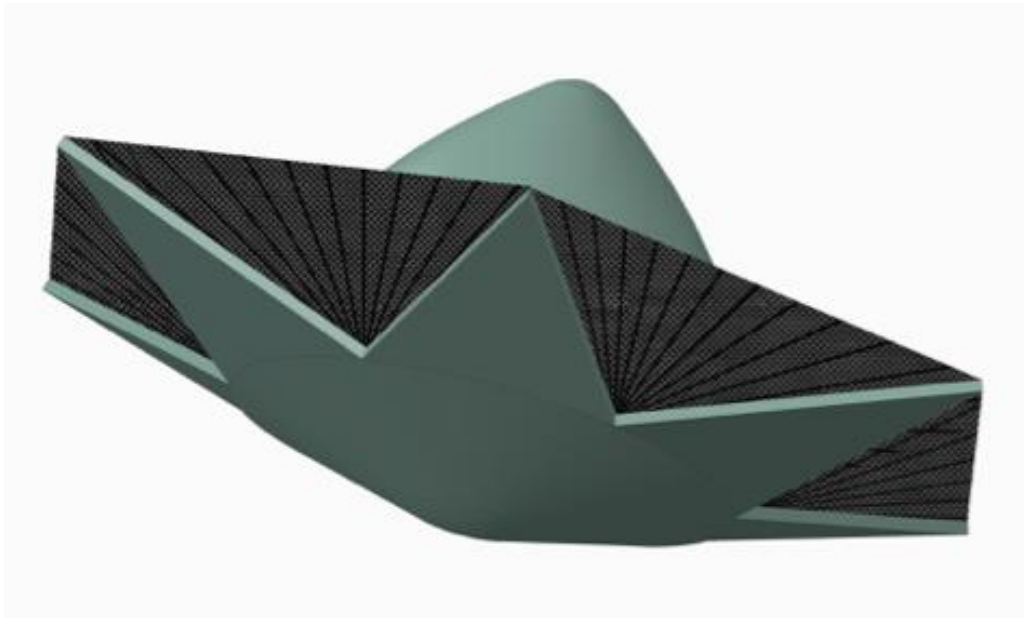
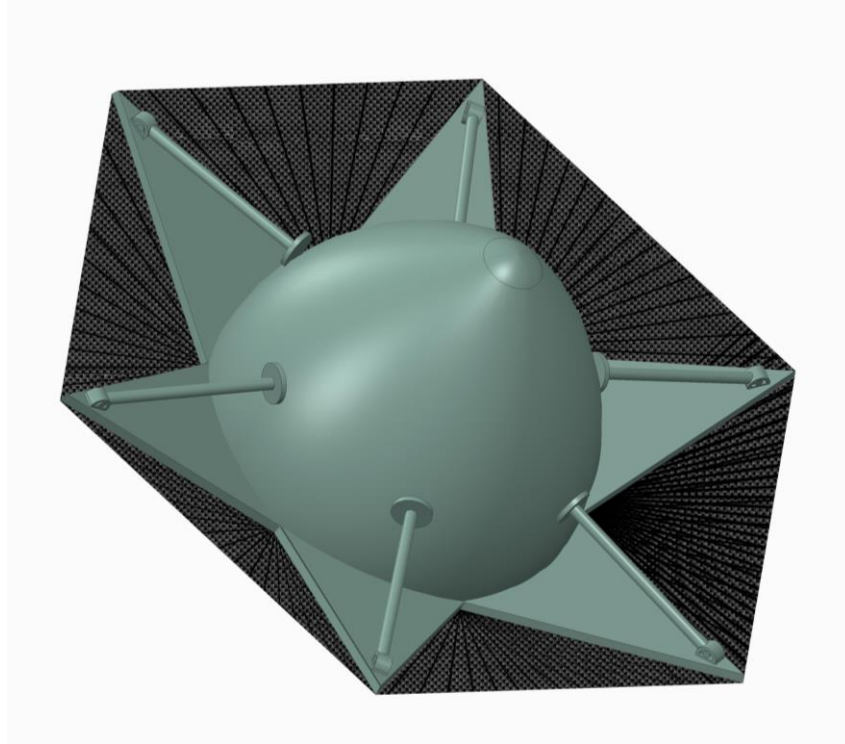


Figure 45. MDAV/SSRL decelerating aerodynamically at Mars with recessed SRP engines (top and bottom isometric views).

The retropropulsion engines are stored behind bay trapdoors while the trapdoors are also deployed as thrust vectoring surfaces for protection of the lander structures from ejecta and cratering during terminal phase landing. In the landing configuration, the webbing forms a skirt to protect other surface infrastructure elements from ejecta. The structure of the morphing aerobrake system becomes the landing gear with six legs spanning very wide to provide stability

and straddle the blast erosion area. Previous lander concepts in the literature and in NASA studies have not been able to reconcile a deployable aerobrake with deployable landing gear that must protrude through a heat shield, which is undesirable. This MDAV/SSRL concept solves the landing gear protrusion issue, and even creates an innovative aerobrake while using the legs as structural braces. By incorporating the landing gear, aerobrake and engine blast protection functions all into one system, significant mass savings and risk reduction could be achieved.

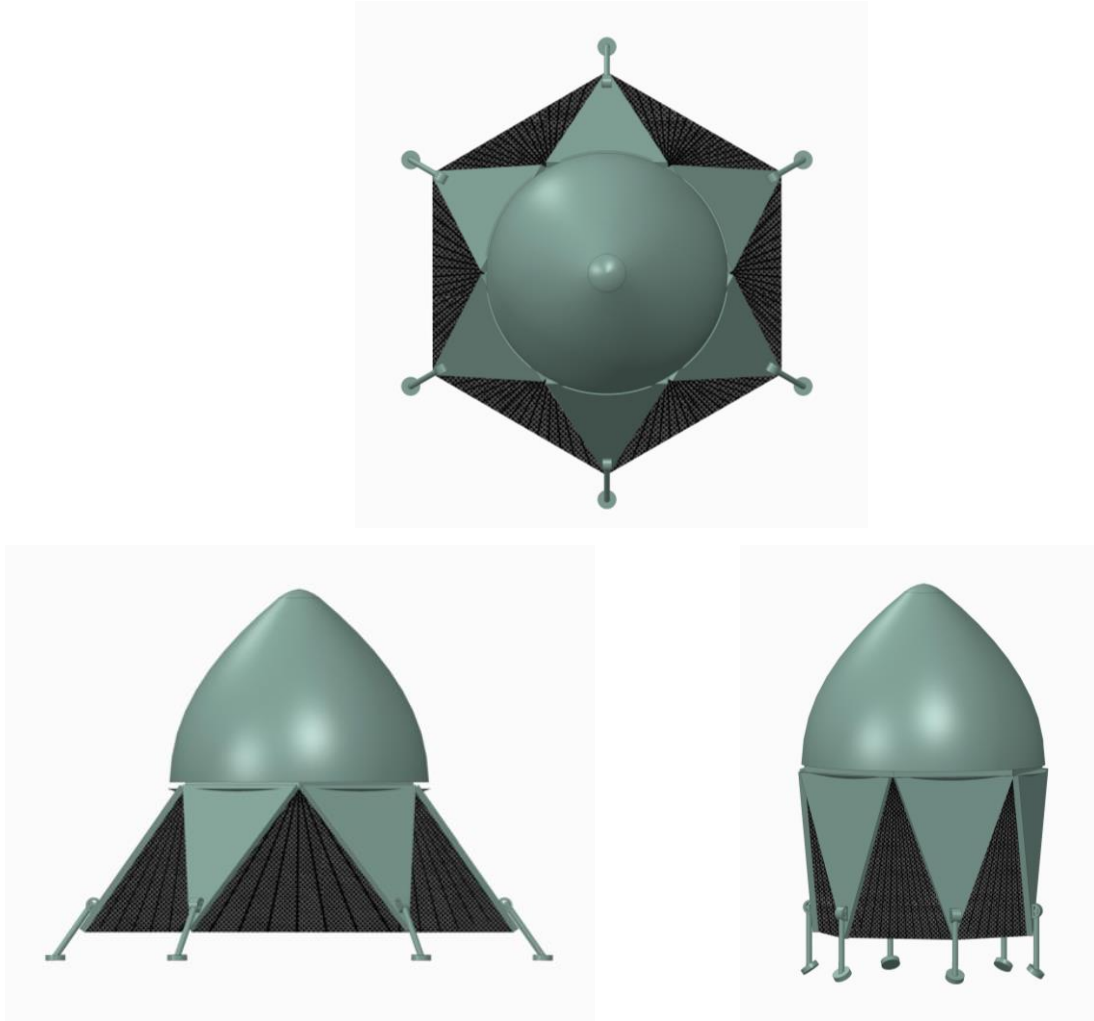


Figure 46. Configuration for landing at Mars (top and left) and for ascent from Mars after launch (right).

Once the MDAV/SSRL has landed, then cargo unloading is an issue on most Mars lander concepts due to the height of the lander. In our concept the landing gear can rotate to provide a “kneel down” capability for cargo offloading. The propellant tanks are packaged above the cargo bay so that the cargo can roll out onto the surface with the aid of a lightweight deployable ramp, which can be supported by the aerobrake petal structures, eliminating additional mass.

During Mars launch the entire aerobrake/skirt system can be vectored to a vertical configuration to allow a streamlined launch to take place. While Phase I only included first-concept analysis

focused mainly on mass and volume of the MDAV/SSRL, our Phase II work will develop the MDAV/SSRL systems based on expected performance, adherence to design standards, and ability to integrate with the other elements. A more rigorous Mars launch model will be developed to assess viability of the MDAV/SSRL concept, with assistance from Tara Polsgrove of the Lander Design Group at the NASA Marshall Space Flight Center (MSFC), who will be consulted for this project. Single-stage-to-orbit launch vehicles are notoriously difficult to achieve due to the low payload mass fractions involved, in addition, reusability incurs additional mass penalties. Figure 45 below shows that the Hercules study MDAV/SSRL propellant mass fraction (PMF) achieved ~79% with an assumed heat shield mass fraction of 10%. The resulting launch stage wet mass is 95 t for Hercules. The same SSRL carries a 20 t payload to the surface of Mars. (Arney et al, 2010)

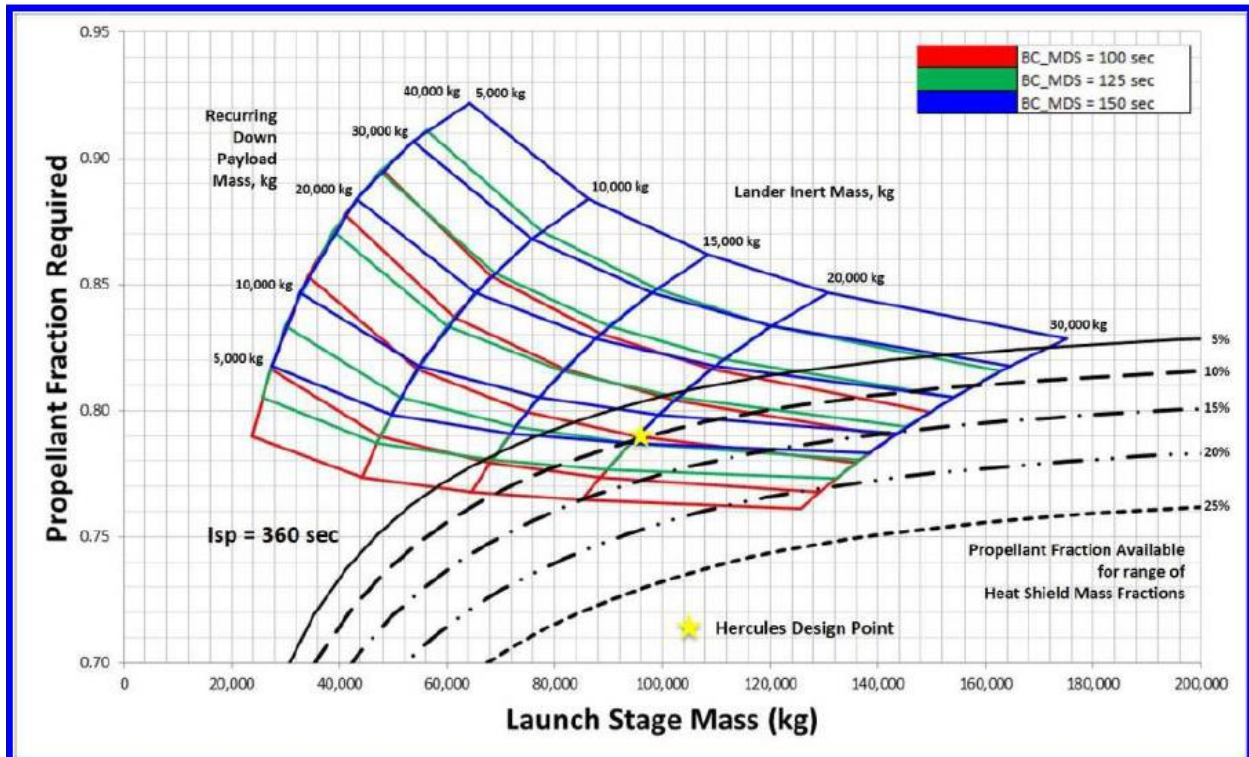


Figure 47. Comparison of required and available PMF for Hercules SSTO design space.

In our study, we use parameters similar to those used for Hercules, which allows for comparison and benchmarking. At liftoff, the Hercules MDAV/SSRL has a mass of 94 t, which includes the ISRU propellant used. The inert mass of the MDAV/SSRL is 18 t, and the recurring landed payload capacity is 20 t. The MDAV/SSRL requires an ascent crew cabin, which NASA studies have shown to be between 3 t and 4t. To be conservative, we use 4 t, which leaves 16 t payload available for other cargo to be landed, or 20 t can be landed in the cargo lander version. Orbital maintenance requires 0.46 t of propellant, and deorbit and entry orientation require 1.3 t. For the EDL of our lander, 8.5 t of propellant is required (6.98 t O₂ and 1.52 t CH₄).

Calculations show that the CH₄/O₂ propellants required to raise the MDAV+ CH₄ for EDL (25 t) from LMO to HMO amounts to 11.3 t of ISRU propellant made on the surface, which must be launched in the MDAV/SSRL and used for an orbit-raising burn. This indicates that the Mars

NIAC FY16: Mars Molniya Orbit Atmospheric Resource Mining

Molniya architecture lander dry mass would be larger than the Hercules lander dry mass (Table 15) to account for the extra tank mass and associated structure. When analysis is performed to size the MDAV/SSRL launch propellants mass needed to launch 11.3 t of propellant with a 25 t MDAV/SSRL (36.3 t total) at launch, the result is 110.9 t of CH₄/O₂. When the propellants and lander masses are summed the resultant MDAV/SSRL liftoff weight is 147 t, which is feasible but larger than existing concepts.

Table 15. Reference: Hercules Lander Inert Mass Breakdown

Stage Inert Mass Breakdown	Mass, kg	Comments
Dry Mass w/ Growth	15,156	
Structures	4,377	
Primary	1,244	8.8 m diameter; composite structures
Secondary	304	5% of total structure mass
Tank Support	386	0.5% of supported tank + propellant mass
Payload Support	500	2.5% of supported payload mass
Thrust Structure	606	Composite structure
Landing Legs	1,338	3.5% of landed mass
Deployable Heat Shield	4,496	10% of entry mass
Main Propulsion System (MPS)	3,738	
Fuel Tanks & Feed	1,127	4 fuel and 2 oxidizer cylindrical aluminum-lithium tanks at 275 kPa w/ MLI for passive thermal control on-orbit
Oxidizer Tanks & Feed	1,155	
Pressurization Systems	107	Autogenous system using engine heat exchanger
Engines	1,349	4 x 334 kN pump-fed engines delivering 360 sec Isp
Reaction Control System (RCS)	478	
Fuel Tanks & Feed	149	8 x 1,550 kPa spherical graphite-wrapped aluminum tanks w/ MLI for passive thermal control on-orbit
Oxidizer Tanks & Feed	188	
Pressurization Systems	8	2 x 41 MPa spherical graphite-wrapped aluminum tanks
Thrusters	134	16 x 445 N pressure-fed thrusters delivering 325 sec Isp
Power, Thermal & Avionics	677	
Solid Oxide Fuel Cells	116	3 x 2 kW; consumables scavenged from MPS residuals
Power Mgmt & Distribution	91	400 Hz, 115 volt AC w/ 10 kW peak power @ 90% eff.
Heat Acquisition & Transport	176	Ammonia fluid loop collecting 6 kW heat
Heat Rejection	95	Body-mounted radiator rejecting 6 kW
Command & Control	44	
Guidance & Navigation	47	
Communications	74	
Cabling & Instrumentation	35	
Mass Growth Allowance	1,391	15% of dry mass
Unusable Propellants	2,980	
RCS Reserves	197	5% of usable propellant
RCS Residuals	79	2% of usable propellant
RCS Helium Pressurant	38	
MPS Residuals	2,165	3% of usable propellant
MPS Boiloff	0	
MPS Autogenous Pressurant	501	
Inert Mass	18,136	

In Phase II, the architecture will be revisited to see if other ConOps are feasible, perhaps with other elements or combinations. Note that in our ConOps, shown in Figure 4, the MDAV/SSRL is launched and delivers the crew directly to HMO while the RCV and MTCS stack are raised using an integrated and augmented SEP system that uses the RCV EES as well as solar power with deployed photovoltaic panels and electric thrusters.

Since the propellant is all made via ISRU, the lander has empty tanks during the down trip and is capable of delivering similar cargo mass as Hercules can. However it must make substantially more propellant than Hercules to account for raising the MDAV/SSRL back to HMO with 1.5t of CH₄ for EDL. Packaging and volumetric aspects of the MDAV/SSRL must be examined but this is deferred to Phase II. It is envisioned that our initial concept shown here could evolve into a stretch version of the MDAV/SSRL concept CAD model shown in Figure 44, Figure 45, and Figure 46. The ogive section can be raised, and a cylindrical section can be added to accommodate the propellant tanks. The cylinder is a parametric feature that can be expanded or contracted as needed by the sizing models. In Phase II an integrated analysis model will drive the CAD model to generate a realistic and data-driven CAD model.

The crew must be returned to HEO for the journey home, so using ISRU propellants for transportation to HMO allows for a truly reusable system while Hercules remains in LMO and the transportation propellant for the crew must be brought from Earth and stored for 1.5 years in LMO in a separate crew taxi vehicle. These trades and cost/benefits will be examined in Phase II.

The MDAV/SSRL could use modular common CH₄/O₂ rocket engines as shown in Figure 28 that are scaled up in size to 334,000 kN. With a liftoff wet mass of 147 t and a thrust of 0.7 Earth *G*'s needed (Arney et al., 2010), this results in 3 334,000 kN engines being required for an MDAV/SSRL launch. Since four engines are needed in the landing phase, this would provide an engine-out capability during launch, which makes the system much safer for the crew going back home.

7. TECHNOLOGY ROADMAPS

This novel Mars mission architecture involves a large number of technologies, most of which are developed under other NASA programs beyond the scope of this study. The notional roadmaps below focus on the key technologies of our revolutionary concept.

7.1 Reusable Hypersonic CO₂ Collector and MHD Energy Generator

- TRL 1-3: Higher fidelity CFD simulations for specific entry conditions and vehicle for MHD generator panel (NIAC Phase II scope)
Advanced Multiphysics modeling for physics-based designs (begins in NIAC Phase II)
- TRL 3-5: Experiments to test performance curves of ~2.5 cm. flat single panel (NIAC Phase II)
Progress to multiple flat panels to 1 m scale
Progress to multiple panels on vehicle aeroshell profile
Full-scale gas velocity experiments (e.g., hypersonic shock tube w/artificial ionization)
- TRL 6-7: Sounding rocket tests (accelerated downward entry in Earth upper atmosphere)
ISS-release experiments or “booster stage” payload experiments for long duration tests
- TRL 8-9: Operational technology demonstration with MSR

7.2 Fast-Charging Electrical Energy Storage (EES) and Augmented Solar Electric Propulsion (SEP)

The development of EES will leverage heavily on the rapid advances at various scales of several technologies in industry such as electric vehicles, off-grid power storage, and superconducting magnetic storage. The EES may be able to store enough energy to augment an orbit raising SEP system as well. This needs to be investigated in Phase II.

- TRL 1-3: Development of updated EES performance analysis tool with current technologies (Phase II)
 - Assessment of feasibility and packaging of an EES-augmented SEP system
 - Investigation of potential technologies under Mars aerobraking conditions (low/high temperatures, charge decay profiles) (NIAC Phase II scope)
- TRL 3-5: Experiments with optimal power extraction (technology coupling with MHD)
 - Advanced modeling for parametric analysis
 - Development of power management and distribution for large in-flight EES
 - Development of a concept for an EES-augmented SEP system
- TRL 6-7: Integration experiments in Earth upper atmosphere: ISS-release or “booster stage”
- TRL 8-9: Operational technology demonstration with MSR

7.3 Large-Scale Solid Oxide Electrolysis (SOE)

The development of large-scale solid oxide fuel cells (SOFC) in industrial applications for hydrogen production and energy storage is expected to set the pace for space applications of technologies such as the one studied in our NIAC.

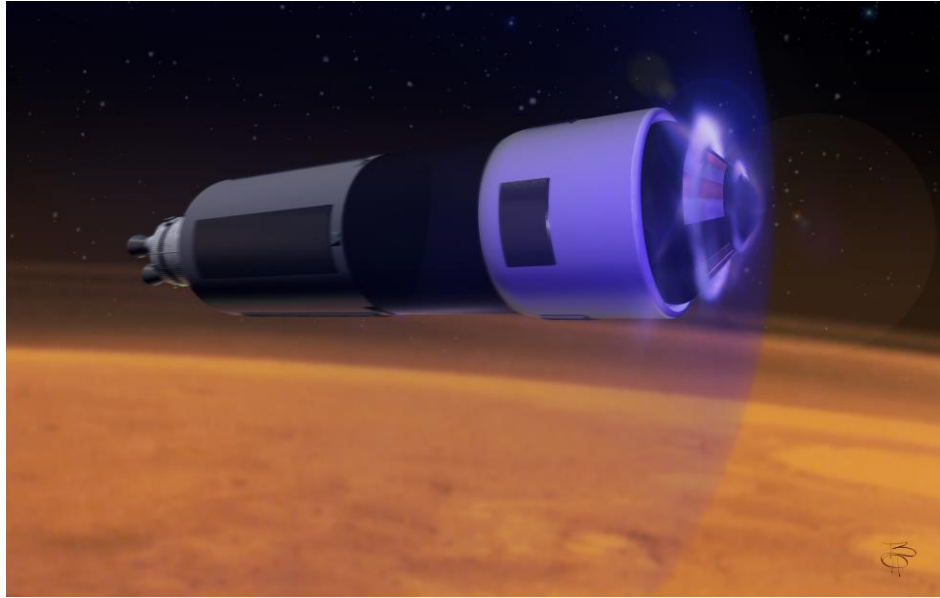
7.4 Mars Descent Ascent Vehicle

Technology Area	Major Technical Challenges
Propulsion	<ul style="list-style-type: none"> • Developing large engines capable of throttling with sufficient thrust for human-scale payloads (300s of kN) • Demonstrating reliable engine startup and throttling to 10 % against supersonic flow
Aerodynamics/ Aerothermodynamics	<ul style="list-style-type: none"> • Understanding and predicting SRP aerodynamics (static and dynamic forces and moments) and aerothermodynamics (surface heating) • Developing and validating CFD models and tools needed to build full-scale aerodynamics and aerothermodynamics databases
GN&C	<ul style="list-style-type: none"> • Developing algorithms and systems to dynamically control and stabilize the entry vehicle in the presence of complex fluid dynamic interactions

NIAC FY16: Mars Molniya Orbit Atmospheric Resource Mining

<p>Integrated Systems, Engineering and Analysis</p>	<ul style="list-style-type: none"> • Configuring the SRP engines on candidate entry vehicle geometries to satisfy the required system performance • Packaging the propulsion system within the volume and mass constraints of the EDL system • Verifying and validating the integrated SRP system performance models (propulsion, flight mechanics, aerodynamics, aerothermodynamics, GN&C, thermal, structural) • Developing entry trajectory simulations using validated models
<p>Analytical Models</p>	<ul style="list-style-type: none"> • Validating all models that feed into entry system SRP configuration and performance analyses (mass, engine performance, aerodynamics, flight mechanics, etc.)
<p>Ground Testing</p>	<ul style="list-style-type: none"> • Testing in ground facilities that can achieve relevant environments for engine, aerodynamics, and aerothermodynamics experiments • Providing a database for validation of analytical methods (e.g., CFD)
<p>Flight Testing</p>	<ul style="list-style-type: none"> • Successfully executing stable and controlled instrumented flight tests at sufficient scale and complexity to satisfy TRL 5 and 6

8. SUMMARY OF THE MARS MOLNIYA ORBIT ATMOSPHERIC RESOURCE MINING CONCEPT



While ISRU has been proposed on the surface of Mars, using atmospheric mining of resources while in orbit is a new and innovative concept. This study has examined the case for a reusable Mars space transportation system that can repeatedly launch and land on Mars, without ever relying on transportation of propellant from Earth by using propellant and electrical energy generated on orbit via plasma-harnessing, scooping, and ram-compressing the 95% CO₂ Martian atmosphere, and by using indigenous resources on the surface of Mars (CO₂, H₂O) as well for the launch and landing mission segments. The concept was investigated in the context of an enabling architecture with an associated concept of operations, mission elements, and technologies needed.

In Phase I we showed that a 4-crew reusable Mars lander human class mission can be supplied with LO₂ in Mars orbit prior to executing a supersonic retro-propulsive EDL to the surface. A Resource Collector Vehicle (RCV) performing 81 orbital scooping passes into the upper Martian atmosphere, with each atmospheric scoop varying in duration from 7.1 minutes to 5.3 minutes, can ingest approximately 431 kg of CO₂ per scoop and compress it via a hypersonic ram compression system. The total amount of CO₂ captured and stored is about 34,939 kg. The use of solid oxide electrolysis and a conservative calculation of efficiency losses results in the on-board production of O₂ at an estimated 20% of the captured CO₂ mass - resulting in 6,986 kg O₂ for EDL propulsion to provide thrust for de-orbit, re-orient for entry, supersonic retro-propulsion (SRP) and propulsive precision landing. A concept has been developed and the scooping analysis indicates feasibility, but more detailed analysis and design scaling of technologies is required in Phase II to optimize it and work out details of the aerodynamics and compression thermodynamics. After the CO₂ has been captured, then it is processed into O₂ using solid oxide electrolysis, while in orbit. Subsequently the O₂ is used with CH₄ (that is brought from Earth on the first mission and then from the surface of Mars in subsequent missions) as propellants to enable EDL with SRP. Once landed, the MDAV is re-fueled with propellants made by surface ISRU systems and it launches directly to HMO and then repeats the cycle. The RCV stack is raised independently from LMO to

HMO via an onboard deployable augmented Solar Electric Propulsion (SEP) system. A crew exchange occurs at HMO every 26 months as a sustainable pioneering presence on Mars becomes reality.

An alternative trade was considered whereby the MDAV launches to LMO and does a rendezvous with the RCV and MTCS. Propellant brought from Mars on the MDAV was considered for the MDAV+RCV+MTCS stack LMO to HMO burn, but transporting this propellant through the ΔV of 4.2 km/s creates a large launch propellant penalty, which made the MDAV size prohibitive, so this method was rejected. A new way was found to raise the RCV + MTCS from LMO to HMO without using propellant from the surface of Mars. There is excess MHD electrical energy created during aerobraking, so if the energy can be stored, it could be used to augment a deployable SEP system that is part of the RCV. AT LMO the SEP is then used to boost the RCV + MTCS back to HMO, while the MDAV proceeds directly to HMO with less propellant requirements, so that it is feasible to bring the crew to the Crew Transit Vehicle (CTV) for a return to Earth without an intermediate docking maneuver, which decreases risk to the crew.

A variety of new technologies are required such as MHD electrical energy generation and storage, EES-augmented SEP, heat storage and release and deployable decelerators. The systems and technologies are listed in our roadmap in section 7.0, with proposed TRL development strategies.

Phase II efforts will focus on detailed analysis of the proposed technology concepts and other mission architectures. Our results will be benchmarked against these previous studies to show the relative benefits:

- Human exploration of Mars, NASA Design Reference Architecture 5.0 (Drake et al, 2010)
- Jet Propulsion Lab, “A Minimal Architecture for Human Journeys to Mars” (Price, 2015)
- NASA Langley Research Center, “Sustaining Human Presence on Mars Using ISRU and a Reusable Lander” (Arney, 2015)

A successful collaboration between NASA Swamp Works and Georgia Tech has created a team of experts that have developed a set of computer models that allow rapid simulations of various concepts and ideas. This systems model will be the basis for solving the challenges identified in Phase I. The “unknown unknowns” have been identified and are now “known unknowns,” forming a solid basis for further investigation in Phase II.

9. TECHNICAL CHALLENGES THAT REMAIN TO BE ADDRESSED IN FORWARD WORK

The following tasks and challenges were identified from the Phase I study and are listed below by mission phase. The most important and relevant challenges will be pursued in Phase II:

9.1 Launch and Near-Earth Assembly

- Refine launch manifest and associated payloads and propulsion stages.
- Assess ground operations impacts and ability to meet launch cadence requirements.
- Rendezvous and docking activities in HEO.
- Define and refine Earth departure astrodynamics and operations scheduling.
- Perform cryogenic propellants boiloff management.

9.2 Arrival in Mars system

- Aerocapture at Mars: Define operations and investigate dual-use heat shields on the RCV and MDAV. Aerocapture has never been demonstrated in spaceflight operations and involves high heat rates, autonomous flight, and targeting with high uncertainties in flight environment.

9.3 Mars Molniya Operations (orbital maneuvering, aerobraking, CO₂ collection and processing)

Aerobraking occurs in a hypersonic regime and involves potentially very high heating on edges, which must be modeled. Ingestion of CO₂ gas requires a hypersonic inlet that can ingest over a very large range of Mach numbers, and may need to be of variable geometry. Significant challenges exist in the engineering of gas deceleration and compression, adsorption into storage, and cool mixture without causing choking issues.

- Develop a nonlinear trajectory and optimization simulation/solver for the atmospheric scooping/aerobraking analysis. Determine pressures and velocities of CO₂ during scooping.
- Aerobraking: Computational fluid dynamics (CFD) of gas ingestion with reacting flow to understand chemical composition effects (will probably affect ingestion efficiency and MHD). Assess heat exchanger and gas storage. Perform structural assessment of inlet.
- Develop analysis methods for aerodynamics and thermodynamics modeling at the RCV inlet scoop.
- Develop a non-ablating blunt body sphere-cone heat shield/compressor cone for RCV CO₂ ingestion, compression and storage. Identify TPS of the cone.
- Capture compression, capture, and liquefaction system for CO₂.

- Develop large-scale SOEC designs (DoE heritage) and integrate them with thermal storage material for processing of the CO₂ into O₂. LOX cryogenic ZBO storage.
- Reduce mass of the RCV stack to reduce propellant requirements in the LMO→HMO boost mission segment,
- Develop analysis methods for external MHD energy generation, fundamental analysis.
- Computational fluid dynamics and some testing of experimental hardware have established the basic feasibility of generating power during a Mars entry. Identify potential need for plasma seeding during MHD energy generation.
- Develop energy storage solutions with extremely high energy (MW) being available during atmospheric scooping passes via plasma MHD, and rapid energy generation management. Identify potential charging impacts on spacecraft.

9.4 EDL, SRP at Mars

The current state-of-the-art for Mars EDL is 1– 2 t so everything above this threshold calls for new solutions. SRP has to be demonstrated at Mars, and many problems exist, including placement of nozzles, heating next to nozzles, interaction of plume exhaust products with the freestream and potentially higher heating rates on the forebody, changes in the vehicle's center of gravity with propellant usage, transition events between stages, flipping the drag skirt “out” for landing, terminal descent under a deployable decelerator, structural integrity of the decelerator and system integration and operational sequencing. Reusable heat shield technology that does not have to be maintained has never been developed.

- Perform heating assessment, perform reusable TPS and heat propagation calculations, and assess packaging of payload with retropropulsion system.
- Include terminal descent maneuver into EDL simulation. Perform landing/precision landing assessment.
- Assess design of the reversible deployable skirt and perform structural assessment.
- Investigate plume effects of the rocket engines during landing. Assess debris ejecta and mitigation via the MDAV skirt structure.

9.5 Mars Liftoff

- Refine Mars ascent model for RPSCL and MDAV. Trade single-stage and two-stage options, fly-back first stage option, and orbital targets for rendezvous with Earth transport. Assess design of the reversible and deployable skirt and perform structural assessment.
- Assess engine-out capability.

9.6 RCV Stack LMO to HMO maneuver

- Perform detailed architecture analysis to identify optimal orbital parameters and sequencing.
- Investigate rendezvous and docking with the CTV at HMO.
- Investigate use of an SEP module integrated with EES on board the RCV as an electrical energy source. Optimize MHD to generate sufficient excess energy for SEP.

9.7 Architecture

- Develop alternate ConOps and new elements if necessary.
- Develop cost estimates and cost-benefit analysis.
- Perform risk analyses.
- Investigate mitigating communications blackout during EDL by using high-power communications.
- Perform sensitivity studies and parametric studies.
- Enhanced software dashboard for an integrated computer model linked to a CAD model: Determine if rapid trades will be possible.
- Use high-speed computing for EDL simulations.
- Assess packaging and sizing of all mission element concepts. Develop Master Equipment Lists (MELs).
- Perform benchmarking against existing (already identified) studies for Mars human missions.

10. CONCLUSIONS

Mars Molniya Orbit Atmospheric Resource Mining was investigated in this NIAC Phase I project, in order to determine if it is feasible at all. Our NASA KSC Swamp Works/Georgia Tech Aerospace Department team has examined the case for a reusable Mars space transportation system that can repeatedly launch and land on Mars, without ever relying on transportation of propellant from Earth. This space transportation system uses propellant and electrical energy generated on orbit via plasma-harnessing, scooping, and ram-compressing the 95% CO₂ Martian atmosphere, and also uses indigenous resources on the surface of Mars (CO₂, H₂O) for the launch and landing mission segments.

The study considered the space missions that would be required to implement this system, and an associated space mission architecture was generated and tested by analysis. It shows that the concept can support a pioneering presence by humans on Mars with precursor robots deployed to prepare the ISRU aspects and robotic surface systems to keep the astronauts safe by autonomously making propellant from local resources in the atmosphere and regolith, for the journey home.

In Phase I of this NIAC study, two major applications for Mars Molniya Orbit Atmospheric Mining mission architecture concepts were studied. Both mission concepts are aligned with NASA's top priorities for Mars exploration in the next three decades:

- A path for further architecture and technology development and eventual implementation is proposed by proving this technology as part of an **ISRU/Mars Sample Return (MSR) demonstration mission**.
- The eventual goal for this revolutionary and breakthrough space mission architecture is to enable **landing humans (4 crew) on the surface of Mars with all associated equipment** needed to allow them to survive and thrive. This will require landing very large vehicles, from 20 t to 60 t in mass. A breakthrough method is required to make this technically and economically feasible.

Other solar system destinations and related space transportation systems have been deferred to Phase II of the study. It is likely that the same orbital resource mining architecture being developed for Mars in this study could also be viable at other outer Solar System destinations.

This study has concluded that atmospheric mining at Mars is feasible. In a human-class mission with 81 orbital scooping passes at 79 km altitude, with each atmospheric scoop varying in duration from 5.3 minutes to 7.1 minutes, at speeds ranging from 3.57 km/s to 4.5 km/s, approximately 431 kg of CO₂ can be ingested per scooping pass at periapsis. This can be compressed and stored by an RCV hypersonic ram compression system. The total amount of CO₂ captured and stored is about 34,939 kg, which is processed with the SOE chemical conversion process—resulting in 6,986 kg O₂ for EDL propulsion to provide thrust for deorbit, reorientation for entry, SRP, and propulsive precision landing.

The mission elements can all be delivered to Mars using the existing and projected SLS rocket in the 70 t payload version for a Mars sample return mission and the 105 t payload version for the human-class missions. The number of launches needed are comparable to other human Mars

mission studies, and less total mass is needed than in the NASA Mars DRA 5.0 reference architecture. The RCV vehicle is projected to achieve a full payback in terms of mass transported from Earth after two missions by making O₂ propellant on orbit, which eliminates the transportation stages and extra Earth launch operations and associated risk. After that, an Earth-independent Mars descent/ascent system for crew and cargo will be available at no further cost for transportation of mass from Earth. By amortizing the costs over the subsequent missions, substantial cost savings and mission flexibility can be achieved.

New technologies are required to make this concept feasible, such as HEO departures that use a lunar-gravity assist, aerocapture at Mars, atmospheric ram compression at hypersonic speeds, magnetohydrodynamic electricity generation and storage, large-scale solid oxide electrolysis to make O₂ from CO₂, phase-changing thermal storage materials, zero boiloff cryogenic storage, advanced deployable aerodynamic decelerator systems, novel lander configurations and designs, 10% throttling CH₄/O₂ rocket engines, supersonic retropropulsion, autonomous excavation and propellant production on the Mars surface, automated propellant loading systems, augmented solar electric propulsion systems, and automated rendezvous and docking. These are just some of the technologies needed; others are identified in our report and associated technology roadmap.

In conclusion, our study has shown that a novel architecture using Mars Molniya Orbit Atmospheric Resource Mining is feasible. This will enable an Earth-independent and pioneering, permanent human presence on Mars by providing a reusable, single-stage-to-orbit transportation system. This will allow cargo and crew to be routinely delivered to and from Mars without transporting propellants from Earth, therefore reducing the massive logistics burden facing human mission to Mars and giving flexibility to operations at Mars.

More work remains to be done in Phase II of this study to analyze the details. The NASA/Georgia Tech team has developed expertise and analysis tools that are ready to support further investigations of this exciting and revolutionary NIAC concept.

11. FORWARD WORK

Our Phase II work plan is presented in Table 15. The dates represented by NTP+X month indicate the expected start of the task and the team members involved. The percent effort for each personnel refers to percent of Level 1 Task total.

Table 15. Work Plan: Work Breakdown Structure (WBS), Resource Allocation & Schedule

Task	Key Milestone or Accomplishment	PI	Co-I	Collab.	Grad. St.
0.0	Start NIAC Phase II project – Notice to Proceed (NTP)				
1.0	Develop Mars Molniya ISRU Architecture – Phase II	33%	10%	31%	26%
1.1	Define key remaining unknowns, assumptions, risks & path forward	NTP+1 month	NTP+1 month	NTP+1 month	NTP+1 month
1.2	Trade Arch. ConOps from Phase I for Phase II selection	NTP+2	NTP+2	NTP+2	NTP+2
1.3	Define a Cis-Martian transportation system using in-situ MHD energy production & propellant production: depots	NTP+2	NTP+2	NTP+2	NTP+2
1.4	Evaluate integrating advanced propulsion: MHD for SEP orbit raising of RCV, SEP for cargo from Earth	NTP+7	NTP+7	NTP+7	NTP+7
1.5	Evaluate Mars – Earth Cyclers as a transportation method using Mars vicinity propellants to get on/off	NTP+12	NTP+12	NTP+12	NTP+12
1.6	Evaluate extensibility of orbital atmospheric mining to the rest of the solar system	NTP+14	NTP+14	NTP+14	NTP+14
2.0	Key Enabling Technology Modeling and Analysis	30%	5%	45%	20%
2.1	Refine Atmospheric and surface ISRU Model – Large scale SOE, etc.	NTP+2		NTP+2	
2.2	Develop advanced Mars Surface ISRU Model: water mining, Sabatier etc.	NTP+2		NTP+2	
2.3	Refine Orbital Mechanics Model – Mars Launch, Mars Aerocapture, Aldrin cyclers etc.	NTP+6	NTP+6		NTP+6
2.4	Advance Magneto-Hydrodynamic Model, create proof of concept testing devices in lab (synergy with PhD* - see section 1.3.3)	NTP+3	NTP+3	NTP+3	NTP+3
2.5	Modeling and experimental verification of MHD multi-magnet side-by-side configuration (synergy with PhD* - see section 1.3.3)		NTP+9	NTP+9	NTP+9
2.6	Create a MHD-EES performance model			NTP+6	NTP+6
2.7	Develop a method for passive heat storage in phase change material on orbit for SOE operation	NTP+3		NTP+3	
2.8	RCV & MDAV/SSRL stack hypersonics dynamics and design drivers, aerodynamics and heat loading of RCV configuration, pressure lines, velocities: Newtonian panel analysis to determine pressure aero loads on RCV. Thermal and structural requirements will come from this Aero analysis.		NTP+9		NTP+9
2.9	Refine the RCV aerobraking/scooping model for Mars Molniya Orbital Mining of CO ₂ atmosphere	NTP+3		NTP+3	NTP+3
2.10	Refine Entry, Descent & Precision Landing (ED&PL) modeling with Supersonic Retropropulsion (SRP) using POST & all available SRP data from recent tests	NTP+4	NTP+4		NTP+3
2.11	Develop Elements & Spacecraft concepts and CAD Models, sub-systems Master Equipment Lists (MEL).	NTP+6	NTP+6	NTP+6	NTP+6

NIAC FY16: Mars Molniya Orbit Atmospheric Resource Mining

	Define Mass, power, volume for each element & integrate them into a viable system concept and model				
2.12	Propellant trade study – non ISRU vs ISRU for quantitative impact assessment and gear ratio definition	NTP+5		NTP+5	
2.13	Rapid iteration analysis and optimization algorithms development for integrated system computer model	NTP+8	NTP+8	NTP+8	NTP+8
3.0	Perform Architectural Trade Studies and Sensitivity Analysis	30%	5%	45%	20%
3.1	Develop a dashboard that ties all the models together for efficient trade studies	NTP+7	NTP+7	NTP+7	NTP+7
3.2	Rapid iteration trade studies and analysis with optimization algorithms in integrated model	NTP+10	NTP+10	NTP+10	NTP+10
3.3	Sensitivity Analysis of architectures and element concept designs	NTP+10	NTP+10	NTP+10	NTP+10
3.4	Develop power profile for the surface and orbital operations	NTP+3		NPT+3	NPT+3
4.0	Final Reporting	30%	5%	45%	20%
4.1	Develop CAD concepts for RCV & MDAV/SSRL	NTP+4	NTP+4	NTP+4	NTP+4
4.2	Generate concept graphics and data visualization	NTP+9	NTP+9	NTP+9	NTP+9
4.3	Organize data and results of all analysis for a final system architecture definition with a technology roadmap and technology gaps identified	NTP+20	NTP+20	NTP+20	NTP+20
4.4	Write, Deliver, Present Final NIAC Phase II Report	NTP+22	NTP+22	NTP+22	NTP+22

12. ACADEMIC INVOLVEMENT AND ACKNOWLEDGEMENTS

The work performed during Phase I revealed many interdependent connections between the overall architecture, the local architectures at Mars, and the systems that build them; and it quickly became a multidisciplinary study rich in questions about multi-physics phenomena, chemical and energetic processes, as well as flight dynamics and more. Consequently, the association of NASA personnel and academic personnel at Georgia Tech was fully used to involve graduate students and young researchers in the study. Several face-to-face meetings were organized on the campus of Georgia Tech to stimulate concept brainstorming and rapid iterations of elements in the architecture. Doctoral candidates Keir Goneiya and Hisham Ali became full partners in the project and provided state-of-the-art expertise on orbital mechanics, aerobraking, EDL, and MHD and associated systems. Their contributions were guided by Co-I Prof. Bobby Braun, who is their doctoral advisor, and Co-I Dr. Brandon Sforzo, who also contributed his expert knowledge in hypersonic dynamics and atmospheric entry phenomena.

Hisham Ali is a doctoral candidate who has been supported by the NASA Graduate Student Researchers Project (GSRP). His funding is due to expire, and should Phase II be awarded, Mr. Ali's studies will be supported by a portion of the NIAC budget. This would be a continuation of NASA's investment in a promising future leader in the aerospace field.

In addition, PI Robert Mueller and Co-I Dr. Laurent Sibille gave an invited lecture to a special-topic class at Georgia Tech on surface ISRU systems and led a discussion on the applicability of these systems to advanced exploration architectures such as the one being studied in the Phase I work.

In Phase II, our team will continue these relationships with graduate students at Georgia Tech and will expand our outreach within the academic research departments through lectures and discussions. In addition, we will pursue opportunities to engage students and faculty in conversations about specific technologies within their field of expertise and studies that could increase the feasibility of the overall concept and would allow them to participate in the project. This outreach effort will also be expanded to include students at University of Colorado in Boulder, where Prof. Braun is now Dean of the Engineering Department.

We would like to acknowledge and thank the NIAC management team program officers at NASA HQ in Washington DC for their encouragement, support and understanding:

- **Jason Derleth**, NIAC Program Executive (PE): responsible NASA official, overall leadership
- **Alvin Yew**, NIAC Program Manager (PM): co-manager of NIAC programmatic
- **Ron Turner**, NIAC Senior Science Advisor: POC for any technical program or process issue
- **Kathy Reilly**, NIAC Strategic Partnerships Manager: POC for any media, event, outreach
- **Barb Mader**, NIAC Resources Administrator

NIAC FY16: Mars Molniya Orbit Atmospheric Resource Mining

At Kennedy Space Center (KSC), we would like to acknowledge and thank Mr. Bob Cabana, Karen Thompson, Josie Burnett, Jeff Smith, Khoa Vo, Nancy Zeitlin, Tom Moss, Carolyn Mizell, Tracy Gill, the members of the KSC Research and Technology Management Board (RTMB), and the outstanding team at the KSC Swamp Works.

At NASA MSFC, we would like to acknowledge and thank Tara Polsgrove and her team for consulting and technical advice related to Mars MDAV/SSRL.

At Georgia Tech, we would like to acknowledge and thank the Department of Aerospace Engineering and its faculty.

13. REFERENCES AND CITATIONS

- Ali, K.A., and Braun, R.D., (2015) “Effects of Magnetohydrodynamic Energy Generation on Planetary Entry Vehicle Flight Dynamics,” AIAA 2015-4179, Propulsion and Energy Forum, Orlando, FL, July 2015.
- Ali, K.A., Gonyea, K., and Braun, R.D., (2016) “Magnetohydrodynamic Energy Generation and Atmospheric Breathing SRP for Mars Descent,” IEEE Aerospace Conference, March 2016.
- Allen, H.J. and Eggers Jr, A.J., (1958) *A study of the motion and aerodynamic heating of ballistic missiles entering the Earth’s atmosphere at high supersonic speeds*, NACA.
- Arney, D.C., Jones, C.A., Klovsstad, J., Komar, D.R., Earle, K., Moses, R., & Shyface, H., (2015) “Sustaining Human Presence on Mars Using ISRU and a Reusable Lander,” AIAA SPACE 2015 Conference and Exposition, p. 4479.
- Braun, R.D., & Manning, R.M. “Mars exploration entry, descent and landing challenges.” *J. Spacecraft and Rockets*, 2007, 44, 310-323.
- Braun, R.D., Mitcheltree, R.A., and Cheatwood, F.M., (1997) “Mars microprobe entry analysis,” in *1997 Aerospace Conference Proceedings., IEEE*.
- Button, E.C., Lilley, C.R., Mackenzie, N.S., and Sader, J.E., “Blunted-cone heat shields of atmospheric entry vehicles,” *AIAA journal*, 2009, vol. 47, no. 7, 1784-1787.
- Byrnes, D.V., Longuski, J.M., & Aldrin, B., “Cycler orbit between Earth and Mars,” *J. Spacecraft and Rockets*, 1993, 30(3), 334-336.
- Capriotti, B., (2013) *PROFAC and PHARO: Changing Perceptions of an Idea in Aerospace*, Doctoral dissertation, Worcester Polytechnic Institute.
- Chen, H., Cong, T. N., Yang, W., Tan, C., Li, Y., and Ding, Y., “Progress in electrical energy storage system: A critical review,” *Progress in Natural Science*, vol. 19, 2009, pp. 291–312.
- Davies, C., and Arcadi, M., (2006) *Planetary mission entry vehicles quick reference guide. Version 3.0*, NASA-SP-2006-3401, NASA.
- Demetriades, S., “A Novel System for Space Flight Using a Propulsive Fluid Accumulator.” *Journal of the British Interplanetary Society* 17 (1959-60): 114-119.
- Demetriades, S.T., (1960) *Design and Applications of Propulsive Fluid Accumulator Systems*. Astro Systems and Research Laboratories. Northrop Corporation, Hawthorne, CA.
- Demetriades, S.T., and Kretschmer, C., (1958) *The Use of Planetary Atmospheres for Propulsion*. Aerojet-General Corporation, Azusa, CA.
- Drake, B., (2009) *Human Exploration of Mars Design Reference Architecture 5.0*, NASA-SP-209566, NASA.
- Drake, B.G., Hoffman, S.J., & Beaty, D.W., “Human exploration of Mars, NASA Design Reference Architecture 5.0,” IEEE Aerospace Conference 2010, 1-24.
- Drake B. et al, (2014) NASA/SP–2009-566-ADD2, Human Exploration of Mars Design Reference Architecture 5.0, Addendum #2

- Foster, C., & Daniels, M. (2010). Mission opportunities for human exploration of nearby planetary bodies. In AIAA SPACE 2010 Conference & Exposition (p. 8609).
- Gonyea, K., Auslender, A.H, and Braun, R.D., (2014) “Propulsion System Design for a Martian Atmospheric Breathing Supersonic Retropropulsion Engine,” AIAA 2014-3449, AIAA Propulsion and Energy Forum, Cleveland, OH, June 2014.
- Gordon, S., and McBride, B.J., (1994) “Computer Program for Calculation of Complex Chemical Equilibrium Compositions and Applications,” Cleveland, Ohio 1994.
- Jones, C., Masse, D., Glass, C., Willhite, A., & Walker, M., (2010) “PHARO—Propellant harvesting of atmospheric resources in orbit,” In 2010 Aerospace Conference, IEEE, 1-9.
- Kerr, R.A., “Hang on! Curiosity is plunging onto Mars,” *Science*, 2012, 336(6088), 1498-1499.
- Kim, M., and Boyd, I.D., “Effectiveness of a Magnetohydrodynamics System for Mars Entry,” *Journal of Spacecraft and Rockets*, vol. 49, 2012, pp. 1141–1149.
- Kleinhenz, J.E. and Paz, A., (2017) “An ISRU Propellant Production System to Fully Fuel a Mars Ascent Vehicle.” AIAA SciTech Forum 2017. American Institute for Aeronautics and Astronautics, AIAA-2017-0423.
- Macheret, S.O., Shneider, M.N., Candler, G.V., Moses, R.W., and Kline, J.F., (2004) “Magneto Hydrodynamic Power Generation for Planetary Entry Vehicles,” 35th AIAA Plasma Dynamics and Lasers Conference, Portland, Oregon, 28 June – 1 July 2004.
- Mahaffy, P.R., Webster, C.R., and Al., E., “Abundance and Isotopic Composition of Gases in the Martian Atmosphere from the Curiosity Rover,” *Science*, vol. 341, 2013, pp. 263–266.
- Morring, Frank Jr., “Data-sharing deal will help SpaceX land Falcon 9 on Earth and NASA put humans on Mars,” *Aviation Week & Space Technology*, Oct 20, 2014.
- Moses, R. W. (2005, February). Regenerative aerobraking. In M. S. El-Genk, & M. J. Bragg (Eds.), *AIP Conference Proceedings* (Vol. 746, No. 1, pp. 1361-1370). AIP.
- Moses, R.W., Kuhl, C.A., and Templeton, J.D. (2005). “Plasma Assisted ISRU at Mars,” 15th International conference on MHD Energy Conversion, Moscow, Russia, 24-27 May 2005.
- NASA Office of Chief Technologist, (2010) “Space Technology Grand Challenges,” available at https://www.nasa.gov/offices/oct/strategic_integration/grand_challenges_detail.html
- Obama, B.H., (2010), Speech on US Space Policy at NASA Kennedy Space Center, available at http://www.nasa.gov/news/media/trans/obama_ksc_trans.html
- Palaszewski, B., (2005), *Atmospheric mining in the outer solar system*, National Aeronautics and Space Administration Glenn Research Center, Cleveland, Ohio, October, NASA/TM-2006-214122.
- Palaszewski, B., (2007) “Atmospheric Mining in the Outer Solar System: Mission Scenarios and Options for In-Situ Resource Utilization,” in 43rd AIAA/ASME/SAE/ASEE Joint Propulsion Conference & Exhibit, p. 5598.
- Percy, T., McGuire, M., and Polsgrove, T. (2015). In-space transportation for NASA’s Evolvable Mars Campaign. In AIAA SPACE 2015 Conference and Exposition (p. 4519).

- Prabhu, D., and Saunders, D., "On Heatshield Shapes for Mars Entry Capsules," in *Aerospace Sciences Meetings*, AIAA 2012-0399, American Institute of Aeronautics and Astronautics, 2012.
- Price, H., Baker, J., & Naderi, F., "A Minimal Architecture for Human Journeys to Mars," *New Space*, 2015, 3(2), 73-81.
- Program to Optimize Simulated Trajectories 2 (POST 2), NASA Manual.
<https://post2.larc.nasa.gov/latest-version/>
- Rapp, D., (2008) *Human Missions to Mars: Enabling Technologies for Exploring the Red Planet*, Praxis Publishing, Chichester, U.K.
- Rapp, D., (2012) *Use of Extraterrestrial Resources for Human Space Missions to Moon or Mars*," Springer Science & Business Media.
- Rapp, D., (2013) *Extraterrestrial Resources for Human Space Missions to Moon or Mars*, Praxis Publishing, Chichester, U.K.
- Regan, F.J., Anandakrishnan, S.M., *Dynamics of atmospheric re-entry*, AIAA, 1993.
- Steeves, C.A., Wadley, H.N.G., Miles, R.B., and Evans, A.G., "A Magnetohydrodynamic Power Panel for Space Reentry Vehicles," *J. Applied Mechanics*, 2007, vol. 74, p. 57.
- Strickland, J., (2014) "The incredible, expendable Mars Mission,"
<http://www.thespacereview.com/article/2618/1>
- Tauber, M. and Wright, M. J. (2008) *Cone Angle Choices for Atmospheric Entry Vehicles: A Review*, Georgia Institute of Technology.
- Vizcaino, J., and Manish, M., (2015) "Quantification of plume-soil interaction and excavation due to the sky crane descent stage," AIAA SciTech, Kissimmee, FL, 2015, pp. 10.
- Von Braun, W. (1991) *The Mars Project*, University of Illinois Press.
- Wilkes, J., and Klinkman, P., (2007) "Harvesting LOX in LEO: Toward a Hunter-Gatherer Space Economy." AIAA SPACE 2007 Conference.
- Zubrin, R., Baker, D., and Gwynne, O., (1991) "Mars direct: a simple, robust, and cost effective architecture for the space exploration initiative," in 29th Aerospace Sciences Meeting, AIAA (pp. 91-0326), January 1991.

APPENDIX A. MANAGEMENT STRUCTURE AND TEAM MEMBERS



The NIAC Team working in a Technical Integration Meeting (TIM) at Georgia Tech. (From left to right: Dr. Laurent Sibille, Dr. Brandon Sforzo, Keir Gonyea, Hisham Ali, Rob Mueller, not shown: Dr. Robert Braun)



*Dr. Robert D. Braun,
Adjunct Professor, Georgia Institute of Technology
Dean, College of Engineering & Applied Science, University of Colorado, Boulder*

Robert P. Mueller, NASA Kennedy Space Center, Principal Investigator (PI). He was responsible for the success and technical integrity of the task and was the final authority on all management and technical issues. He will present results at conferences and write papers for journal submission. He provided spaceflight architecture expertise, ISRU expertise, systems engineering, and aerospace/mechanical engineering design; and he performed analysis, feasibility studies, and relevant trade studies. He worked jointly with Dr. Sforzo, Dr. Braun, Dr. Sibille and Georgia Tech graduate students in the analysis, report writing, and dissemination. Mr. Mueller has previous experience as a NIAC fellow—He was a Co-I for the NIAC award: *“Regolith Derived Heat Shield for a Planetary Entry, Descent System with In-Situ Fabrication.”* He was also the NASA agency lead for the ISRU task in the Human Spaceflight Architecture (HAT) team from 2014 to 2016.

Dr. Brandon Sforzo, Georgia Institute of Technology, Co-Investigator (Co-I). He performed analysis of orbital mechanics and EDL concepts and trade studies. He worked jointly with Mr. Mueller and Dr. Sibille in generating the space mission and campaign architecture generation; performing related analysis, trade studies, feasibility studies, report writing, and dissemination. Dr. Sforzo had previously been involved in the primary analysis of vehicle performance for a NASA and SpaceX data sharing partnership to advance the state of supersonic retropropulsion for planetary entry. He led a team of students in the development of a methodology for the design of a novel hypersonic inflatable aerodynamic decelerator, which advanced to final competition in the NASA Big Idea Challenge. His research has also involved developing new numerical models, including novel aerodynamic models of supersonic parachutes for planetary entry.

Dr. Robert D. Braun, Georgia Institute of Technology, Co-Investigator (Co-I). He provided consulting expertise and performed a peer review of all work to ensure that it was beyond state of the art in technologies, concepts, and applications. Dr. Braun is a recognized international expert on Entry, Descent, and Landing (EDL) and has been involved in developing new technologies for all recent NASA Mars landing missions. He is the former Chief Technologist for the NASA agency and was responsible for restarting the NIAC program after a hiatus in the mid-2000s. Dr. Braun is presently the Principal Investigator of the NASA STMD Propulsive Descent Technologies project, which is focused on advancing the technology readiness of supersonic retropropulsion for application to Mars EDL. This project is being performed in collaboration with researchers at the NASA Johnson Space Center, NASA Langley Research Center, the Jet Propulsion Laboratory, and SpaceX.

Dr. Laurent Sibille, Engineering Support Contract (ESC), NASA Kennedy Space Center, Co-Investigator (Co-I). He supported this project by performing analysis of ISRU, physics, development of chemical engineering concepts, feasibility studies, and trade studies. He worked jointly with Mr. Mueller, Dr. Sforzo, and Dr. Braun in generating the mission architecture and performing related analysis and trade studies, feasibility studies, report writing, and dissemination at conferences and journals. Dr. Sibille is a 2011 NIAC fellow and he was a Co-I for two other NIAC awards. He also supports the NASA agency ISRU task in the Human Spaceflight Architecture (HAT) team and has recently been involved in developing the NASA “Evolvable Mars Architecture” for landing humans on Mars in the 2030s.

Graduate Students, Georgia Institute of Technology, Collaborators. Two PhD candidate graduate students worked with Dr. Sforzo (Keir Gonyea and Hisham Ali), performing analysis of orbital mechanics, EDL concepts, magneto-hydrodynamic plasma power generation and storage, precision landing performance requirements, feasibility and associated modeling and trade studies. These graduate students were full team members and provided analysis and engineering support. One graduate student, Hisham Ali, is a NASA Graduate Research Fellow, pursuing doctoral research in MHD and related EDL technologies with Dr. Braun and Dr. Sforzo as PhD advisors.

APPENDIX B. SPACE MISSION CAMPAIGN: ARCHITECTURE GROUND RULES & ASSUMPTIONS

B.1 General Architecture

Objective: Develop a mission campaign concept that provides a technical solution for achieving multiple landings of large spacecraft (>20 t payload) on the surface of Mars using the acquisition of Mars atmospheric CO₂ during orbital operations and processing the CO₂ into propellant for the landing phase. The solution will leverage any assets currently in use by NASA or in development by NASA's Exploration Systems Development (ESD) Division for the Evolvable Mars Campaign and other campaign architectures, in addition to those developed by academic institutions and private space companies whose aim is to land large vehicles on Mars. New concepts and systems shall be developed to meet NIAC goals. Goal is a set of high-level GR&A (i.e., at the system interface level). System teams may maintain a lower level of GR&A detail. Periodically update GR&A during team meetings.

Ground Rule: A constraining parameter set by the study leadership, Principal Investigators (R. Mueller, R. Braun, B. Sforzo), not to be traded or changed without leadership team approval.

Assumption: An initial constraining parameter set by the system leads, which may be traded within a set range of values.

Note: The unit "t" is a metric ton, 1000 kg.

B.1.1 Ground Rules

Extensibility: The campaign concept shall be informed by and compared to current NASA assets (e.g., ISS), NASA assets in final stages of development (e.g., SLS, Orion, ARM-SEP, within 5 years of availability) and assets developed during NASA's Mars DRA 5.0 studies and HEOMD Evolvable Mars Campaign study concluded in FY16. Other capabilities (e.g., transportation, navigation techniques, EDL, near zero-g operations, Mars operations) developed by other non-NASA entities shall be considered when they provide specific attributes beneficial to the mission concept in terms of feasibility and sustainability toward the execution of long-duration human missions to the Mars surface.

- **Rationale:** Maximizes compatibility of mission concept with existing NASA assets and engage participation of non-NASA developers and stakeholders.

Focus on Mars Vicinity Operations: The scope of the Phase I NIAC mission concept shall be focused on the operations in the Mars system that enable four crew members to descend to the Mars surface, ascend from the Mars surface, and rendezvous with a Earth-Mars transportation system. The Mars operations shall include the concept of capturing gases from the Mars atmosphere while in an optimized orbit, to produce propellant for a vehicle to descend to the surface. Mars operations may also include EDL, surface operations, and ascent to Mars orbit.

- **Rationale:** Scope of the NIAC project is limited to the study of the Mars system operations while creating assumptions about the Earth to Mars transportation system.

Continuous Human Exploration Cadence: The campaign concept shall only include mission sequences that maintain a continuous human exploration cadence, having no large gaps in human space exploration activity.

- Rationale: Maintains public excitement and demonstrates value to stakeholders.

Robotic Precursor Missions: The campaign concept could use robotic precursor missions to develop and test capabilities required for sustainable human exploration.

- Rationale: Reduces risk by assessing destination characteristics and demonstrating capabilities in destination environments prior to crew launch.

Mass Margin Policy: The systems analyses shall use the following mass margin policy:

Level I Customer Reserve – 0% on wet payload stack (+ adapter) mass

- Rationale: At this point we are Level One, and mission content is still in a great degree of flux with respect to what is needed.

2.5% launch vehicle adapter mass on wet payload stack mass unless supported by analysis greater than parametric

- Rationale: SLS/Orion has worked numbers beyond the parametric level, and unique EMC stacks may require unique integration approaches

5% Flight Performance Reserve on ΔV s for parametric assessments unless supported by detailed simulation or demonstrated performance

- Rationale: Fidelity/Maturity of assessments should drive margins

Elements Mass Margins – AIAA standards used as a guideline, not to exceed 30% MGA

- Rationale: Fidelity/Maturity of assessments should drive margins

Power Margin Policy: The systems analyses shall utilize the following power margin policy:

Elements Power Margins – 0% for heritage systems, 5% for heritage systems used in evolved elements in the 2020s, 10% new systems post-2020, SEP power margin based upon transportation analysis

- Rationale: Fidelity/Maturity of assessments should drive margins

Low TRL Concepts Margin Policy: Uncertainties may require high margins for low TRL concepts such as MAGNETOHYDRODYNAMIC (MHD) energy generation.

B.2 Assumptions

ISS Transition: ISS Transition will occur between 2024 and 2028.

- Rationale: January 2014 announcement by Office of Space Technology Policy to extend life on ISS until at least 2024.
- Trades: transition occurs in 2030

Human Mission Timeline: If using NASA assets, the political Mars threshold will be to send humans to Mars system and return them safely to Earth by the mid-2030s.

- Rationale: 2010 National Space Policy of the United States of America.
- Trades: Use of SpaceX Red Dragon-based mission architecture (if enough is known).

Vehicle Aggregation: The vehicle stacks for the Mars missions will be assembled in highly elliptical Earth orbit (HEO) for rendezvous with the crew and additional required elements (*e.g.*, life limited in-space propulsion elements). The stack will depart for deep space following rendezvous and test/checkout.

- Rationale: EMC study showed that HEO is an appropriate departure and return orbital location for efficient Trans-Mars Injection. LDRO was also baselined by EMC but not in this study to avoid tying the mission concept to lunar missions.
- Trades: Departure orbits other than HEO.

Crew Delivery and Return: Orion will deliver the crew from Earth to HEO staging area and return the crew from the staging area to Earth at mission end.

- Rationale: Orion is the vehicle planned by NASA to transport the mission crew to and from Earth, independent of architecture or trajectory. Data is available on Orion.
- Trades: Commercial or partner crew excursion vehicles if enough data is available (*e.g.*, SpaceX).

In Situ Resource Utilization (ISRU): The mission concept shall include ISRU of the Martian atmosphere during orbital operations to produce propellant for the Mars Descent and Ascent Vehicle/Single-Stage Reusable Lander (MDAV/SSRL).

- Rationale: The use of ISRU in orbital operations at Mars provides a potential solution to the EDL of large vehicles at Mars. Successful implementation of ISRU decreases the required launch mass from Earth and increases sustainability of human exploration of Mars. Ultimately, it leads to logistical independence of Mars missions from Earth through the optimal use of accessible resources with the Mars planetary system.
- Trades: Full logistics support from Earth (methane fuel is assumed if brought from Earth), propellant trade available in orbital ISRU, oxygen extracted from water acquired from Mars regolith, methane production on Mars surface using hydrogen from regolith and atmospheric carbon dioxide, use of resources from the lunar surface, and ARM-redirected asteroid in LDRO.

Exploration Atmosphere: The environmental control and life support systems (ECLSS) of habitable volumes will maintain an atmosphere of 14.7 pounds per square inch-absolute (psia) at 21% O₂ during all long-duration microgravity mission segments.

- Rationale: Atmospheric configuration with the most understood physiological effects; minimizes risk of fire.
- Trades: 10.2 psia at 26.5% O₂; 8.2 psia at 34% O₂

Development Timeline Philosophy: The duration between PDR and hardware delivery to KSC is 6 years for Phobos and Mars human mission elements. The duration between PDR and hardware delivery to KSC is 3 years for robotic missions. A 1-year duration is assumed between hardware delivery to KSC and launch.

- Rationale: Heritage from EMC assumptions.
- Trades: Implement more traditional government development timelines. SpaceX development schedule if known.

B.3 Space Transportation

B.3.1 Ground Rules

Conjunction Class Trajectories to Mars System: The architecture will implement a conjunction-class trajectory for crew transit from Earth to the Mars system. Maximum round-trip duration limited to 1100 days from Earth departure to Earth arrival.

- Rationale: Opposition-class mission not viable with SEP/chemical propulsion.

Number of Crew and Mars Vicinity Mission Duration: Four crew will stay in the Martian vicinity for a minimum of 300 (TBD) days.

- Rationale: Stay time driven by in-space transportation capabilities while maximizing Mars vicinity duration.

Mars Crew transit propulsion: The in-space transportation system used for crew travel between Earth and Mars will be based on chemical propulsion.

- Rationale: Reduce the transit time for crew and make in-space transportation compatible with emerging concepts of propellant depots in the Earth-Moon system.

B.3.2 Assumptions

Space Launch System (SLS) Nominal and Surge Launch Rates: From 2021 through 2027, the SLS nominal launch rate of one per year can support one crewed mission, with surge

capabilities of two launches (crew or cargo) per year. Starting in 2028, the nominal launch rate is two per year (crew or cargo) with a surge capability of three launches per year.

- Rationale: HQ/Explorations Systems Division direction during August 2014 Face-to-Face at Caltech. Expected initial program funding limits launch rate to one crewed SLS per year; KSC infrastructure can support 120-day turn around period between launches.
- Trades: TBD.

SLS Block Upgrade Timeline: Starting in 2021, the available SLS launches will transition to the 105 t to LEO (Block 1B) variant. In 2028, the available SLS launches will transition to the 130 t to LEO (Block 2B) variant. Crew will also launch on Block 2B.

- Rationale: HQ/Explorations Systems Division direction during August 2014 Face-to-Face at Caltech, driven by the existing stockpile of solid rocket booster segments.
- Trades: COTS/EELVs to deliver cargo.

SLS Launch Fairing: Assume a 9.1 m useable envelope within 10 m Earth launch fairing.

- Rationale: SLS design
- Trades: None

Orion/CTV Remains in Earth System: The Orion will not depart the Earth system during crewed missions to the Mars system.

- Rationale: Decreases round-trip mass to Mars system; decreases Orion mission lifetime requirement; decreases Orion Earth reentry speed requirement; HQ direction during April 2014 Core Team Meeting.
- Trades: Use of a non-NASA crew module designed for travel to Mars.

Deep Space Habitat Volume: Habitat should provide 25 m³/p (HRP/BHP Consensus Session 2014). Also assume that no Orion volume is leveraged to reduce the habitable volume requirement, as Orion is nominally not transported with Transit habitat in many mission concepts.

- Rationale: TBD
- Trades: TBD

Habitat Docking Ports: Habitat should provide 3 docking mechanisms with hatches.

- Rationale: Intended to support aggregation, transit and destination operations.
- Trades: TBD

Mars Cargo Transit Propulsion: Mars cargo and unmanned vehicle transit propulsion technology will utilize up to 159 kW (12x13.25kW thrusters) and 16 t xenon prop solar-electric systems extensible from the Asteroid Redirect Vehicle (ARV) Block 1A spacecraft bus

- Rationale: Lower transportation costs for unmanned transit.

- Trades: All chemical propulsion for cargo/unmanned vehicles.

B.4 Mars Orbit/Moons

B.4.1 Ground Rules

TBD

B.4.2 Assumptions

Crew Descends to Mars Surface after MDAV/SSRL Is Fueled by ISRU system: Mars surface bound crew will remain in Mars orbit until verification that the MDAV/SSRL has been fueled by the ISRU system at the Martian destination.

- Rationale: Ensures that MDAV/SSRL ISRU elements have generated propellant for crew descent prior to committing the crew to landing. Ascent propellants shall be made on the Mars surface.
- Trades: Assume a more averse risk posture with ascent propellant made on orbit and landed with the MDAV/SSRL.

Mars Parking Orbit: Crewed Mars missions bound for Phobos, Deimos, and Mars Surface will utilize one sol orbit (approx. $200 \times 33,000$ km altitude) as an intermediate waypoint prior to transferring among Martian destinations.

- Rationale: Supports arrivals and departures for Earth-Mars trajectories.
- Trades: Consider 5-sol orbit (approx. $200 \times 60,000$ km altitude) and other orbits.

B.5 Mars Surface

Note: All Ground Rules and Assumptions from the Mars Moons section remain valid unless contradicted by statements in this section.

B.5.1 Ground Rules

Mars Surface Site: The mission concept shall target all precursors, technology demonstrations, pre-emplaced systems and crewed missions to a single long duration site on the Mars surface.

- Rationale: A single-surface site enables an efficient aggregation of infrastructure for a sustained human presence on Mars.

Landing Site Limitation: Assume MAV departs from $\pm 30^\circ$ from the Martian equator.

- Rationale: Initial sizing point and overlap with science goals.

Site Buildup Strategy: Crew and cargo are delivered to a single Mars surface destination where the infrastructure from previous visits is leveraged for following missions

- Rationale: EMC guiding principle – reuse of exploration elements

Nuclear Power: The long-duration site will incorporate modular 10 kWe nuclear power systems.

- Rationale: Enables ISRU strategies; reduces power system mass delivered to Martian surface; provides continuous high-power generation.

B.5.2 Assumptions

Lander Delivered Mass: The lander delivered mass will be 20 t.

- Rationale: Heritage from EMC.
- Trades: Consider 18 t, 27 t, and 40 t.

Initial Mars Surface ISRU: The Mars surface site will incorporate atmospheric oxygen and methane generation ISRU systems for propellant production in its initial phase of development. Production durations assumed: 18 months.

- Rationale: Reduces required mass of MDAV/SSRL vehicle propellant delivered to Martian surface. 18 months is heritage from EMC.
- Trades: Bring CH₄ from Earth, cargo delivers regolith-based ISRU in the initial phase of development (i.e., icy or hydrated regolith processing for oxygen and methane propellant production, landing site stabilization if needed)

Mars Descent-Ascent Vehicle Sizing: The Mars Descent-Ascent Vehicle (MDAV/SSRL) will be sized to transport a crew of four and 250 kg cargo (includes tare and overhead) during an ascent and rendezvous.

- Rationale: Heritage from EMC to accommodate rendezvous sequence from 44 hours to 5 days and maintains commonality across initial and long stay missions.
- Trades: Cargo, duration.